

HD-A132 178

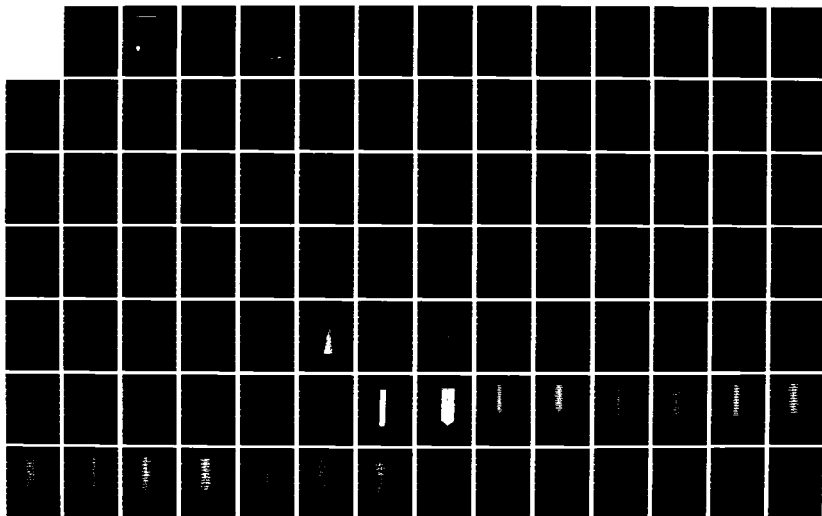
A THEORETICAL ANALYSIS OF NONLINEAR EFFECTS ON THE
FLUTTER AND DIVERGENCE. (U) PRINCETON UNIV N J DEPT OF
AEROSPACE AND MECHANICAL SCIENCES. E CH'NG 02 AUG 77
PUAMS-1343

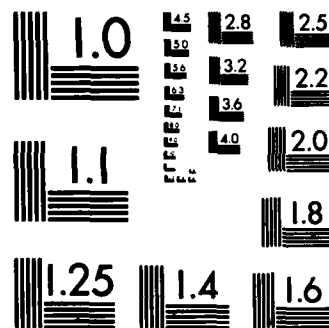
1/2

UNCLASSIFIED

F/G 20/4

NL





MICROCOPY RESOLUTION TEST CHART
NATIONAL BUREAU OF STANDARDS-1963-A

02

ADA132178

Princeton University

A THEORETICAL ANALYSIS OF NONLINEAR EFFECTS ON THE FLUTTER AND DIVERGENCE OF A TUBE CONVEYING FLUID

ENOCH CH'NG, '78

AMS Report No. 1343



PROPERTY
OF THE
ENGINEERING LIBRARY
AEROSPACE COLLECTION

DTIC FILE COPY

Department of
Aerospace and
Mechanical Sciences

DTIC
ELECTE
SEP 07 1983
S E D

This document has been approved
for public release and its
distribution is unlimited.

83 09 02 074

①

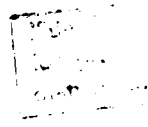
A THEORETICAL ANALYSIS OF
NONLINEAR EFFECTS ON THE FLUTTER AND
DIVERGENCE OF A TUBE CONVEYING FLUID

ENOCH CH'NG, '78

/ AMS Report No. 1343

Department of Aerospace and Mechanical Sciences
Princeton University
Princeton, NJ 08540

August 2, 1977



1

A vertical strip of ten blank, lined pages from a notebook. Each page is white with horizontal ruling lines. The pages are bound on the left side, with visible binder holes. The strip is oriented vertically, showing the sequence of pages from top to bottom.

2.  

DTIC
 COPY
 INSPECTED
 R

ACKNOWLEDGEMENTS

I would like to thank Professor E. H. Dowell for his unfailing assistance in every aspect of this research. His constant encouragement throughout the course of study, his patience and his painstaking review of my work are deeply appreciated.

My thanks also extend to those few who 'live' in the Engineering Quadrangle. Discussions with them have helped me clarify scientific matters.

I am especially grateful to the Dean's office of the School of Engineering and Applied Sciences for funding part of this project, and to Ms. Karen Blackie for typing up this report so professionally.

TABLE OF CONTENTS

<u>Section</u>	<u>Page</u>
Abstract	i
Acknowledgements	ii
Nomenclature	iv
PART I: INTRODUCTION	1
PART II: CANTILEVERED TUBE	4
1. Derivation of Equations of Motion	5
1.1 General Approach	5
1.2 The Nonlinear Tension Effect	7
2. Methods of Solution	10
2.1 Nondimensional Equations of Motion	10
2.2 Galerkin's Method	11
2.3 Numerical Methods	13
3. Numerical Results	16
3.1 Comparison of Numerical and Previous Solutions	16
3.2 Theoretical Limit Cycle Predictions	17
3.3 Mode Shapes and Stress Distribution	17
PART III: SIMPLY SUPPORTED TUBE	19
1. Equations of Motion	20
2. Predicted Characteristics	22
PART IV: CONCLUDING REMARKS	24
References	26
Tables	27
Figures	31
Appendices	95

NOMENCLATURE

a_{jk}	mode shape integral given by Eq. 41
a	cross sectional area of tube
A	notation for matrix
b_{jk}	mode shape integral given by Eq. 42
c_{hi}	mode shape integral given by Eq. A-15
ds	differential length
D	damping factor given in Eq. 9
E	Young's modulus
f_{damp}	damping force
g	acceleration due to gravity
I	moment of inertia of tube section
l	length of tube
m	mass per unit length of tube
m_f	mass per unit length of fluid
\vec{q}	column vector of q_k
q_k	generalized coordinate

q^*	some constant q_k
r	radius of gyration
R	end reaction force
\bar{R}	radius of tube
\bar{R}_1	inside radius of tube
\bar{R}_2	outside radius of tube
t	time
t	thickness (Appendix III)
T	kinetic energy
T_0	tension
U	potential energy
V	velocity of fluid in tube
W	work
x	coordinate
y	displacement of tube
β	nondimensional velocity = $\sqrt{\frac{m_f \ell^2}{EI}} V = 3.52 \sqrt{\frac{\mu}{1-\mu}} \frac{V}{\omega_1 \ell}$
ϵ_x	strain (x-direction)
γ_k	k^{th} cantilever beam mode given in Eq. 34

γ_n	n^{th} simply supported beam mode given in Eq. 63
δ	variation
δ_{jk}	delta function
∇	operator, see Eq. 55
ζ_i	critical damping ratio of i^{th} mode without fluid
λ_k	mode shape constant of Eq. 35
μ	mass ratio = $\frac{m_f}{m_f + m}$
ν	viscous damping parameter = $7.04 \zeta_1 \sqrt{1-\mu}$
ξ	nondimensional coordinate = x/l
ϕ	nondimensional displacement = y/r
σ_k	mode shape constant of Eq. 35
σ_x	stress (x direction) in psi
τ	nondimensional time = $\sqrt{\frac{EI}{(m_f+m)l^4}} t$
θ_1, θ_2	angles of deflection
ω	frequency
$\bar{\omega}_1$	natural frequency of i^{th} mode without fluid
Ω	nondimensional frequency = $\sqrt{\frac{(m_f+m)l^4}{EI}} \omega$ $= \frac{3.52}{\sqrt{1-\mu}} \frac{\omega}{\bar{\omega}_1}$

Subscripts and Superscripts

c cantilevered

f fluid

ss simply supported at both ends

T true

(\cdot) $\frac{d}{d\tau}(\)$

(\prime) $\frac{d}{d\xi}(\)$

PART I: INTRODUCTION

As early as 1950, the observation of bending vibration of a simply supported petroleum pipeline prompted scientific investigations (2). More recently, it was observed that a short pipeline vibrates in its second circumferential mode at fairly high frequency (300-800 Hz) above a certain critical flow velocity (see Figure 1). The vibrations may sometimes generate a shrill sound (3). If the pipeline is sufficiently long, this instability is then superposed on the flexural oscillatory instabilities (Figure 2). High performance liquid-propellant launch vehicles may require rapid transfer of large quantities of fluid from tanks to pumps through pipes with relatively thin walls. Thus, a study of the influence of fluid velocity on the static and dynamic stabilities of propellant lines (tubes) is necessary (4). Other applications occur in hydraulic lines and human lung airways (5).

The purpose of this paper is to analyze the observed motion of an elastic tube conveying fluid using a mathematical model based upon the following assumptions:

- (a) The three basic classes of operative forces are inertial, elastic and aerodynamic forces coupled by the elastic deformations of the tube.
- (b) The fluid being conveyed in the tube is inviscid, incompressible and non-heat conducting.
- (c) The tube may be approximated by a uniform beam.

Earlier investigations have developed linearized mathematical models capable of describing the behavior of the tube up to and including the threshold of instability. Section 1 of Part II briefly discusses the approach taken by Alan S. Greenwald and John Dugundji (1). To predict the large

amplitude periodic motion after the threshold of instability is exceeded, nonlinearities have to be taken into consideration. One such nonlinearity is due to tension induced by bending and consequent stretching of the line. Its existence is closely examined in Part II, Section 1.2. So far, this study is believed to be the only one conducted on the nonlinear tension effect.

Computer simulation is used to solve the set of ordinary differential equations obtained by applying Galerkin's method to the partial differential equations of motion. Data have been analyzed and the results are presented graphically for two sets of tube boundary conditions, cantilevered (clamped-free) and simply supported-simply supported. The clamped-free tube undergoes limit-cycle oscillations of constant peak amplitude and frequency at a fixed fluid velocity. Unlike what was expected, the maximum stress does not always develop at the root of the cantilevered tube (the clamped end). In fact, the point of maximum stress travels along the length of the tube during one period of the limit cycle oscillation. The stress and deflection of the tube increases as fluid velocity increases. For a simply supported-simply supported tube, a static deflection occurs above the threshold of instability whose amplitude increases as the flow velocity increases. At still higher velocity, the tube enters into a dynamically unstable region.

PART II: CANTILEVERED TUBE

Section 1

Derivation of Equations of Motion

1.1 General Approach*

To obtain a differential equation of motion describing the tube, an energy approach has been utilized to account for all the major forces acting on the nonconservative system. Hamilton's principle states

$$\delta \int_{t_1}^{t_2} (T-U) dt + \int_{t_1}^{t_2} \delta W dt = 0 \quad (1)$$

The total kinetic energy of the system is the sum of the kinetic energy due to the motion of the line, and the kinetic energy due to the flowing fluid. In other words,

$$T = T_{\text{line}} + T_{\text{fluid}} \quad (2)$$

where

$$T_{\text{line}} = \frac{1}{2} \int_0^l m \left(\frac{\partial y}{\partial t} \right)^2 dx, \quad (3)$$

$$T_{\text{fluid}} = \frac{1}{2} \int_0^l m_f |\vec{V}|^2 dx \quad (4)$$

In this paper, the x and y components of the fluid velocity are approximated as**

$$\left. \begin{aligned} v_x &\sim v \\ v_y &\sim \frac{\partial y}{\partial t} + v \frac{\partial y}{\partial x} \end{aligned} \right\} \quad (5)$$

* A similar discussion was previously reported in reference 1.

** See figure 3.

Then
$$T_{\text{fluid}} = \frac{1}{2} \int_0^{\ell} m_f [V^2 + (\frac{\partial y}{\partial t} + V \frac{\partial y}{\partial x})^2] dx \quad (6)$$

and
$$T = \frac{1}{2} \int_0^{\ell} \{m(\frac{\partial y}{\partial t})^2 + m_f [V^2 + (\frac{\partial y}{\partial t})^2 + 2V \frac{\partial y}{\partial t} \frac{\partial y}{\partial x} + V^2 (\frac{\partial y}{\partial x})^2]\} dx \quad (7)$$

The total potential energy of the system consists of elastic strain energy of bending and the elastic energy stored in tension due to gravity. By assumption (c) of Part I, the concept of simple beam theory may be applied. In mathematical notation the total potential energy may be written as

$$U = \frac{1}{2} \int_0^{\ell} EI (\frac{\partial^2 y}{\partial x^2})^2 dx + \frac{1}{2} \int_0^{\ell} mg(\ell-x) (\frac{\partial y}{\partial x})^2 dx \quad (8)$$

A structural damping force and a shear force are assumed to be the two major nonconservative forces. Furthermore it is assumed that this structural damping is a viscous damping force of the form

$$\begin{aligned} f_{\text{damp}} &= D \frac{\partial y}{\partial t} \\ &= 2\zeta_1 \bar{\omega}_1 m \frac{\partial y}{\partial t} \end{aligned} \quad (9)$$

From momentum considerations, the shear force at the end of the line may be given as *

$$R = m_f V [\frac{\partial y}{\partial t}(\ell) + V \frac{\partial y}{\partial x}(\ell)] \quad (10)$$

It then follows that

$$\delta W = - \int_0^{\ell} 2\zeta_1 \bar{\omega}_1 m \frac{\partial y}{\partial t} \delta y dx - m_f [\frac{\partial y}{\partial t}(\ell) + V \frac{\partial y}{\partial x}(\ell)] \delta y(\ell) \quad (11)$$

* See Figure 3.

To derive the general equations of motion from Hamilton's Principle, equations (7), (8) and (1) are substituted into equation (1) first. The procedures of the calculus of variation are then performed. Appendix I details the mathematics involved. After considerable algebra, the partial differential equation of motion is found to be

$$EI \frac{\partial^4 y}{\partial x^4} + (m + m_f) \frac{\partial^2 y}{\partial t^2} + 2m_f V \frac{\partial^2 y}{\partial t \partial x} + m_f V^2 \frac{\partial^2 y}{\partial x^2} + 2\zeta_1 \bar{\omega}_1 m \frac{\partial y}{\partial t} - mg \frac{\partial}{\partial x} [(l-x) \frac{\partial y}{\partial x}] = 0 \quad (12)$$

and the boundary conditions are*

$$EI \frac{\partial^2 y}{\partial x^2} (l) = 0 \quad (13)$$

$$\frac{\partial y}{\partial x} (0) = 0 \quad (14)$$

$$EI \frac{\partial^3 y}{\partial x^3} (l) = 0 \quad (15)$$

$$y(0) = 0 \quad (16)$$

1.2 The Nonlinear Tension Effect**

A very important physical characteristic of the tube undergoing flutter is its large amplitude periodic motion. This can only be explained by taking nonlinear effects into account because no linearized model can predict such a periodic solution.

* In Part III these are changed to those appropriate for simply supported edges.

** Up until now, it has been believed that this is the only study on the nonlinear tension effect on the dynamics of a fluttering propellant line (tube).

Imagine that the tube is deflected as shown in the free body diagram for a differential length, ds (Fig. 4). For small displacements, the approximations

$$\theta_1 \sim \sin \theta_1 \sim \partial y / \partial x \quad (17)$$

$$\theta_2 \sim \sin \theta_2 \sim \frac{\partial}{\partial x} \left(\frac{\partial y}{\partial x} \right) dx \quad (18)$$

may be used. Summing forces in the y -direction due to tension yields a net force of

$$T_0 \frac{\partial y}{\partial x} - T_0 \left(\frac{\partial y}{\partial x} + \frac{\partial^2 y}{\partial x^2} dx \right) = -T_0 \frac{\partial^2 y}{\partial x^2} dx \quad (19)$$

for a tube element of differential length, dx . Assuming that the propellant line is Hookean ideal elastic, then

$$T_0 = \sigma_x a \quad (20)$$

$$E = \frac{\sigma_x}{\epsilon_x} \quad (21)$$

where

$$\epsilon_x = \frac{\Delta \ell}{\ell} \quad (22)$$

The elongated length can be written as

$$ds = \sqrt{(\partial x)^2 + (\partial y)^2} \quad (23)$$

and

$$\begin{aligned} \int_0^\ell ds &= \int_0^\ell \sqrt{1 + \left(\frac{\partial y}{\partial x} \right)^2} dx \\ &= \int_0^\ell \left[1 + \frac{1}{2} \left(\frac{\partial y}{\partial x} \right)^2 + \dots \right] dx \end{aligned} \quad (24)$$

Neglecting higher order terms, equation (22) may be written as

$$\epsilon_x = \frac{\int_0^\ell \left[1 + \frac{1}{2} \left(\frac{\partial y}{\partial x} \right)^2 \right] dx - \ell}{\ell} = \frac{1}{2\ell} \int_0^\ell \left(\frac{\partial y}{\partial x} \right)^2 dx \quad (25)$$

Combining equations (25), (21) and (20) give

$$T_0 = \frac{Ea}{2\ell} \int_0^{\ell} \left(\frac{\partial y}{\partial x}\right)^2 dx \quad (26)$$

With this tension term and using (19) and (26), the equation of motion becomes

$$\begin{aligned} EI \frac{\partial^4 y}{\partial x^4} + (m+m_f) \frac{\partial^2 y}{\partial t^2} + 2m_f V \frac{\partial^2 y}{\partial t \partial x} + m_f V^2 \frac{\partial^2 y}{\partial x^2} + \\ 2\zeta_1 \bar{\omega}_1 m \frac{\partial y}{\partial t} - mg \frac{\partial}{\partial x} [(\ell-x) \frac{\partial y}{\partial x}] \\ - \frac{Ea}{2\ell} \int_0^{\ell} \left(\frac{\partial y}{\partial x}\right)^2 dx \cdot \left[\frac{\partial^2 y}{\partial x^2}\right] = 0 \end{aligned} \quad (27)$$

In most cases, the gravity force is small compared to the other forces and may be neglected. Thus,

$$\begin{aligned} EI \frac{\partial^4 y}{\partial x^4} + (m+m_f) \frac{\partial^2 y}{\partial t^2} + 2m_f V \frac{\partial^2 y}{\partial t \partial x} + m_f V^2 \frac{\partial^2 y}{\partial x^2} + \\ 2\zeta_1 \bar{\omega}_1 m \frac{\partial y}{\partial t} - \frac{Ea}{2\ell} \left[\int_0^{\ell} \left(\frac{\partial y}{\partial x}\right)^2 dx \right] \frac{\partial^2 y}{\partial x^2} = 0 \end{aligned} \quad (28)$$

Section 2

Methods of Solution

2.1 Non-dimensional Equations of Motion

The coordinate system (ξ, ϕ) and time τ chosen to nondimensionalize the equations of motion are defined as

$$\left. \begin{aligned} \xi &= x/l \\ \phi &= y/r, \quad (r^2 = \bar{R}^2/2)^* \end{aligned} \right\} \quad (29)$$

$$\tau = \sqrt{\frac{EI}{(m+m_f)l^4}} t \quad (30)$$

With the above dimensionless quantities substituted into equation (28), the equation of motion is found to be

$$\begin{aligned} & \frac{\partial^4 \phi}{\partial \xi^4} + \frac{\partial^2 \phi}{\partial \tau^2} + \frac{2Vm_f l}{\sqrt{EI(m+m_f)}} \frac{\partial^2 \phi}{\partial \xi \partial \tau} + \frac{m_f V^2 l^2}{EI} \frac{\partial^2 \phi}{\partial \xi^2} \\ & + \frac{2\zeta_1 \bar{\omega}_1 m l^2}{\sqrt{EI(m+m_f)}} \frac{\partial \phi}{\partial \tau} - \frac{a r^2}{2I} \int_0^1 \left(\frac{\partial \phi}{\partial \xi} \right)^2 d\xi \frac{\partial^2 \phi}{\partial \xi^2} = 0 \end{aligned} \quad (30)$$

With $\beta \equiv \sqrt{\frac{m_f l^2}{EI}} V$ (velocity parameter)

$$\mu \equiv \frac{m_f}{m + m_f} \quad (\text{mass ratio})$$

* See Appendix III for the derivation.

$$\nu \equiv \frac{2\zeta_1 \bar{\omega}_1 m \ell^2}{\sqrt{EI(m+m_f)}} * \quad (\text{damping parameter})$$

and the fact that for a thin cylindrical tube, $I = ar^2$, equation (30) can be expressed as

$$\frac{\partial^4 \phi}{\partial \xi^4} + \frac{\partial^2 \phi}{\partial \tau^2} + 2\beta\sqrt{I} \frac{\partial^2 \phi}{\partial \xi \partial \tau} + \beta^2 \frac{\partial \phi}{\partial \tau} - \frac{1}{2} \int_0^1 \left(\frac{\partial \phi}{\partial \xi} \right)^2 d\xi \cdot \left[\frac{\partial^2 \phi}{\partial \xi^2} \right] = 0 \quad (31)$$

Equation (31) has associated boundary conditions

$$\text{at } \xi = 0 \quad \phi = 0, \quad \frac{\partial \phi}{\partial \xi} = 0 \quad (32)$$

$$\text{at } \xi = 1 \quad \frac{\partial^2 \phi}{\partial \xi^2} = 0, \quad \frac{\partial^3 \phi}{\partial \xi^3} = 0 \quad (33)$$

2.2 Galerkin's Method

The partial differential equation discussed in the previous section may be reduced to a set of ordinary differential equations by using Galerkin's method. It is assumed that the solution is of the form

$$\phi(\xi, \tau) = \sum_{k=1}^m \gamma_k(\xi) q_k(\tau) \quad (34)$$

where $q_k(\tau)$'s are unknown functions of time, and $\gamma_k(\xi)$'s are assumed functions satisfying all boundary conditions of the problem. For the uniform cantilever beam considered in this study, $\gamma_k(\xi)$'s are taken to be

$$\gamma_k(\xi) = \cosh \lambda_k \xi - \cos \lambda_k \xi - \sigma_k [\sinh \lambda_k \xi - \sin \lambda_k \xi] \quad (35)$$

Values of λ_k and σ_k are given in Table 1. Substituting equation (34) into equation (31), and using the notations

$$* \bar{\omega}_1 = 3.52 \sqrt{EI/m\ell^4}$$

$$\frac{\partial q_k(\tau)}{\partial \tau} = \dot{q}_k(\tau) \quad \frac{\partial \gamma_k(\xi)}{\partial \xi} = \gamma'_k(\xi) \quad (36)$$

The following equation is obtained

$$\sum_{k=1}^m q_k(\tau) \gamma_k^{iv}(\xi) + \sum_{k=1}^m \ddot{q}_k(\tau) \gamma_k(\xi) + 2\beta\sqrt{\mu} \sum_{k=1}^m \gamma'_k(\xi) \dot{q}_k(\tau) + \beta^2 \sum_{k=1}^m q_k(\tau) \gamma_k''(\xi) \quad (37)$$

$$+ \nu \sum_{k=1}^m \gamma_k(\xi) \dot{q}_k(\tau) - \frac{1}{2} \left[\int_0^1 \left(\sum_{k=1}^m q_k \gamma'_k(\xi) \right)^2 d\xi \right] \cdot \left[\sum_{k=1}^m q_k(\tau) \gamma_k''(\xi) \right] = 0$$

The integral in the last term of equation (37) may be re-written as

$$\int_0^1 \left(\sum_{k=1}^m q_k(\tau) \gamma'_k(\xi) \right)^2 d\xi = \sum_{h=1}^m \sum_{i=1}^m [q_h(\tau) q_i(\tau) \cdot \int_0^1 \gamma'_h(\xi) \gamma'_i(\xi) d\xi] \quad (38)$$

The mode shape integral is evaluated in Appendix II with its values tabulated as c_{hi} in Table 2. Equation (38) then becomes

$$\int_0^1 \left(\sum_{k=1}^m q_k(\tau) \gamma'_k(\xi) \right)^2 d\xi = \sum_{h=1}^m \sum_{i=1}^m c_{hi} q_h(\tau) q_i(\tau) \quad (39)$$

Applying Galerkin's method to equation (37) yields

$$\begin{aligned} & \sum_{k=1}^m \left\{ \left[\int_0^1 \gamma_j \gamma_k^{iv} d\xi \right] q_k + \left[\int_0^1 \gamma_j \gamma_k d\xi \right] \ddot{q}_k \right. \\ & + 2\beta\sqrt{\mu} \left[\int_0^1 \gamma_j \gamma'_k d\xi \right] \dot{q}_k + \beta^2 \left[\int_0^1 \gamma_j \gamma_k'' d\xi \right] q_k \\ & \left. + \nu \left[\int_0^1 \gamma_j \gamma_k d\xi \right] \dot{q}_k - \frac{1}{2} \sum_{h=1}^m \sum_{i=1}^m q_h(\tau) q_i(\tau) c_{hi} \left[\int_0^1 \gamma_j \gamma_k'' d\xi \right] q_k \right\} = 0 \\ & (j = 1, 2, \dots, m) \end{aligned} \quad (40)$$

To simplify equation (40), define

$$a_{jk} = \int_0^1 \gamma_j \gamma_k' d\xi \quad (41)$$

$$b_{jk} = \int_0^1 \gamma_j \gamma_k'' d\xi \quad (42)$$

a_{jk} and b_{jk} have been evaluated in the same manner as c_{hi} . Their values are also tabulated in Table 2. Furthermore,

$$\int_0^1 \gamma_j \gamma_k d\xi = \delta_{jk} \quad (43)$$

$$\int_0^1 \gamma_j \gamma_k^{iv} d\xi = \delta_{jk} \lambda_k^4 \quad (44)$$

where δ_{jk} is the delta function. Equation (40) may be further reduced to

$$\begin{aligned} & \sum_{k=1}^m \{ \delta_{jk} \ddot{q}_k + [2\beta \sqrt{\mu} a_{jk} + \nu \delta_{jk}] \dot{q}_k \\ & + [\delta_{jk} \lambda_k^4 + \beta^2 b_{jk} - \frac{1}{2} \sum_{h=1}^m \sum_{i=1}^m q_h q_i c_{hi} b_{jk}] q_k \} = 0 \\ & (j = 1, 2, \dots, m) \end{aligned} \quad (45)$$

2.3 Numerical Methods

The time history of the tube motion may be determined by solving equation (45) numerically. For simplicity, first consider a two mode analysis for equation (45) without the nonlinear term, that is

$$\sum_{k=1}^2 \{ \delta_{jk} \ddot{q}_k + [2\beta \sqrt{\mu} a_{jk} + \delta_{jk} \nu] \dot{q}_k + [\delta_{jk} \lambda_k^4 + \beta^2 b_{jk}] q_k \} = 0$$

$$(j = 1, 2) \quad (46)$$

In another form,

$$\ddot{q}_1 + [2\beta \sqrt{\mu} a_{11} + \nu] \dot{q}_1 + [\lambda_1^4 + \beta^2 b_{11}] q_1 + 2\beta \sqrt{\mu} a_{12} \dot{q}_2 + \beta^2 b_{12} q_2 = 0 \quad (47)$$

$$2\beta \sqrt{\mu} a_{21} \dot{q}_1 + \beta^2 b_{21} q_1 + \ddot{q}_2 + [2\beta \sqrt{\mu} a_{22} + \nu] \dot{q}_2 + [\lambda_2^4 + \beta^2 b_{22}] q_2 = 0 \quad (48)$$

If one defines

$$q_3 = \dot{q}_4 \Rightarrow q_1 = \dot{q}_3 \quad (49)$$

$$q_4 = \dot{q}_2 \Rightarrow \ddot{q}_2 = \dot{q}_4 \quad (50)$$

equations (47) and (48) may be written in matrix form as

$$\begin{bmatrix} \dot{q}_1 \\ \dot{q}_2 \\ \dot{q}_3 \\ \dot{q}_4 \end{bmatrix} = \begin{bmatrix} 0 & 0 & 1 & 0 \\ 0 & 0 & 0 & 1 \\ -(\lambda_1^4 + \beta^2 b_{11}) & -\beta^2 b_{12} & -(2\beta \sqrt{\mu} a_{11} + \nu) & -2\beta \sqrt{\mu} a_{12} \\ -\beta^2 b_{21} & -(\lambda_2^4 + \beta^2 b_{22}) & -2\beta \sqrt{\mu} a_{21} & -(2\beta \sqrt{\mu} a_{22} + \nu) \end{bmatrix} \begin{bmatrix} q_1 \\ q_2 \\ q_3 \\ q_4 \end{bmatrix} \quad (51)$$

$$\text{In short,} \quad \dot{\vec{q}} = A \vec{q} \quad (52)$$

$$\text{But} \quad \dot{\vec{q}}(\tau) \simeq \frac{\vec{q}(\tau + \Delta\tau) - \vec{q}(\tau)}{\Delta\tau} \quad (53)$$

$$\text{then} \quad \vec{q}(\tau + \Delta\tau) = A \vec{q}(\tau) \Delta\tau + \vec{q}(\tau) \quad (54)$$

for $\Delta\tau$ sufficiently small.

The fact that equation (54) is easily expandable for an m-mode analysis makes it the preferred form for writing the equations of motion.

In the case of four mode nonlinear analysis, the nonlinear term of equation (45) alone generates 256 terms. However, only 20 of them are unique. The size of the matrix can thus be reduced to (8,28).*

The error of the approximated solution can be reduced by using the more accurate finite difference relation.**

$$q(\tau+\Delta\tau) \simeq q(\tau) + \Delta\tau(1 + \frac{1}{2} \nabla + 5/12 \nabla^2 + \dots) \dot{q}(\tau) \quad (55)$$

where $\nabla \dot{q}(\tau) = \dot{q}(\tau) - \dot{q}(\tau-\Delta\tau)$ (56)

and $\nabla^{r+1} \dot{q}(\tau) = \nabla^r \dot{q}(\tau) - \nabla^r \dot{q}(\tau-\Delta\tau)$ (57)

A listing of WATFIV computer programs for four mode linear and nonlinear analysis is given in Appendix IV. They are based on the algorithms discussed in this sections and improved by equation (55). Initial conditions and data used in the program are given in Table 3.

The above approach to determination of nonlinear limit cycle oscillations is similar to that employed by Dowell for plates and shells (7).

* Note that the vector and the matrix have to be conformal.

** The formulas given can be found in Reference 6.

Section 3

Numerical Results

3.1 Comparison of Numerical and Previous Solutions

The three most interesting questions posed are, for a given mass ratio and damping ratio,

- i) What is the fluid velocity at which the tube begins to flutter?
- ii) What is the flutter frequency? and,
- iii) What is the limit cycle amplitude of vibration?

Answers to all the questions above may be obtained from the raw computer data. The most primitive method is the "binary search" method.* The computer program is run at several values of the fluid velocities until the flutter behavior is observed. Binary search is then applied to determine the fluid velocity at which the system is neutrally stable.

Another method is to process the raw data. Frequencies and damping ratios of the different vibration modes are plotted against the nondimensional fluid velocity on the same graph. Flutter velocity and frequency may be readily detected from the graph. Examples of two and four-mode linear analysis are shown in Figures 5 and 6.

To make sure that the numerical results obtained reflect the actual dynamic instabilities of the tube, rather than numerical instabilities, the results from the four mode linear analysis are double checked against the previous solutions derived by Alan S. Greenwald and John Dugundji (1). Although the approaches used are significantly different, the two results are found to be in very close agreement. They are shown in Figures 7a and 7b.

* Concept of Binary Search is given in detail in Reference 8.

3.2 Theoretical Limit Cycle Predictions

From the nonlinear model, one can predict the behavior of a cantilevered tube conveying fluid at low fluid velocity. For a given mass ratio, the amplitude of the vibrations is expected to decay to zero with time. However, above a certain critical velocity, the amplitude would increase first as if there is no upper bound. After a few cycles, the amplitude of the vibrations drops back by a fraction and stays at a constant magnitude indefinitely. This is called a limit cycle. The amplitude of the limit cycle increases with the fluid velocity. Graphical presentations of the relationship between the amplitude and the fluid velocity are given in Figure 8 and 9 for mass ratios of 0.1 and 0.5 respectively.

First and second mode frequencies are identical at the threshold of instability. Beyond that, both frequencies increase with the fluid velocity. This is shown in figures 10 and 11 for mass ratios of 0.1 and 0.5 respectively.

3.3 Mode Shapes and Stress Distributions

Mode shapes of the fluttering tube can be obtained by holding τ in equation (34) constant. Altogether five values of τ are judiciously chosen to represent equal time increments over one-half of the period of the limit cycle oscillations. The mode shapes of the tube at these instances are plotted on the same scale for ease of comparison. Figures 12, 13, 14 show mode shapes of tube of mass ratio 0.1 for three different fluid velocity, β . Figures 15, 16, 17 show the cases where mass ratio is 0.5, and the mode shapes are at $1/2$, $5/8$, $3/4$, $7/8$ and the end of the period.

Stress distribution may be determined by using the following equation

$$\sigma_x = Er \frac{\partial^2 y}{\partial x^2} * \quad (58)$$

$$\begin{aligned} \text{or } \sigma_x &= \frac{Er^2}{l^2} \frac{\partial^2 \phi}{\partial \xi^2} \\ &= \frac{Er^2}{l^2} \sum_{k=1}^m q_k(\tau) \gamma_k''(\xi) \\ &= \frac{Er^2}{l^2} \sum_{k=1}^m q_k(\tau) \cdot \lambda_k^2 [\cosh \lambda_k \xi + \cos \lambda_k \xi - \sigma_k (\sinh \lambda_k \xi + \sin \lambda_k \xi)] \end{aligned} \quad (59)$$

Figure 18 shows the stress distribution in the tube for $\mu = 0.5$ and $\beta = 10.4$ at five different time steps. Unlike what was expected, the maximum stress does not occur at the root of the tube (the clamped end). It appears to be shifting along the length of the tube during the entire cycle of oscillation. This is because the maximum curvature of the tube does not necessarily occur at the root of the tube.

* σ_x is in psi in Fig. 18.

PART III: SIMPLY SUPPORTED TUBE

Section 1

Equations of Motion

The partial differential equation of motion of a simply supported tube is the same as the one for a cantilever tube, i.e., equation 37. The only difference is the set of boundary conditions

$$\left. \begin{array}{l} \text{at } \xi = 0, \quad \phi = 0 \\ \quad \quad \quad \frac{\partial^2 \phi}{\partial \xi^2} = 0 \end{array} \right\} \quad (60)$$

$$\left. \begin{array}{l} \text{at } \xi = 1, \quad \phi = 0 \\ \quad \quad \quad \frac{\partial^2 \phi}{\partial \xi^2} = 0 \end{array} \right\} \quad (61)$$

It is again assumed that the solution is of the form

$$\phi(\xi, \tau) = \sum_{n=1}^m \gamma_n(\xi) q_n(\tau) \quad (62)$$

To satisfy the boundary conditions, the $\gamma_n(\xi)$'s are taken to be

$$\begin{aligned} \gamma_n(\xi) &= \sin n\pi\xi \\ n &= 1, \dots, m \end{aligned} \quad (63)$$

Since everything else is the same as for the cantilevered tube except for $\gamma_n(\xi)$, equation (40) can be reused. The only things that have to be rederived are the mode shape integrals. Mode shape integrals for a tube simply-supported at both ends are evaluated in Appendix V.

As before, define

$$a_{jk} = \int_0^1 \gamma_j \gamma_k' d\xi \quad (64)$$

$$b_{jk} = \int_0^1 \gamma_j \gamma_k'' d\xi \quad (65)$$

$$c_{hi} = \int_0^1 \gamma_h' \gamma_i' d\xi \quad (66)$$

and the equations of motion become

$$\begin{aligned} & \sum_{k=1}^m \left\{ \frac{1}{2} \delta_{jk} \ddot{q}_k + [2\beta \sqrt{\mu} a_{jk} + \frac{1}{2} \nu \delta_{jk}] \dot{q}_k \right. \\ & \left. + \left[\frac{k^4 \pi^4}{2} \delta_{jk} + \beta^2 b_{jk} - \frac{1}{2} \sum_{h=1}^m \sum_{i=1}^m q_h q_i c_{hi} b_{jk} \right] q_k \right\} = 0 \quad (67) \\ & (j = 1, 2, \dots, m) \end{aligned}$$

The computer program written for evaluating the time histories of a cantilevered tube may be readily modified to solve equation (67) by the following changes

$$\delta_{jk} = \begin{cases} \frac{1}{2} & j=k \\ 0 & j \neq k \end{cases} \quad (68)$$

$$\lambda_k = k\pi \quad (69)$$

A listing of the modified program in FORTRAN is given in Appendix VI. Other alternations were made to conserve core storage space and computer time.

Section 2

Predicted Characteristics

For $0 \leq \beta < \pi$, the tube undergoes damped stable vibrations. Examples of these damped vibrations are shown in Figures 19 and 20 for the two limiting cases. The magnitude of the true damping ratio, ζ_1^T , increases with flow velocity. This relation is shown in Figure 21a. First mode frequency, ω_1 , as a function of β is shown in Figure 21b. The frequency of the first mode vibration decreases as β is increased π . In the neighborhood of $\beta = \pi$, the first mode damping ratio becomes very large and the frequency approaches zero. In Figure 22, the product $\zeta_1 \omega_1$ is shown. Note that it varies smoothly with β as β passes through π .

Beyond $\beta = \pi$, the tube was found to undergo divergence by previous investigators, Ref. 5. This is only true for β less than 2π . For $\pi < \beta < 2\pi$, the magnitude of $q_1(\tau)$ grows exponentially with time initially. $q_1(\tau)$ then oscillates near some constant value, say q^* . These transient oscillations decay with time and eventually die out, and $q_1(\tau)$ converges to the steady state amplitude, i.e., q^* . Higher mode oscillations are not very significant and the amplitudes decay to zero. Examples of such behavior for four different values of β are given in Figures 23, 24, 25 and 26. To show the relationship between β and the amplitude of $q_1(\tau)$ more clearly, the non-oscillatory average of $q_1(\tau)$ is plotted against time for the four β 's in Figure 27.

Near $\beta = 2\pi$, all four modes become dynamically unstable. However, the first and second modes are dominant. Four of the relevant time histories are illustrated in Figures 28 to 31.

It was speculated that if at $\beta = \pi$, the first mode becomes statically unstable, and at $\beta = 2\pi$, the second mode becomes important and changes the static instability to a dynamic instability, then at $\beta = 3\pi$, the third mode may become very significant and drastically alter the time history of motion again. However, this is not true. The third and fourth modes are dynamically unstable, but they do not dominate the total motion. For $\beta > 3\pi$, no drastic change in time history is found. It appears to have the same "pulse" or "beat" characteristics as for $\beta < 3\pi$. These are shown in Figures 32 and 33.

A stress analysis was done for $\beta = 5.92$. As was expected, the maximum stress is in the middle between the two ends. Figure 34 shows the stress distribution in the tube.

Although there is no drastic change in the time history for $\beta > 3\pi$, the third mode does appear in the deformation shape during the cycle. At $\beta = 10.0$, the deformation shape of the tube changes from a two mode sine wave to a three mode sine wave and back to a two mode sine wave over a complete cycle of motion. Deformation shapes at 20 equal time increments over the period of the modulated sine wave are shown in Figures 35a-35e. Graphs showing stress distribution in the tube for the 20 corresponding deformation shapes are given in Figures 36a-36e.

The effects of fluid velocity β on the first and second mode peak limit cycle amplitudes are shown in Figure 37a and 37b respectively. These further illustrate the dramatic changes in modal content of the motion which occur near $\beta = 2\pi$.

The first correct linear stability analysis of a simply supported-simply supported pipe was given by Housner (9). The present discussion extends his results to the nonlinear regime.

PART IV: CONCLUDING REMARKS

This study has developed a mathematical model capable of describing the large amplitude periodic behavior of a cantilever or simply-supported propellant line (tube) conveying high velocity liquid. The study has also illustrated the importance of the nonlinear tension effect induced by bending of the tube. Thresholds of instability predicted by the theory are in good agreement with those previously obtained by other investigators. Plans have been made for setting up experiments to confirm the predicted magnitudes of the limit cycles.

The theoretical model might be improved by considering other nonlinearities, e.g., nonlinear modulus of elasticity or nonlinear curvature. Instead of viscous damping, one might consider viscoelastic damping, or better still, a combination of viscous and viscous-elastic damping. The uniform beam assumption could be replaced by the thin cylindrical shell approximation. For cases in which the hanging tubes are very flexible, the gravity term should not be neglected.

References

1. Greenwald, A.S., and Dugundji, J., "Static and Dynamic Instabilities of a Propellant Line", AFOSR 67-1395, United States Air Force, (May 1967).
2. Ashley, H., and Haviland, G., "Bending Vibrations of a Pipeline Containing Fluid", Journal of Applied Mechanics, Transaction of A.S.M.E., vol. 27, pp. 229-232 (1950).
3. Paidoussis, M.P., and Denise, J.P., "Flutter of Cylindrical Shells Conveying Fluid", Journal of Sound and Vibration, vol. 16, pp. 259-261 (1971).
4. Dodds, H.L., and Runyan, H.L., "Effect of High Velocity Fluid Flow on the Bending Vibrations and Static Divergence of a Simply Supported Pipe", NASA TN D-2870, (June 1965).
5. Weaver, D.S. and Paidoussis, M.P., "On the Collapse and Flutter Phenomena in Thin Tubes Conveying Fluid", Journal of Sound and Vibration, vol. 50, pp. 117-132 (1977).
6. Hildebrand, F.G., Introduction to Numerical Analysis, McGraw-Hill Book Co., Inc., New York, pp. 188-9, 92 (1956).
7. Dowell, E.H., Aeroelasticity of Plates and Shells, Noordhoff International Publishing (1975).
8. Gear, C.W., Introduction to Computer Science, Science Research Associates, Inc., Chicago, p. 197 (1973).
9. Housner, G.W., and Hudson, D.E., Applied Mechanics - Dynamics, D. Van Nostrand Company, Inc., New York (1950).
10. Felgar, R.P., Jr., "Formulas for Integrals Containing Characteristic Functions of a Vibrating Beam", Bureau of Engineering Research, The University of Texas, Austin, Texas, No. 14 (1950).
11. Young, D., and Felgar, R. P., Jr., "Tables of Characteristic Functions Representing Normal Modes of Vibration of a Beam", Bureau of Engineering Research, The University of Texas, Austin, Texas, No. 44, p. 19, (July 1, 1949).

Table 1
MODE SHAPE PARAMETERS
(Cantilever Beam)

Mode	σ_k	λ_k	λ_k^4
1	0.73410	1.8751	12.362
2	1.01847	4.6941	485.52
3	0.99923	7.8548	3806.5
4	1.000034	10.9955	14617.

Table 2
MODE SHAPE INTEGRALS
 (Cantilever Beam)

$$a_{jk} = \int_0^1 \gamma_j(\xi) \gamma_k'(\xi) d\xi$$

j/k	1	2	3	4
1	2.0000	-4.7600	3.7840	-4.1200
2	0.7595	2.0000	-6.2220	3.3830
3	0.2157	2.2220	2.0000	-8.1680
4	0.1198	0.6166	4.1680	2.0000

$$b_{jk} = \int_0^1 \gamma_j(\xi) \gamma_k''(\xi) d\xi$$

j/k	1	2	3	4
1	0.8582	-11.7400	27.4500	-37.3900
2	1.8740	-13.3000	-9.0420	30.4000
3	1.5650	3.2290	-45.9000	-8.3350
4	1.0870	5.5410	4.2540	-98.9200

$$c_{hi} = \int_0^1 \gamma_h'(\xi) \gamma_i'(\xi) d\xi$$

h/i	1	2	3	4
1	4.6478	-7.3799	3.9415	-6.5934
2	-7.3799	32.4173	-22.3524	13.5826
3	3.9415	-22.3542	77.2989	-35.6482
4	-6.5934	13.5826	-35.6482	142.4605

Table 3

INITIAL CONDITIONS AND DATA USED

$$\vec{q} = 0.1$$

$$\dot{\vec{q}} = 0$$

$$l = 9.5 \text{ ins.}$$

$$m = 1.21 \times 10^{-6} \text{ lb-sec}^2/\text{in}^2$$

$$I = 46.6 \times 10^{-6} \text{ in}^4$$

$$\bar{\omega}_1 = 25.1 \text{ rad/sec}$$

$$E = 1.07 \times 10^4 \text{ lbs/in}^2$$

$$\zeta_1 = .080$$

$$\nu = .400$$

$$\mu = 0.1, 0.5$$

Table 4

MODE SHAPE INTEGRALS

(Simply Supported Beam)

$$a_{jk} = \int_0^1 \gamma_j(\xi) \gamma_k'(\xi) d\xi$$

j/k	1	2	3	4
1	0.0000	-1.3333	0.0000	-0.5333
2	1.3333	0.0000	-2.4000	0.0000
3	0.0000	2.4000	0.0000	-3.4286
4	0.5333	0.0000	3.4286	0.0000

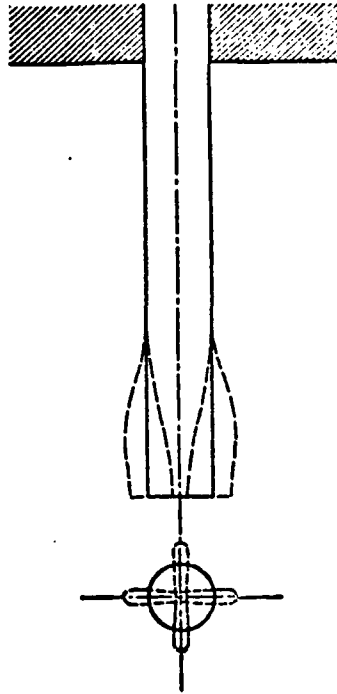


Figure 1. Observed Flutter of Short Tube
(From Reference 3)

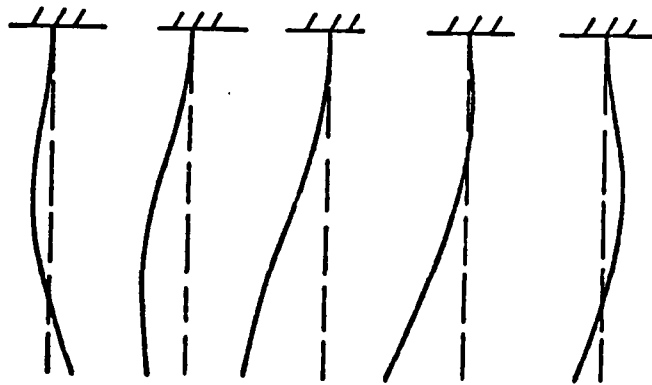
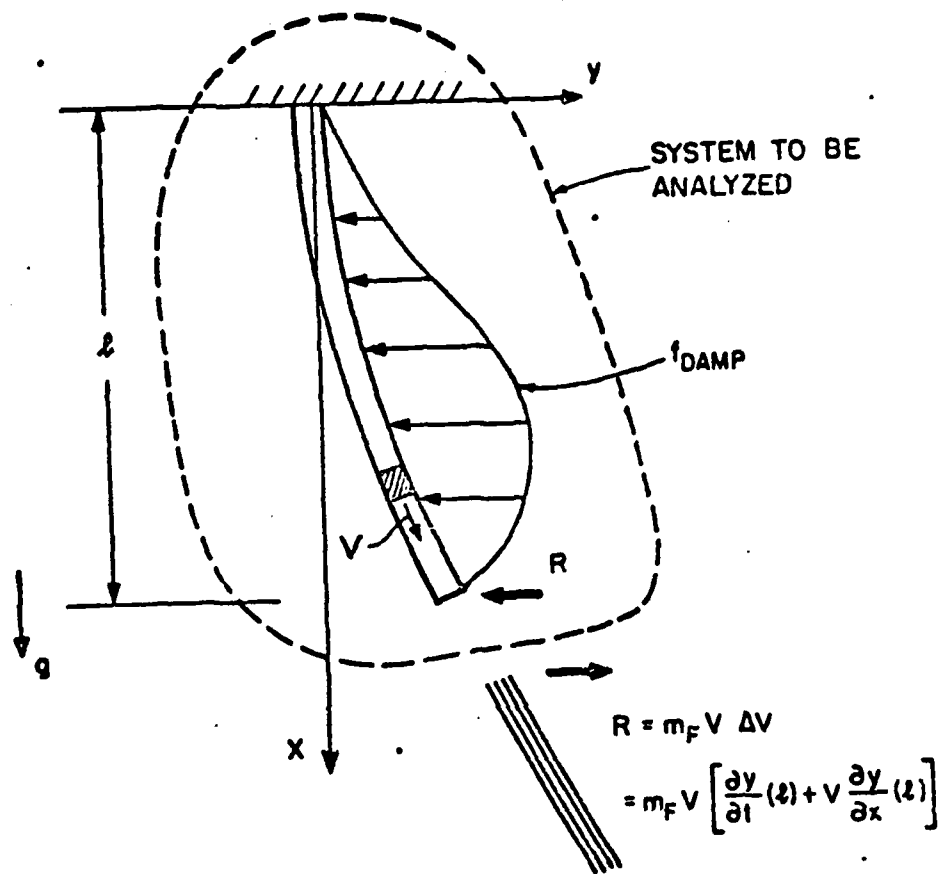


Figure 2. Flexural Oscillatory Instabilities
(From Reference 1)



ABSOLUTE VELOCITY OF FLUID,

$$V_x \approx V$$

$$V_y \approx \frac{\partial y}{\partial t} + V \frac{\partial y}{\partial x}$$

Figure 3. Tube with Flowing Fluid
(From Reference 1)

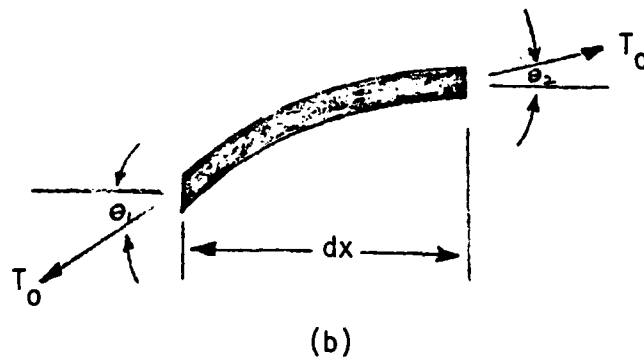
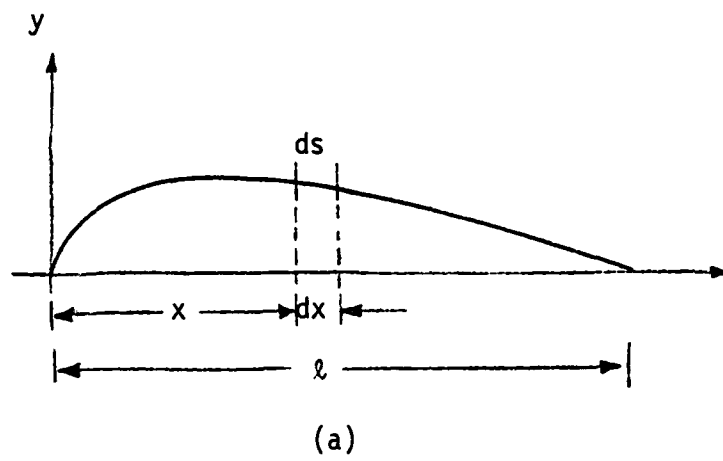


Figure 4. Deflected Beam

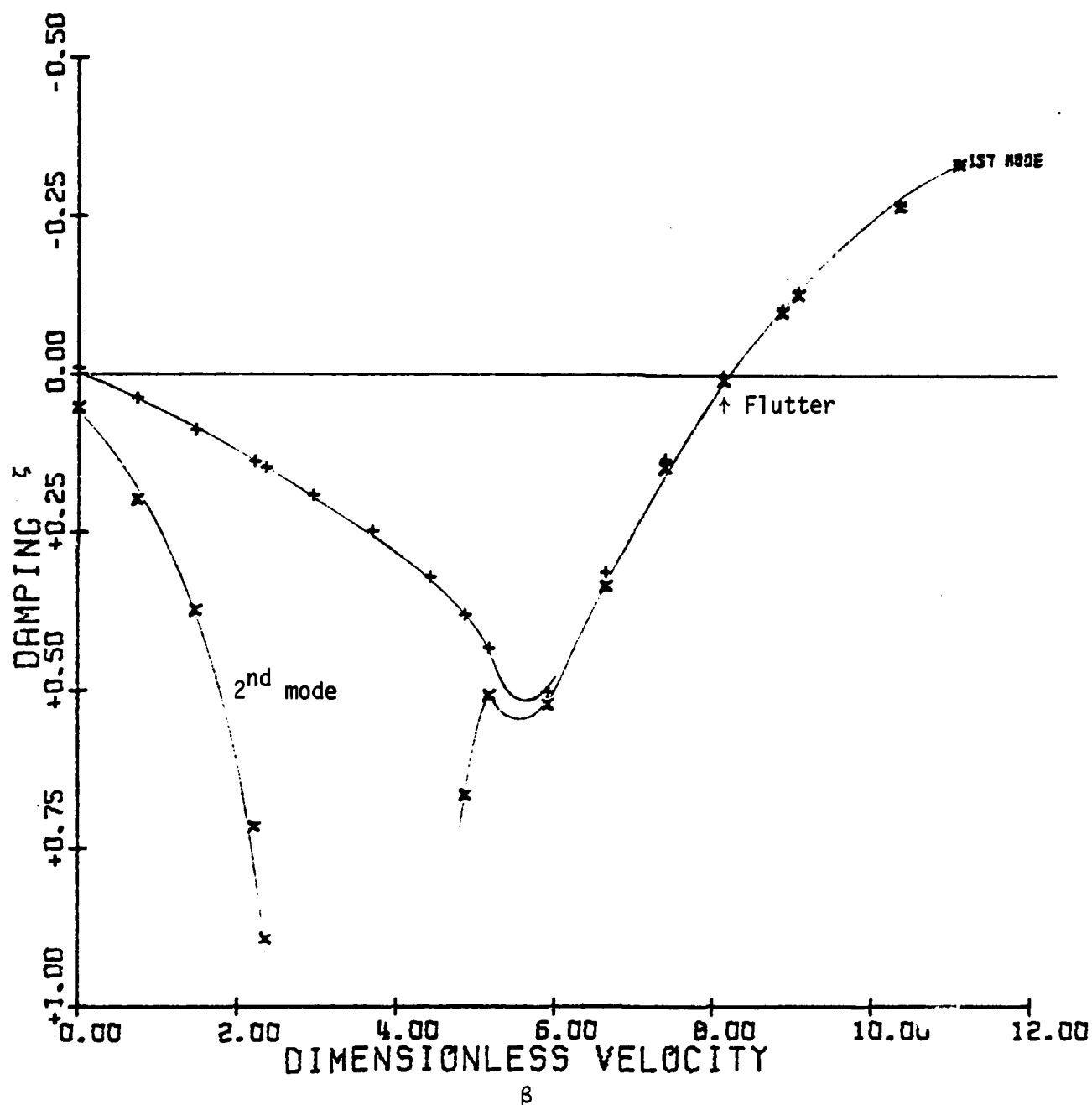


Figure 5. The Effects of Velocity on Damping ($\mu = 0.5$)
(Two Modes)

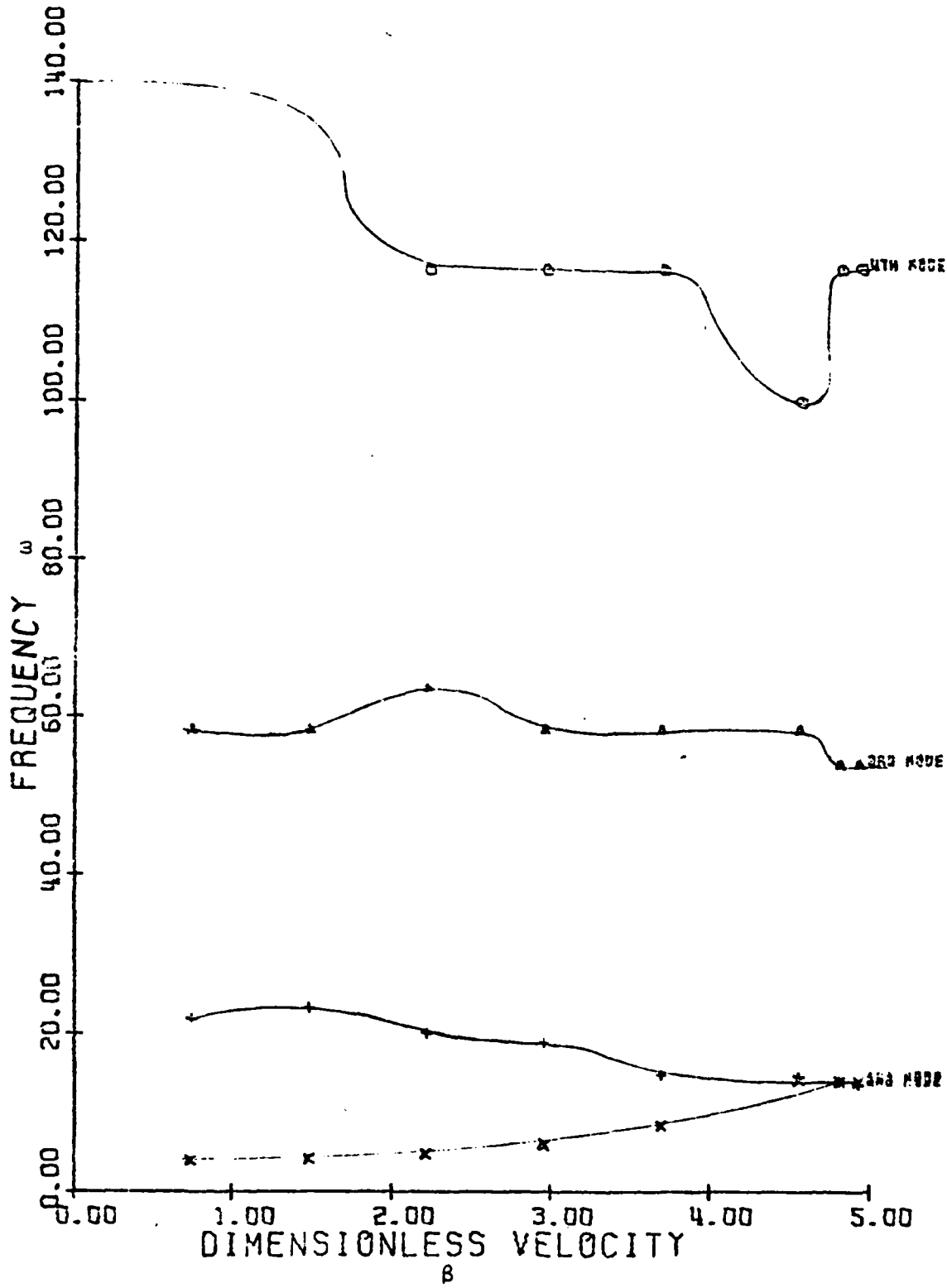


Figure 6a. The Effects of Velocity on Frequency ($\mu = 0.1$)
(Two Modes)

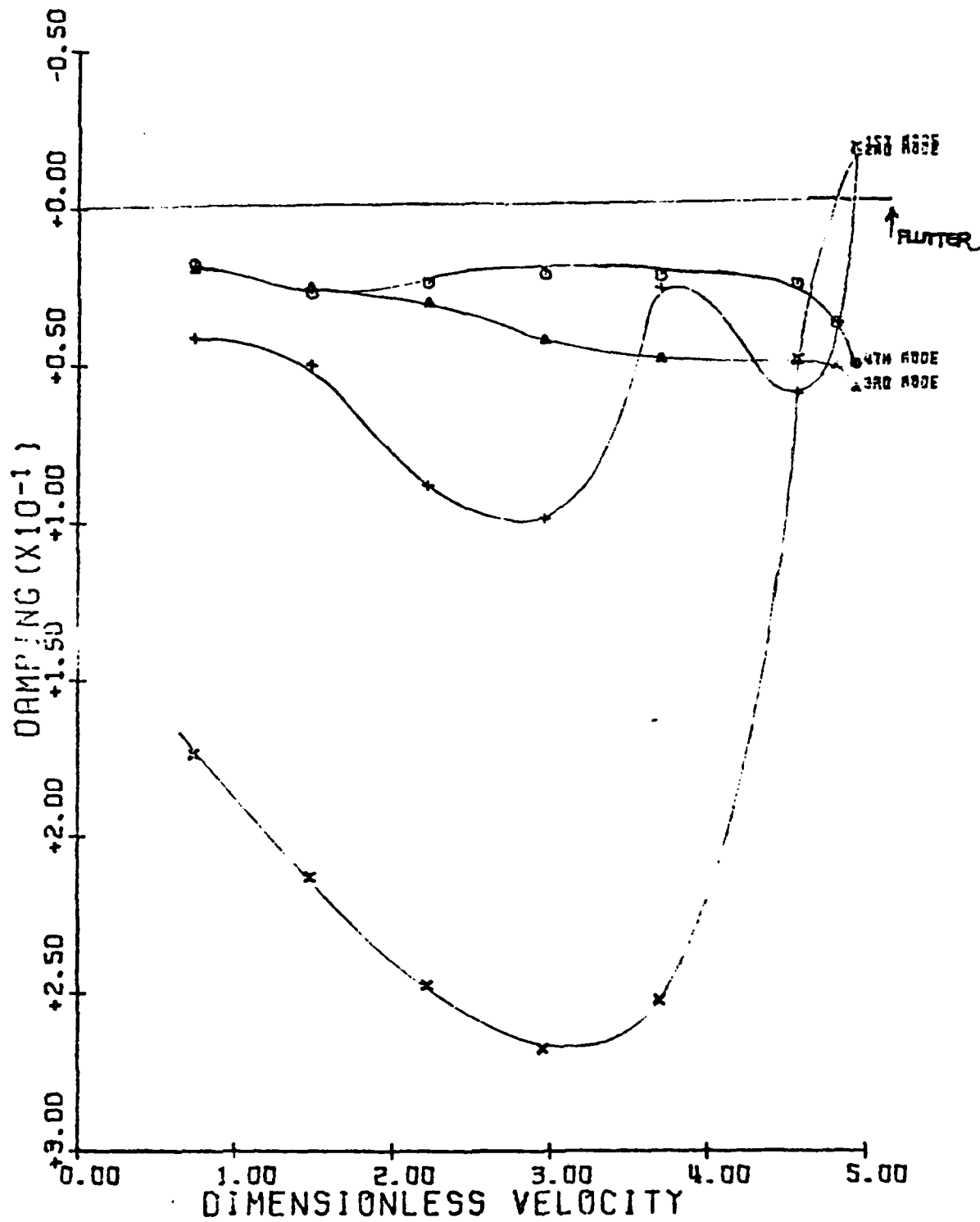


Figure 6b. The Effects of Velocity on Damping
($\mu = 0.1$, Four Modes)

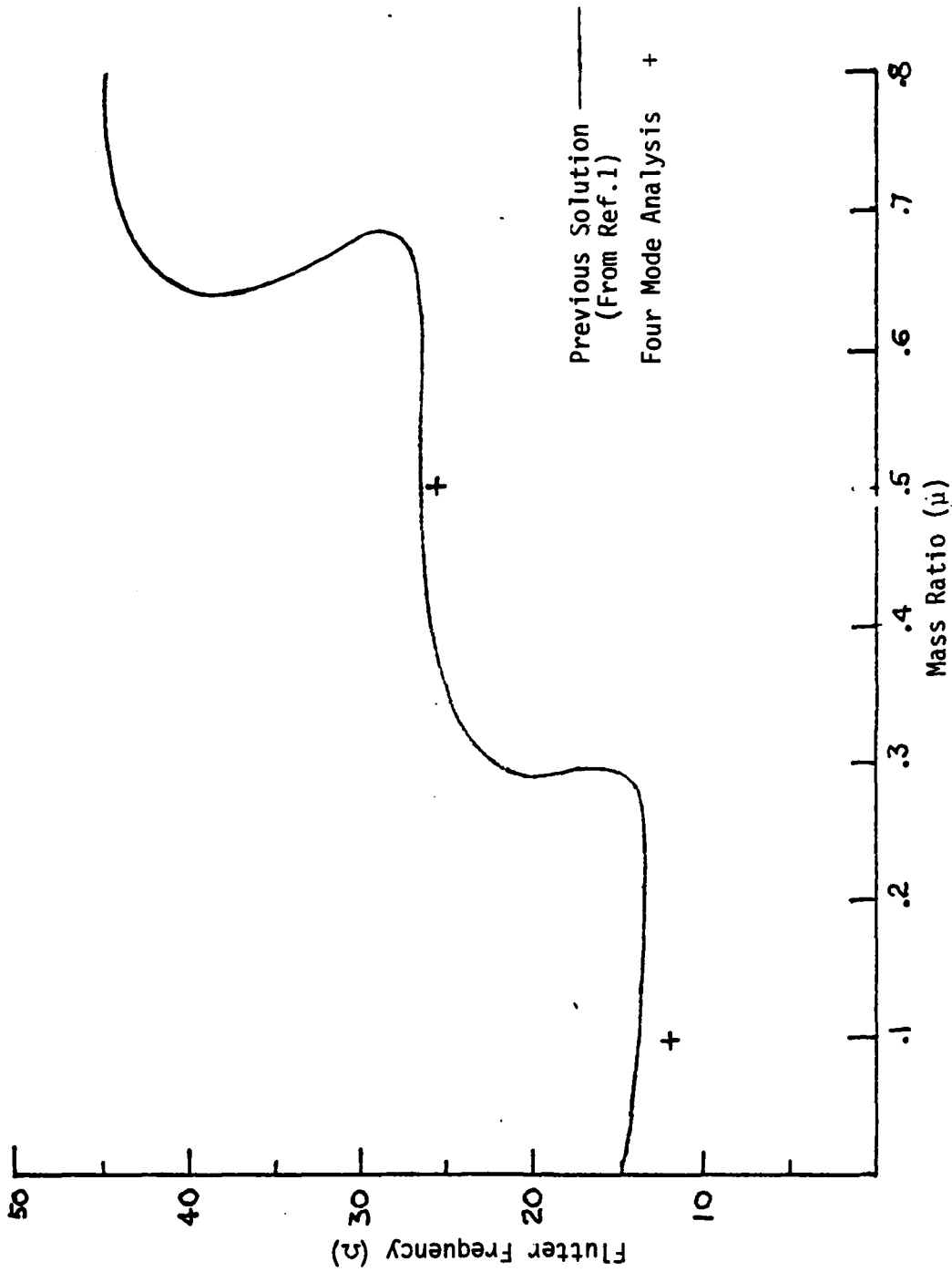


Figure 7a. Comparison of Previous and Numerical Solutions
(Frequency vs. Mass Ratio)

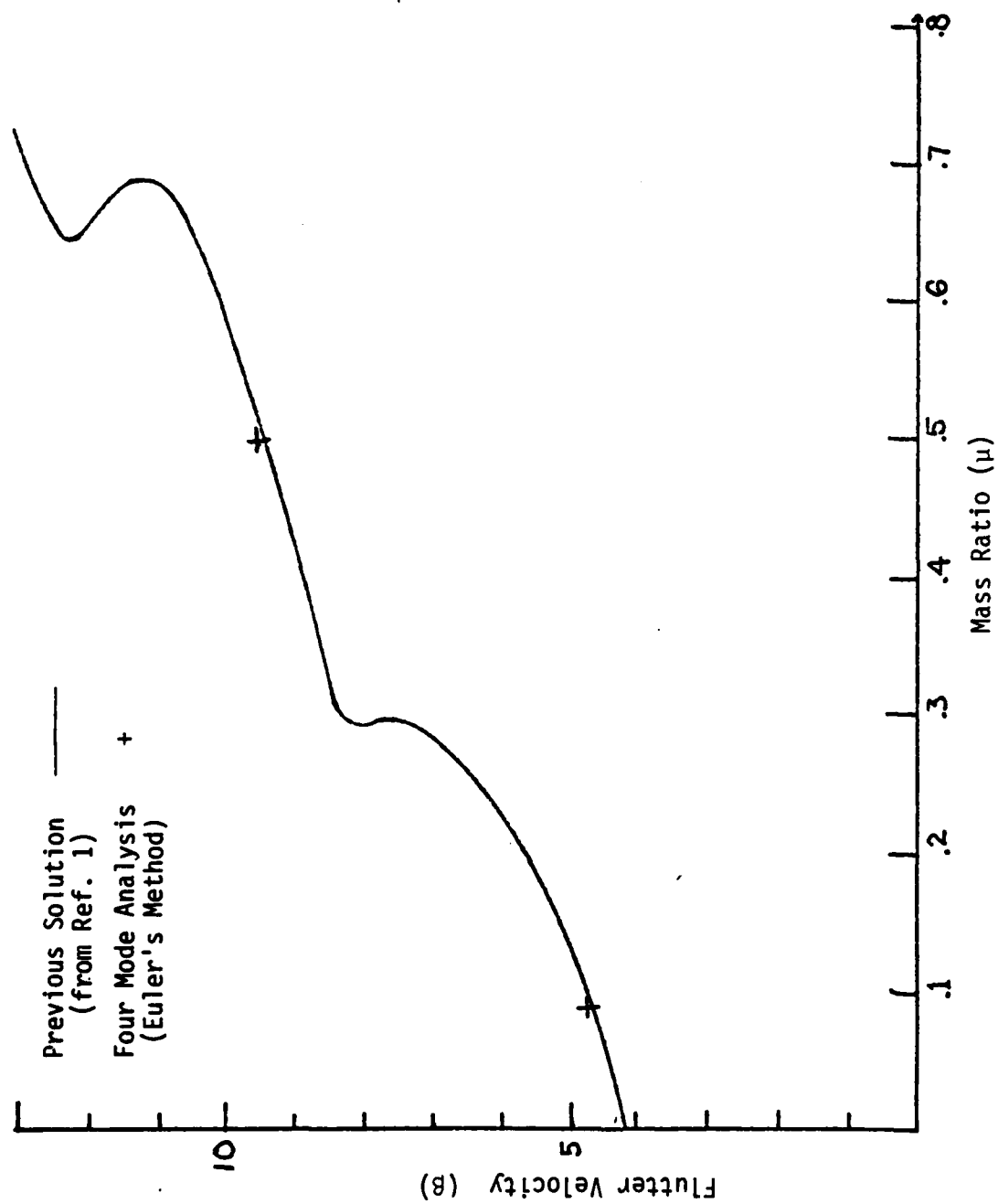


Figure 7b. Comparison of Previous Solution and Numerical Solutions
(Velocity vs. Mass Ratio)

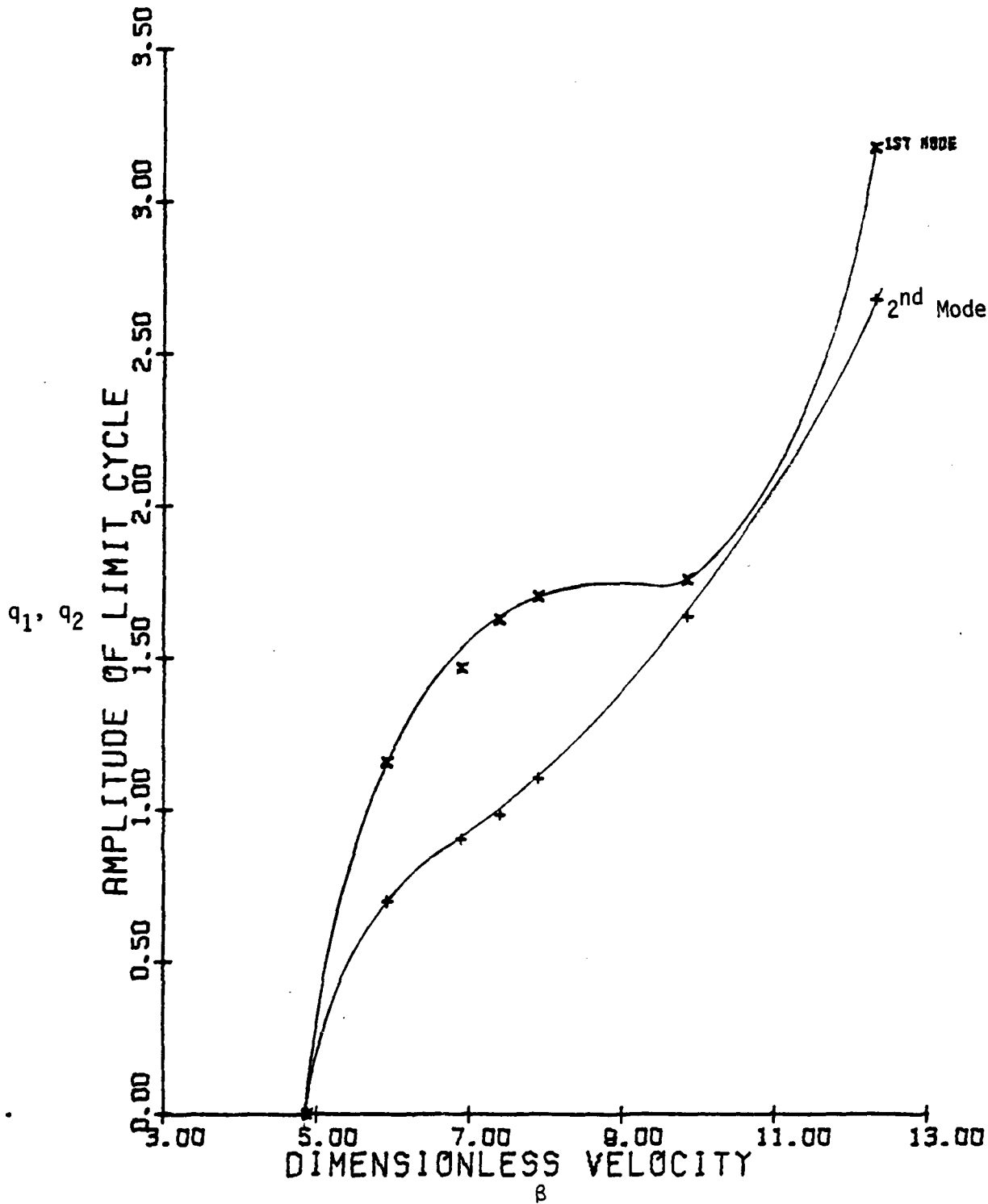


Figure 8. Effects of Velocity on Amplitude of Limit Cycle
($\mu = 0.10$, Four Modes)

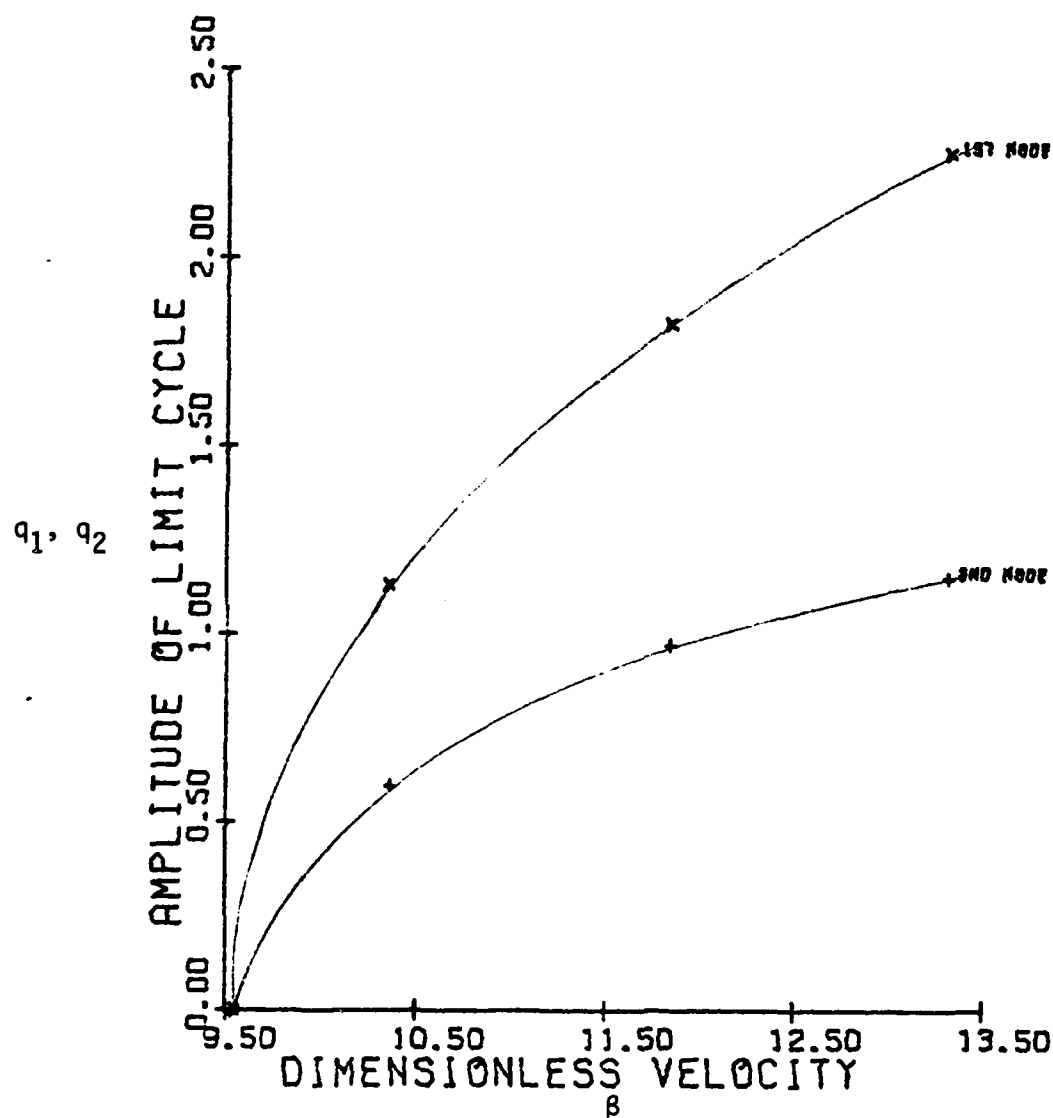


Figure 9. The Effects of Velocity on the Amplitude of Limit Cycle ($\mu = 0.50$, Four Modes)

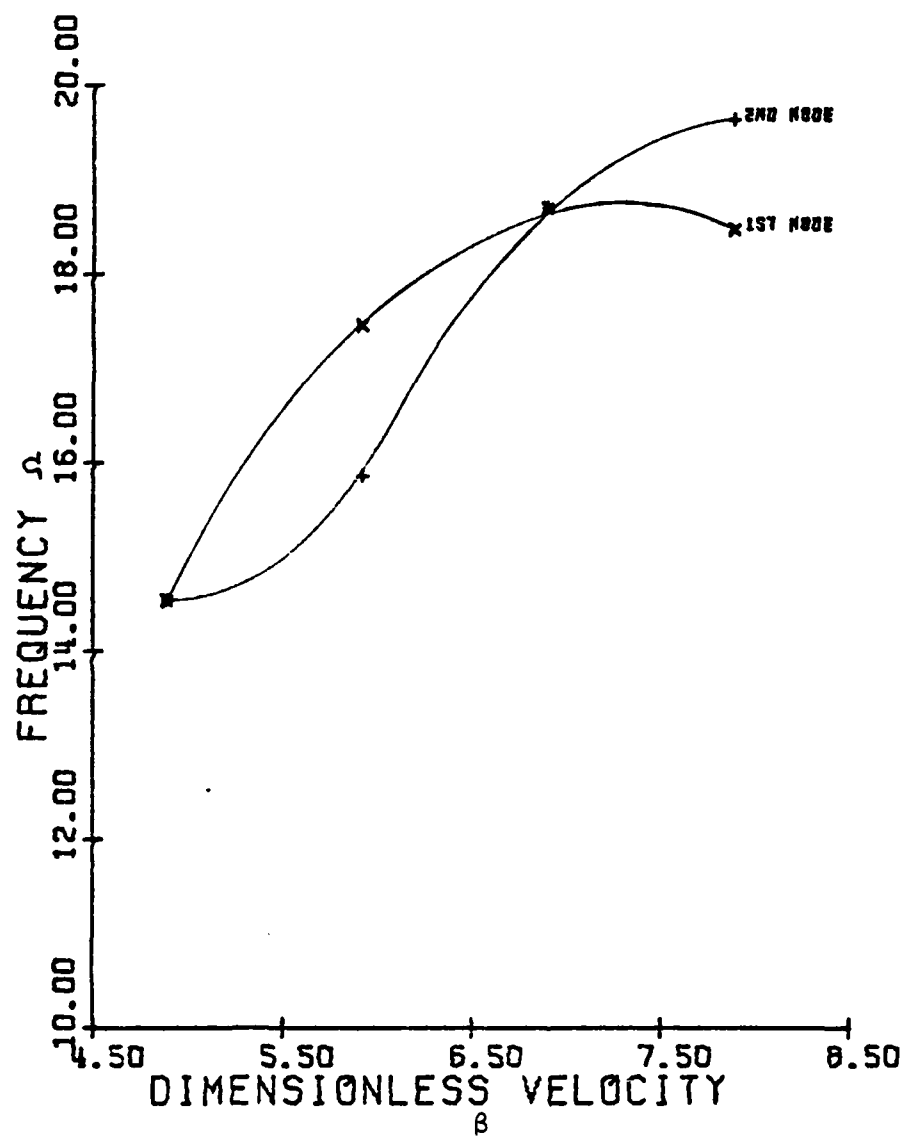


Figure 10. Variation of Frequency Due to Velocity
($\mu = 0.1$, Four Modes)

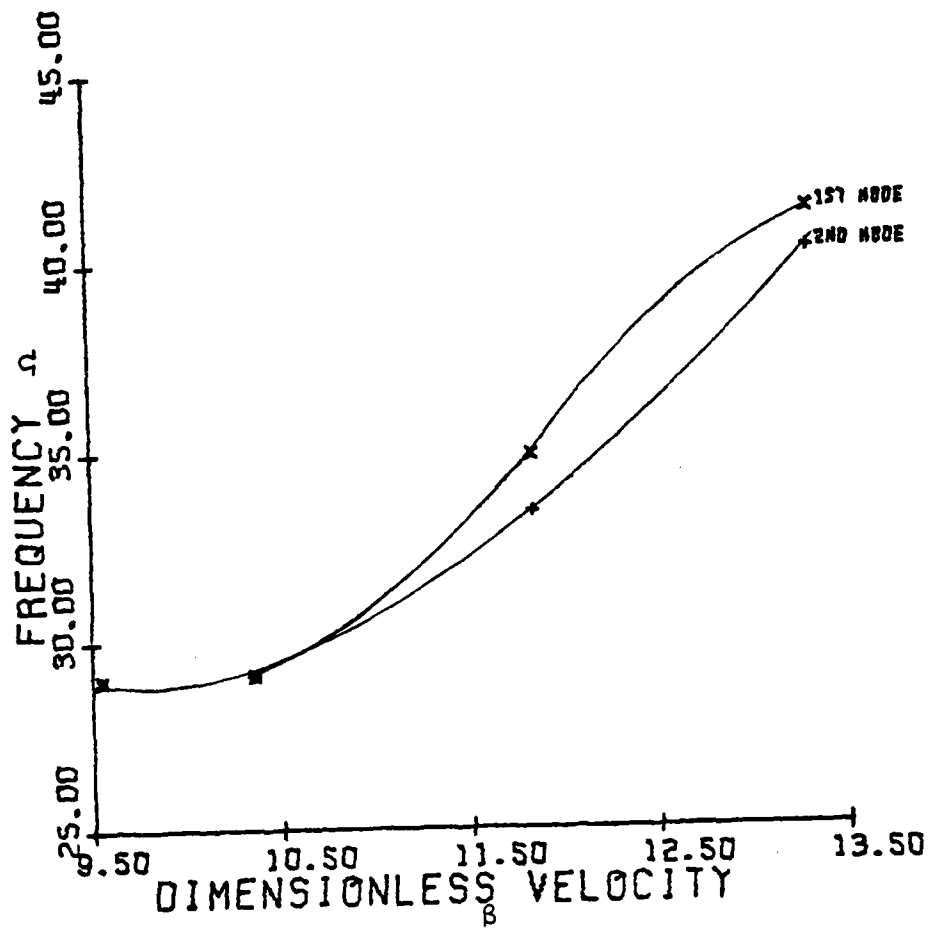


Figure 11. Variation of Frequency Due to Velocity
($\mu = 0.5$, Four Modes)

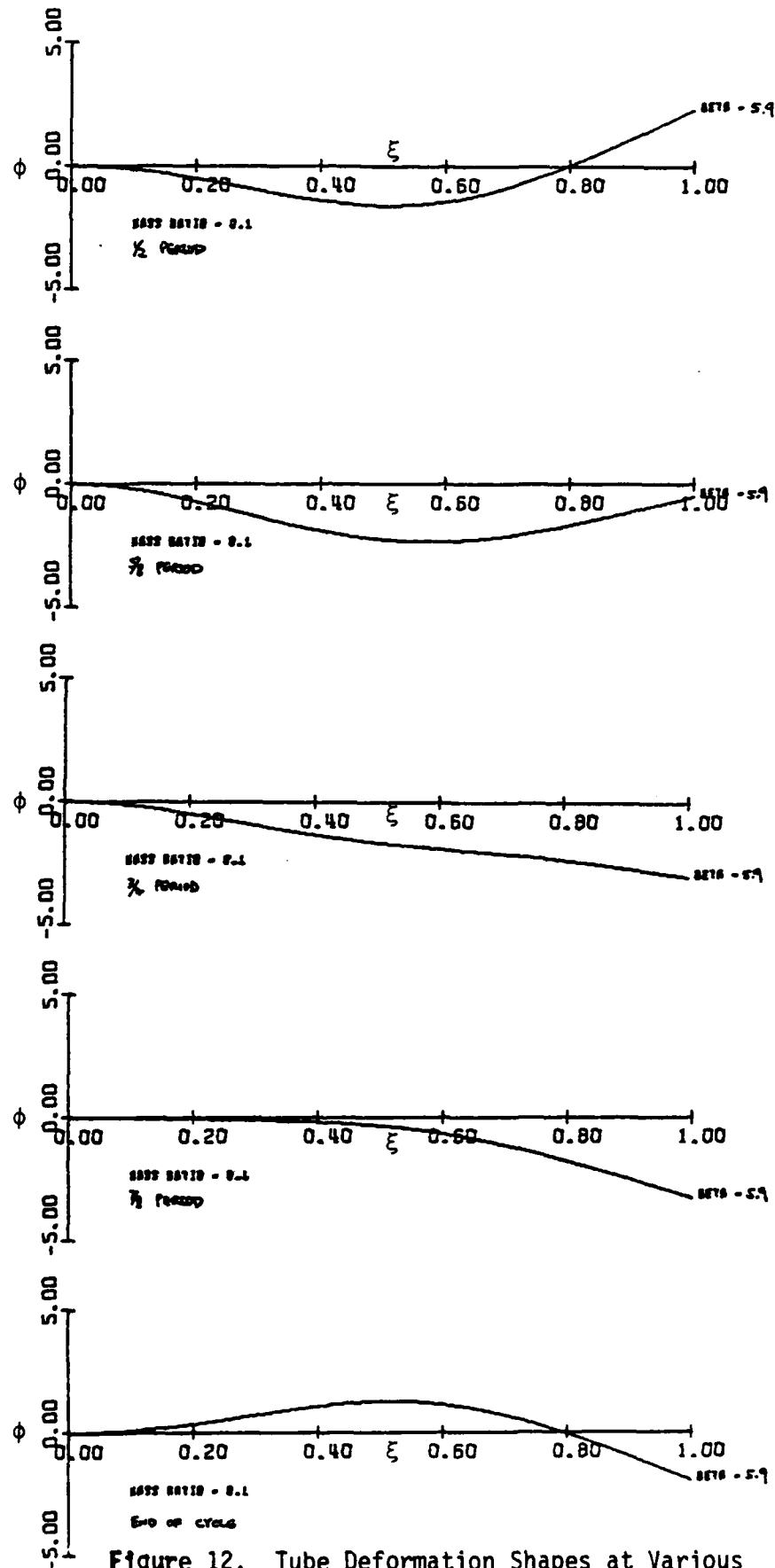


Figure 12. Tube Deformation Shapes at Various Times During Limit Cycle

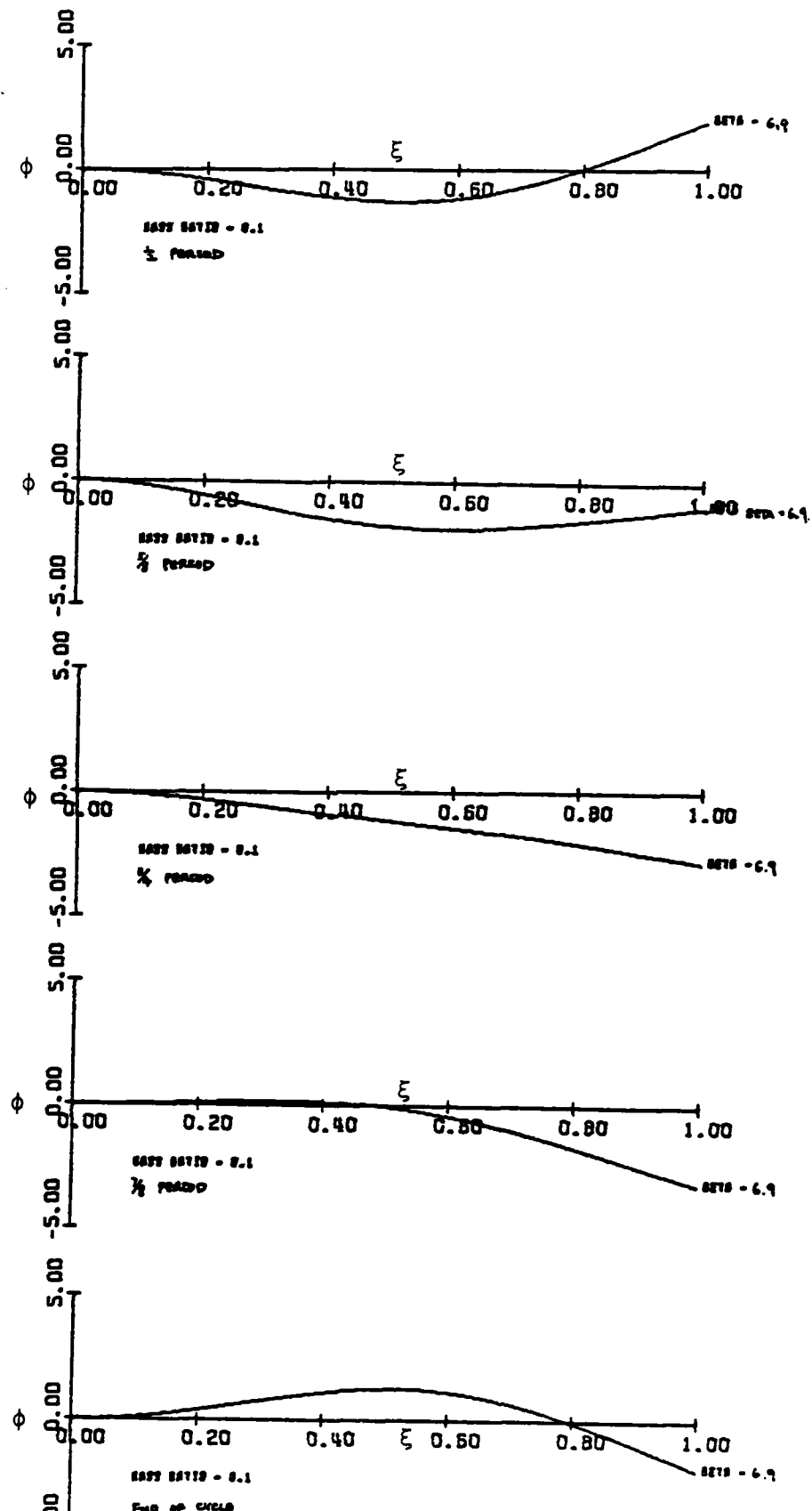


Figure 13. Tube Deformation Shapes at Various Times During Limit Cycle

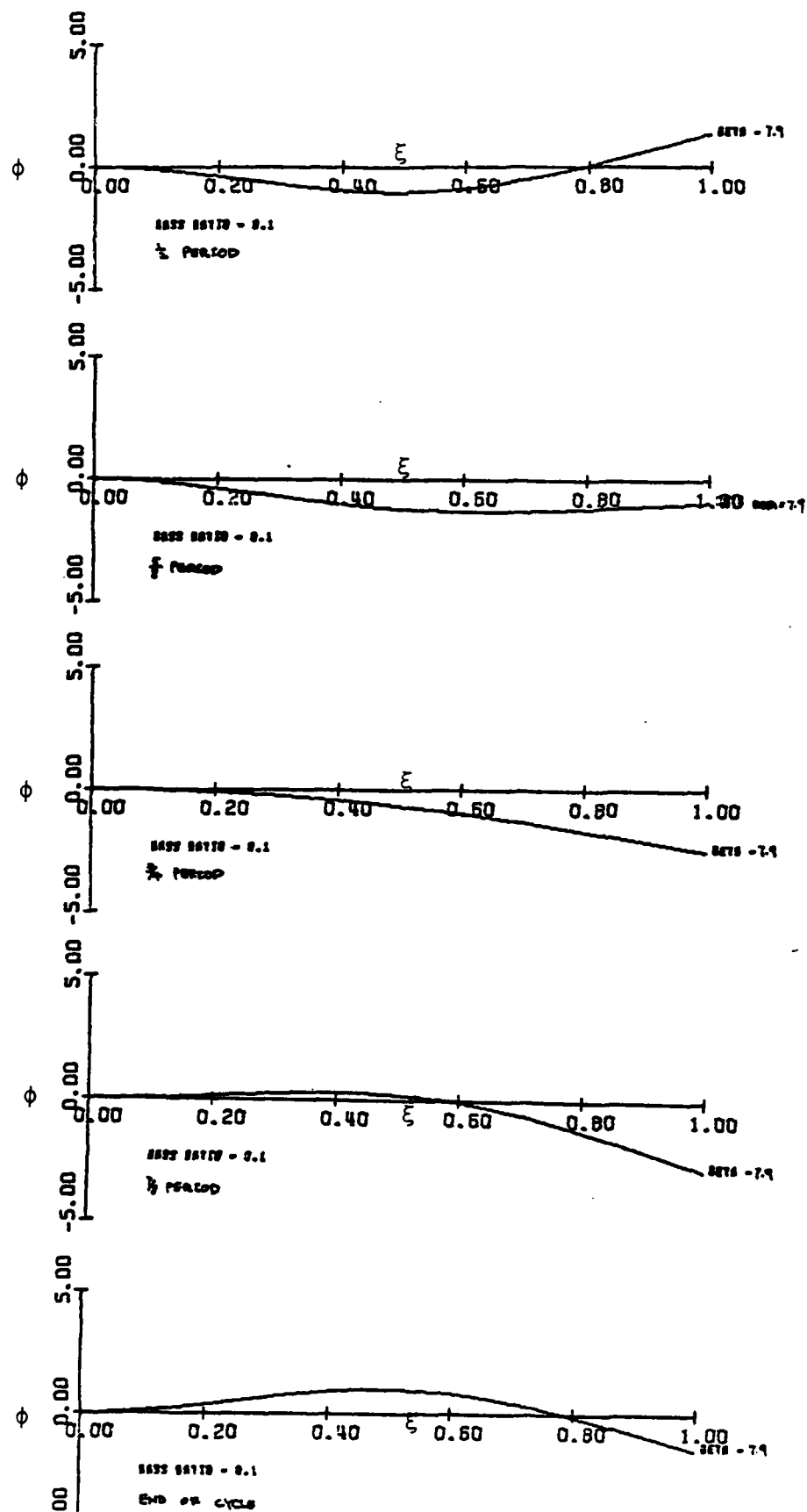


Figure 14. Tube Deformation Shapes at Various Times During Limit Cycle

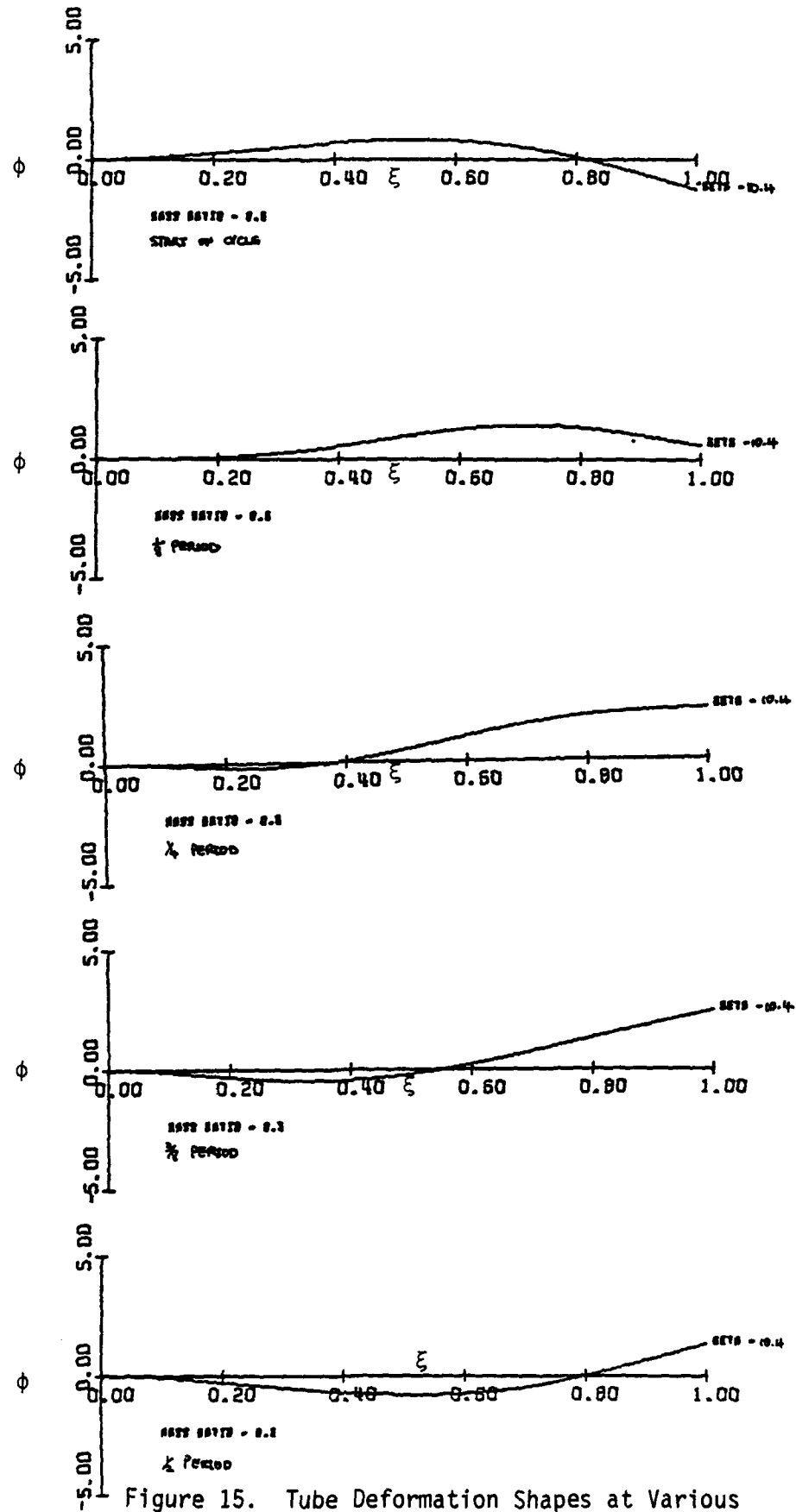


Figure 15. Tube Deformation Shapes at Various Times During Limit Cycle

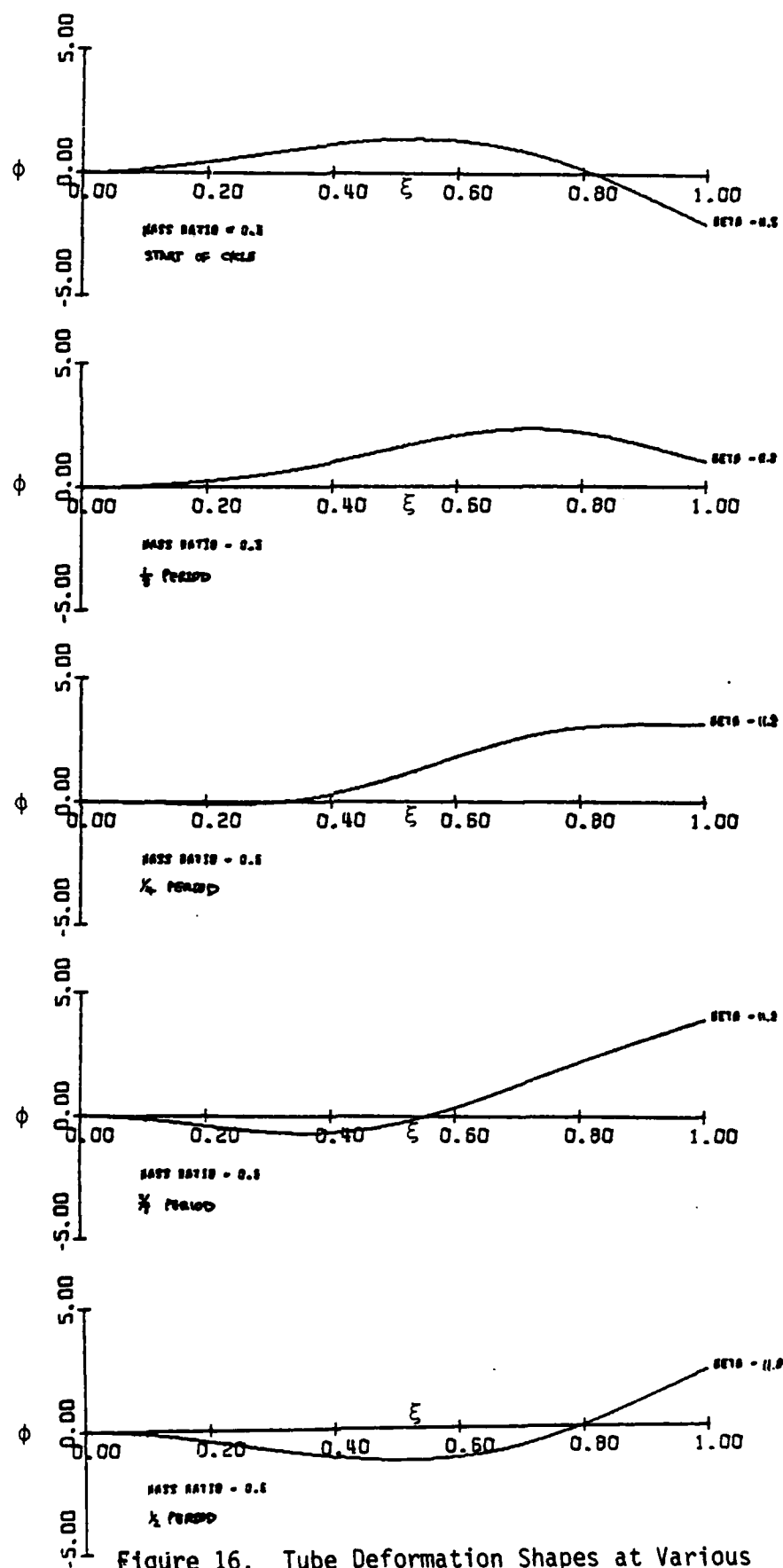


Figure 16. Tube Deformation Shapes at Various Times During Limit Cycle

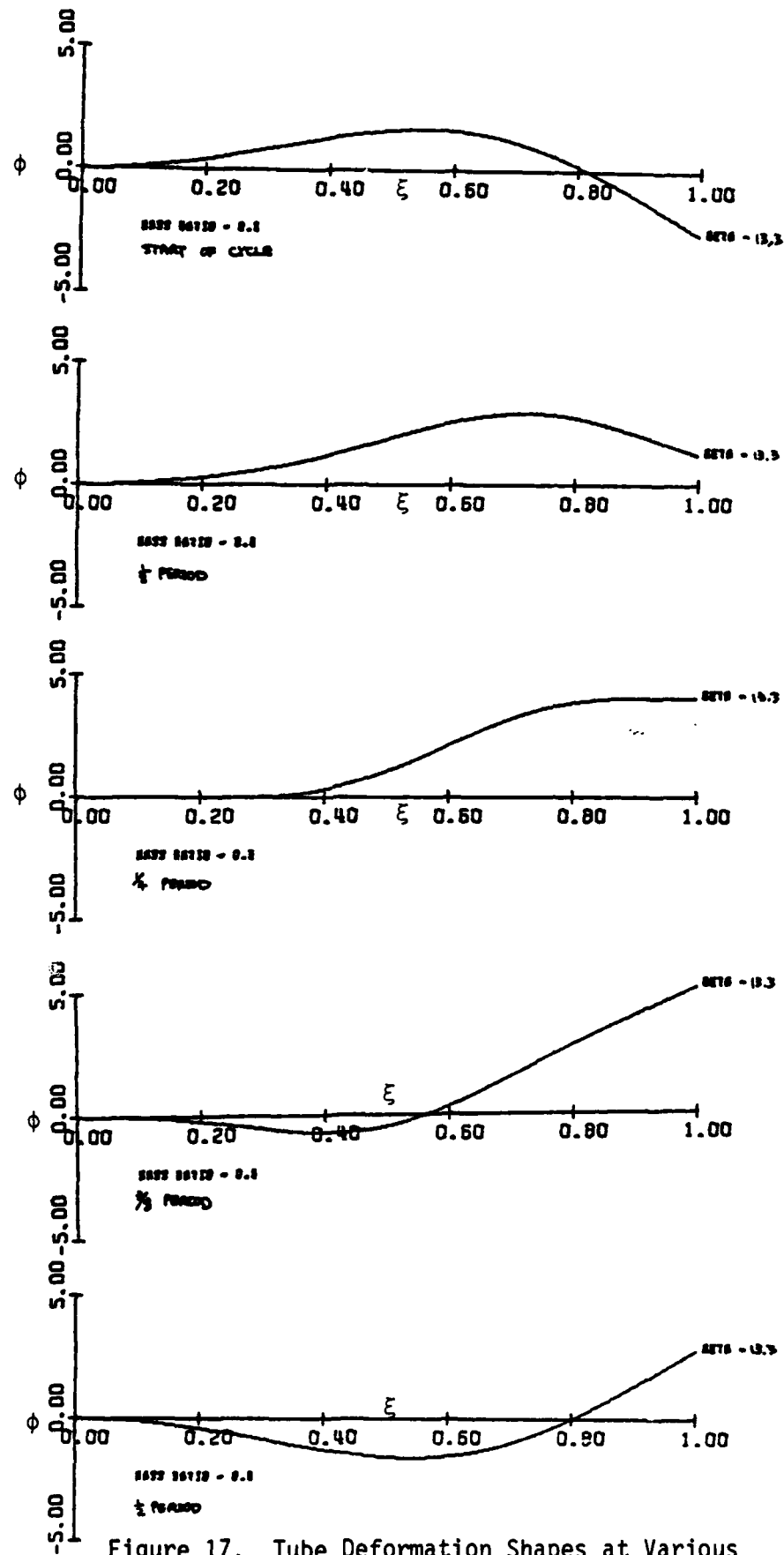


Figure 17. Tube Deformation Shapes at Various Times During Limit Cycle

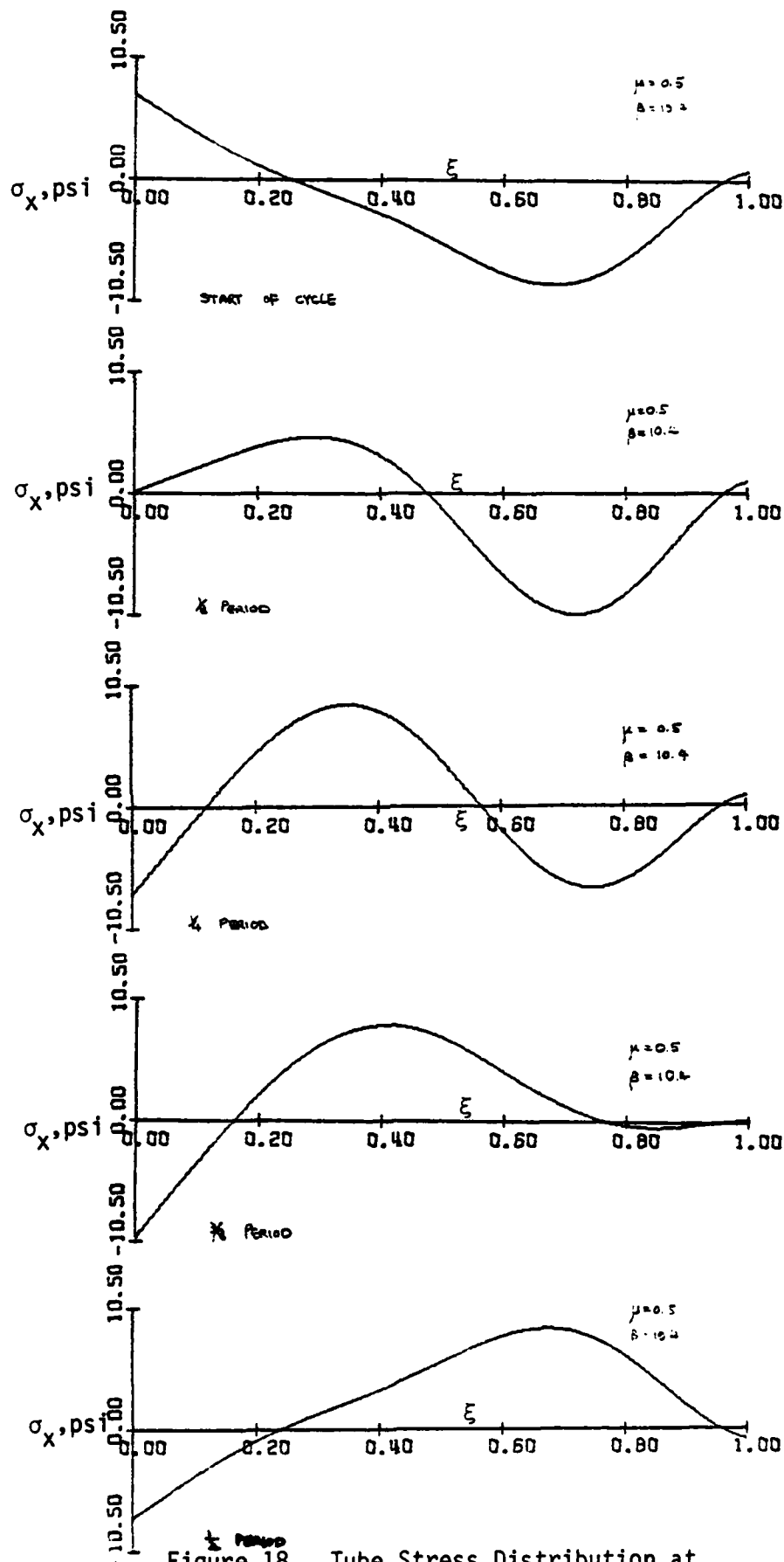


Figure 18. Tube Stress Distribution at Various Times During Limit Cycle

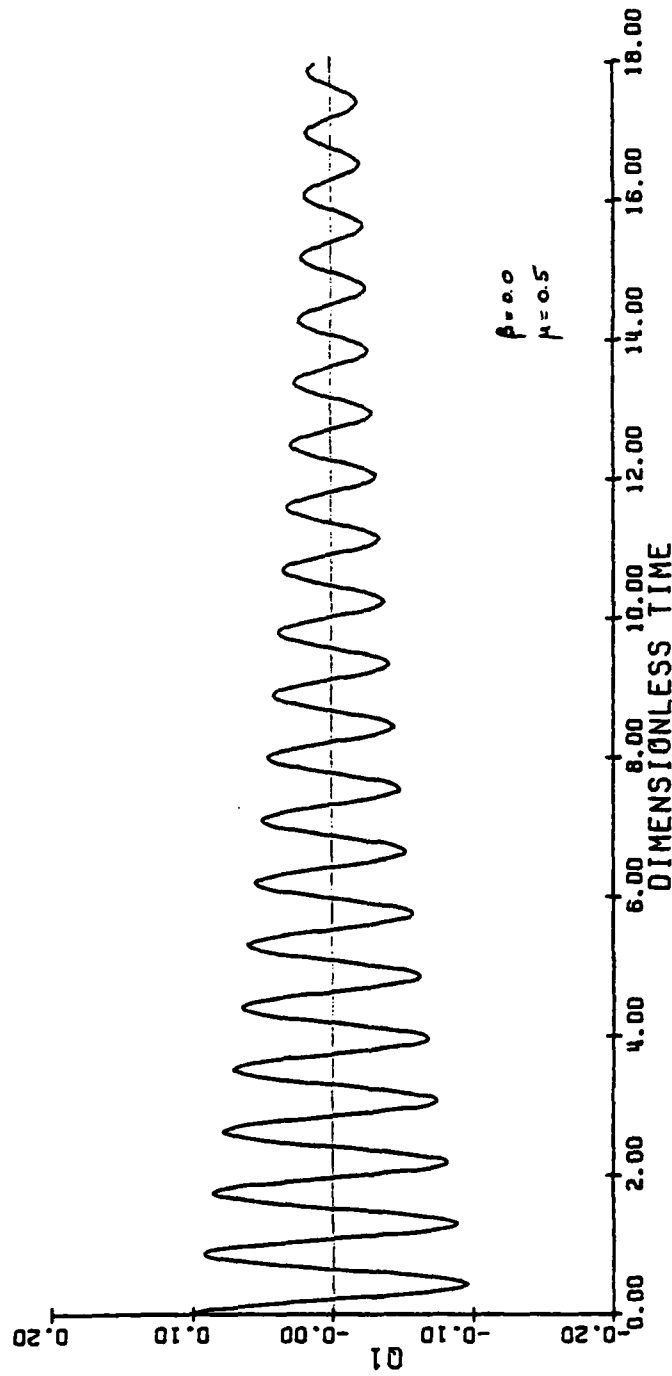


Figure 19a. First Mode Time History of Tube Motion
(Damped Vibration)

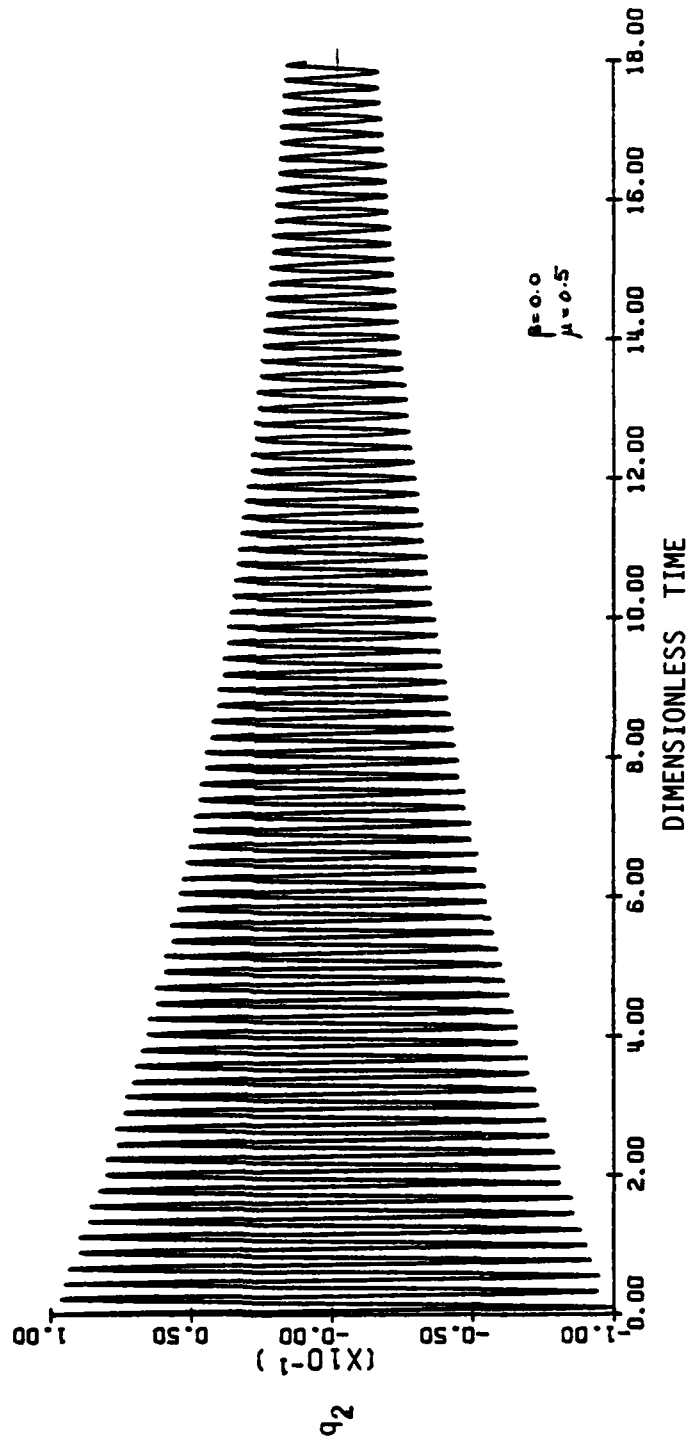


Figure 19b. Second Mode Time History of Tube Motion
(Damped Vibrations)

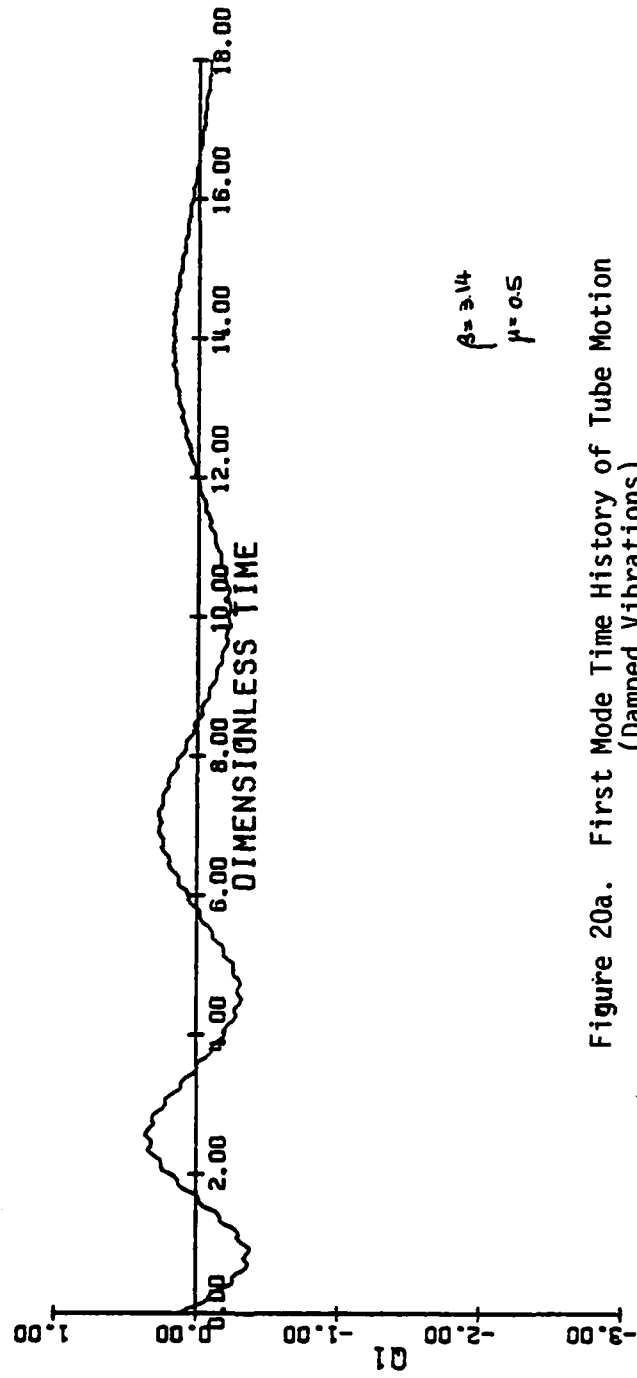


Figure 20a. First Mode Time History of Tube Motion
(Damped Vibrations)



Figure 20b. Second Mode Time History of Tube Motion
(Damped Vibrations)

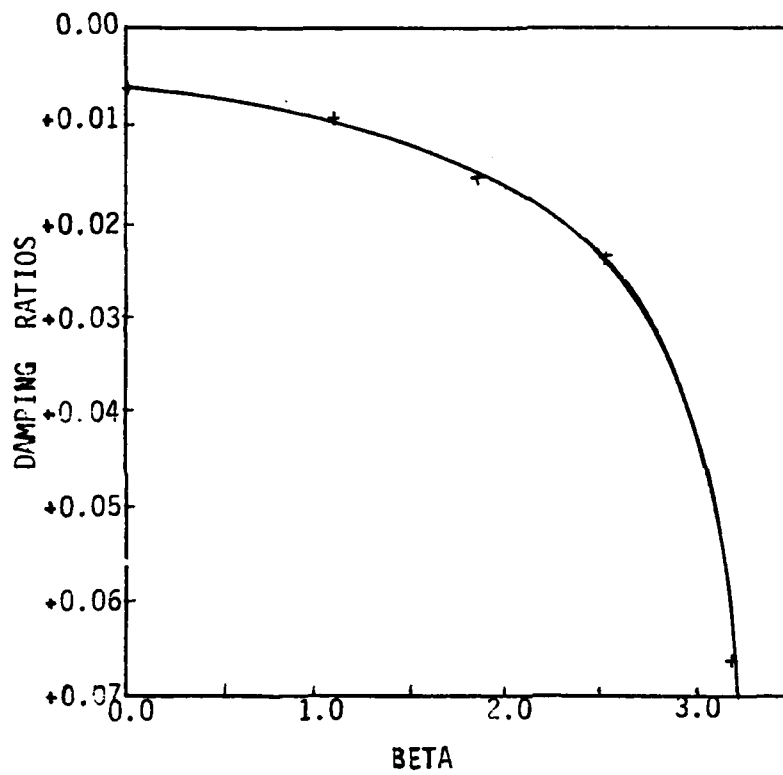


Figure 21a. Effects of Beta on First Mode Damping Ratios ($\mu = 0.1$)

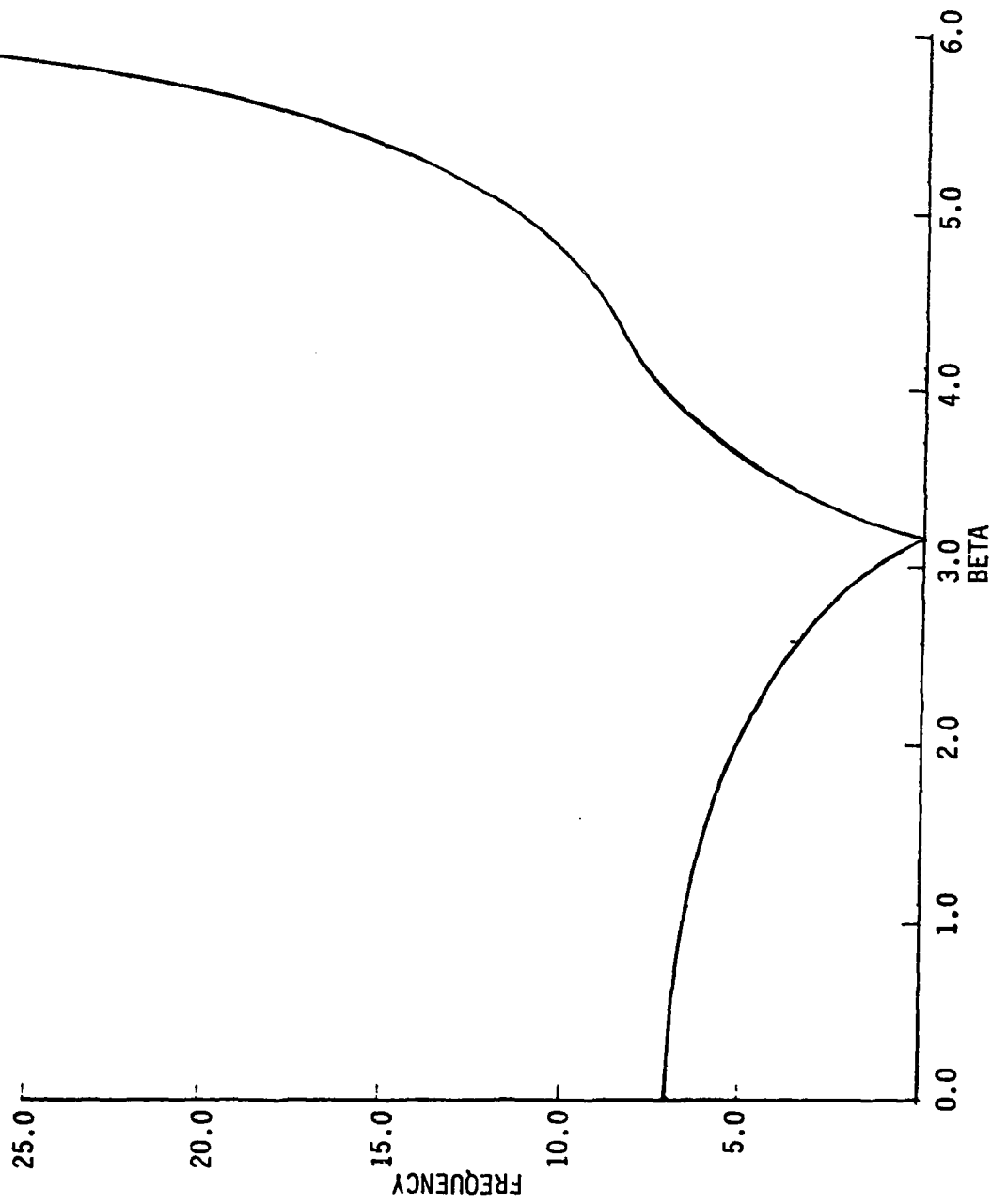


Figure 21b. Effects of Beta on First Mode Frequencies
($\mu = 0.1$)

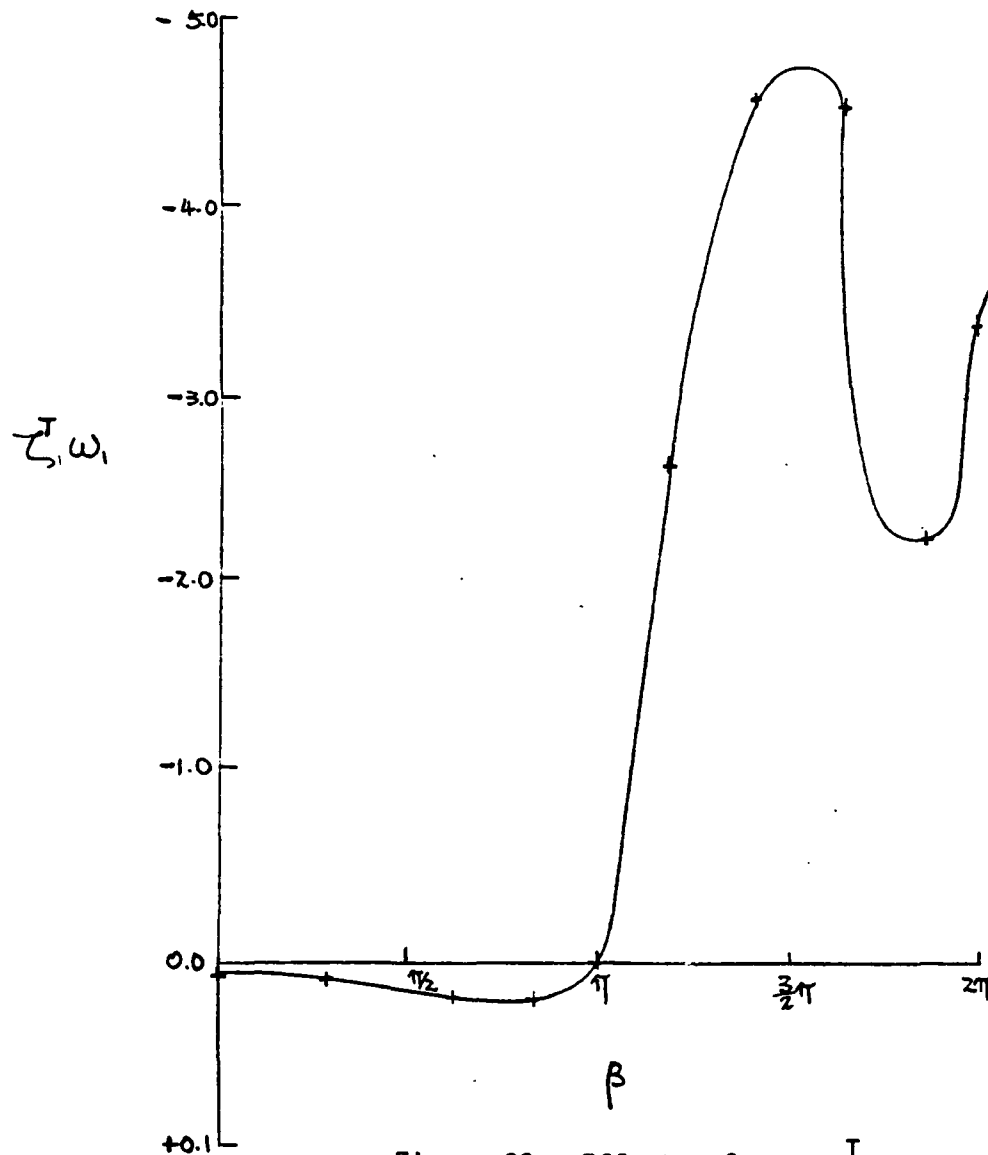


Figure 22. Effects of β on $\zeta_1^T \omega_1$
 Note different scales for positive and
 negative $\zeta_1^T \omega_1$

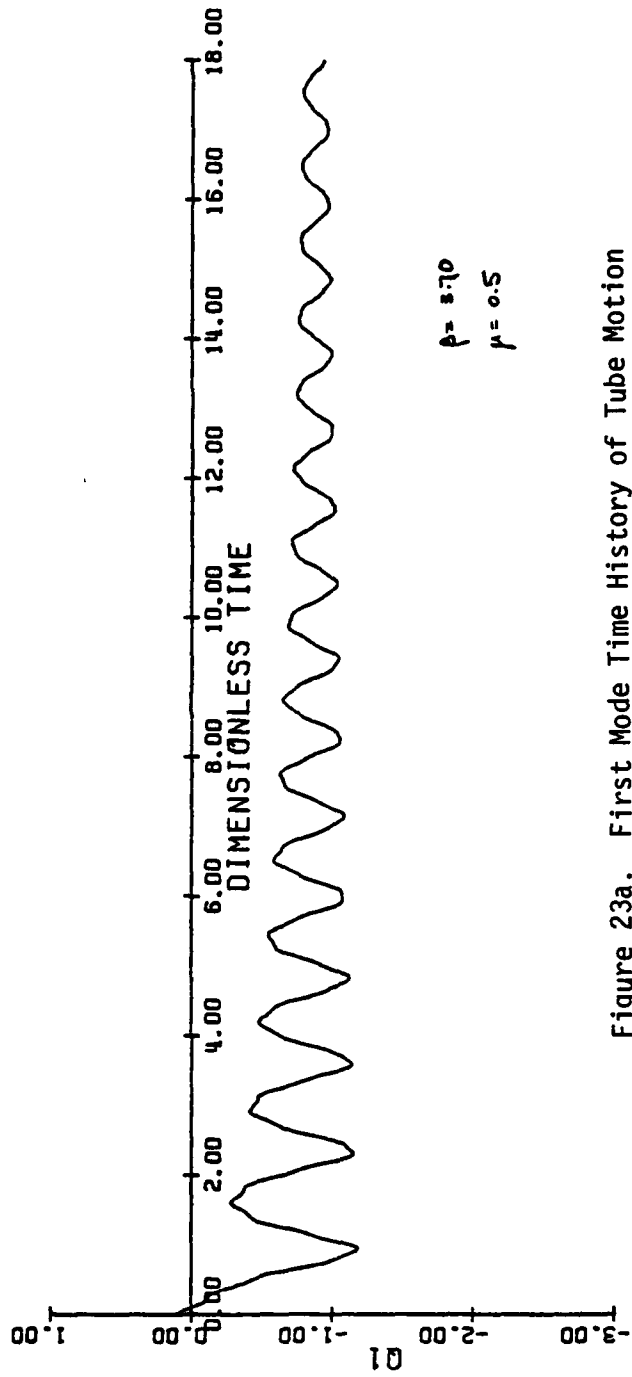


Figure 23a. First Mode Time History of Tube Motion
(Divergence)

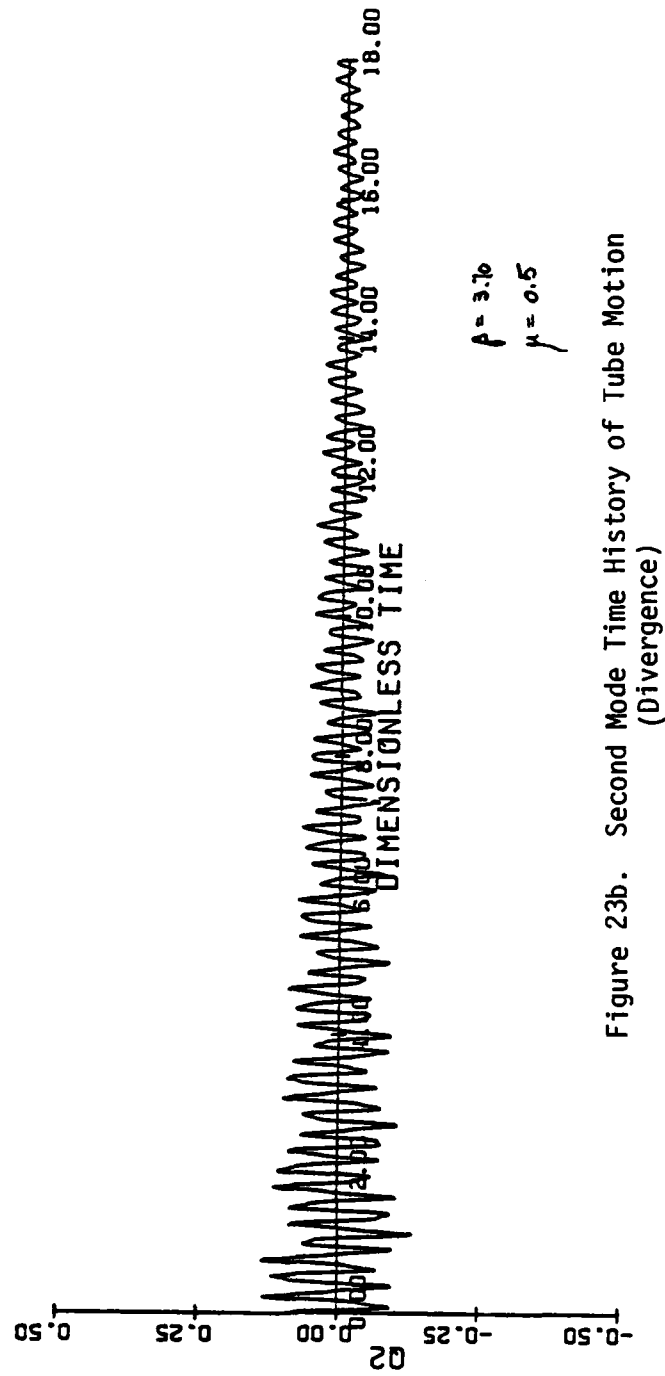


Figure 23b. Second Mode Time History of Tube Motion
(Divergence)

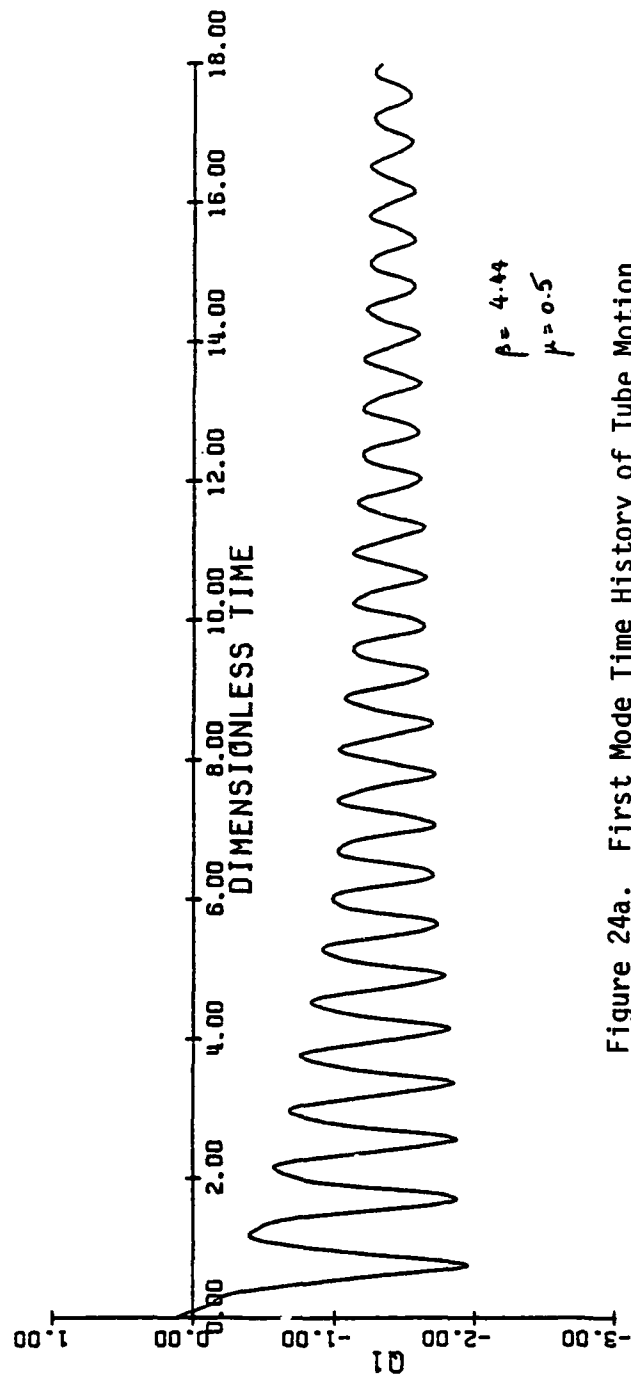


Figure 24a. First Mode Time History of Tube Motion
(Divergence)

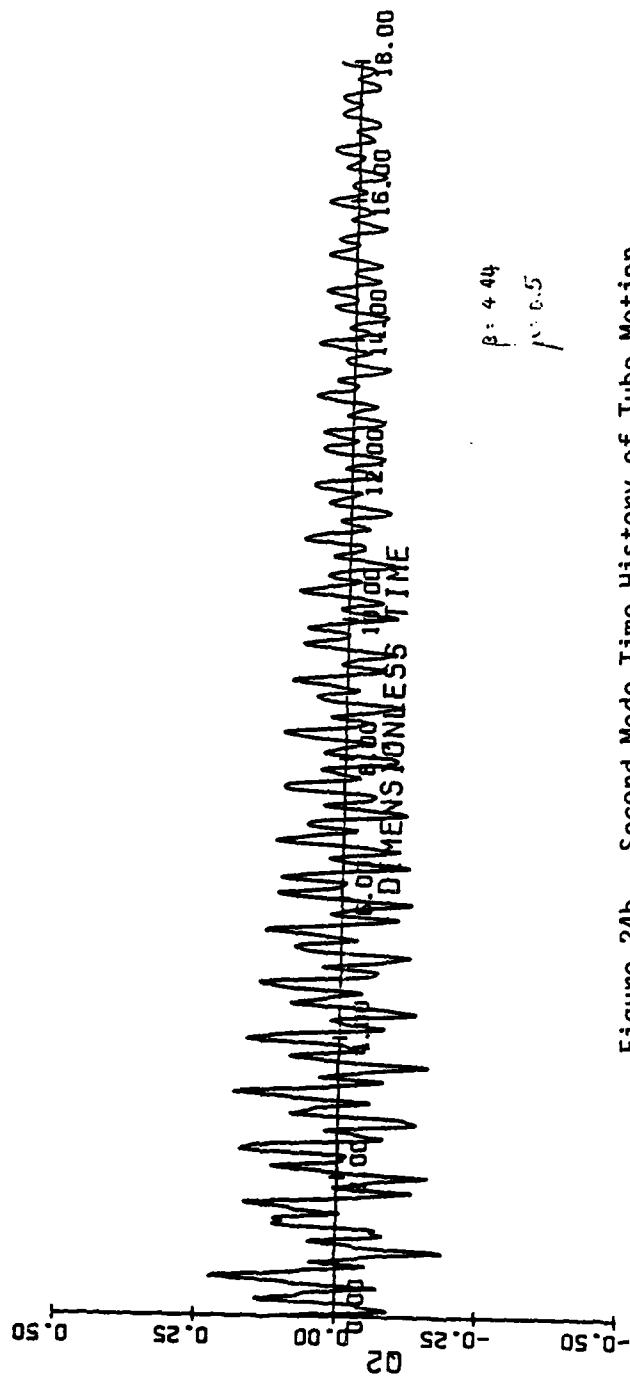


Figure 24b. Second Mode Time History of Tube Motion
(Divergence)

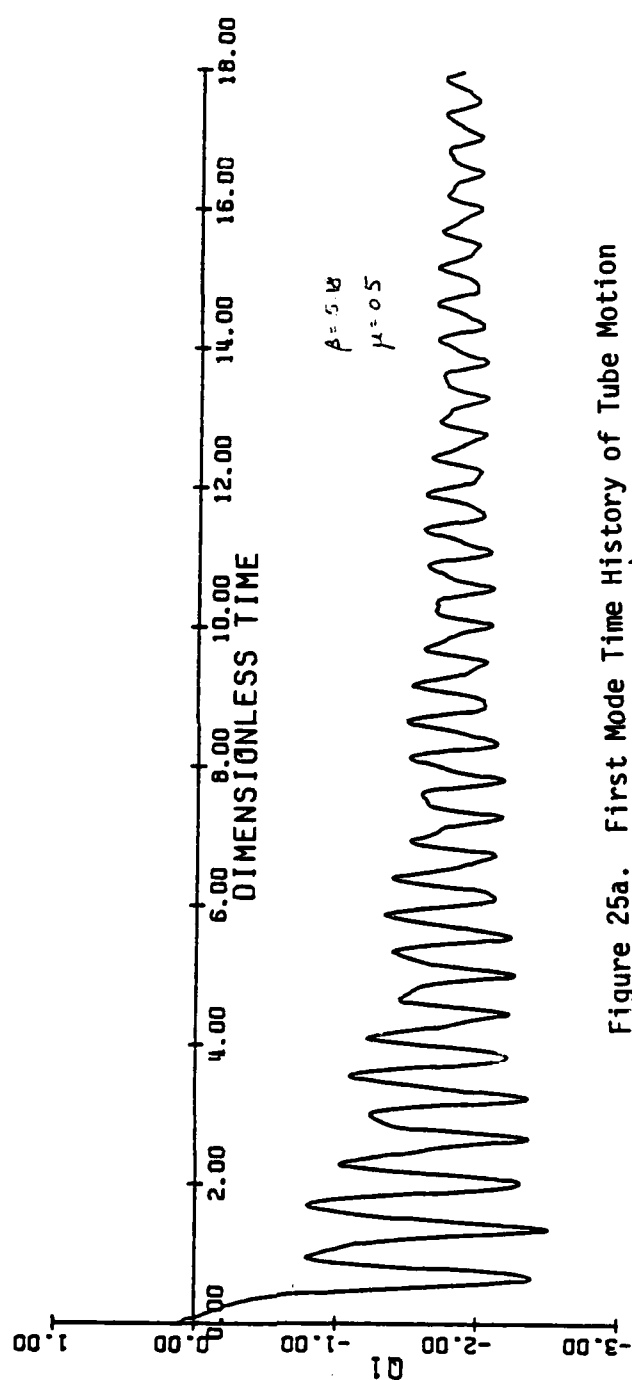
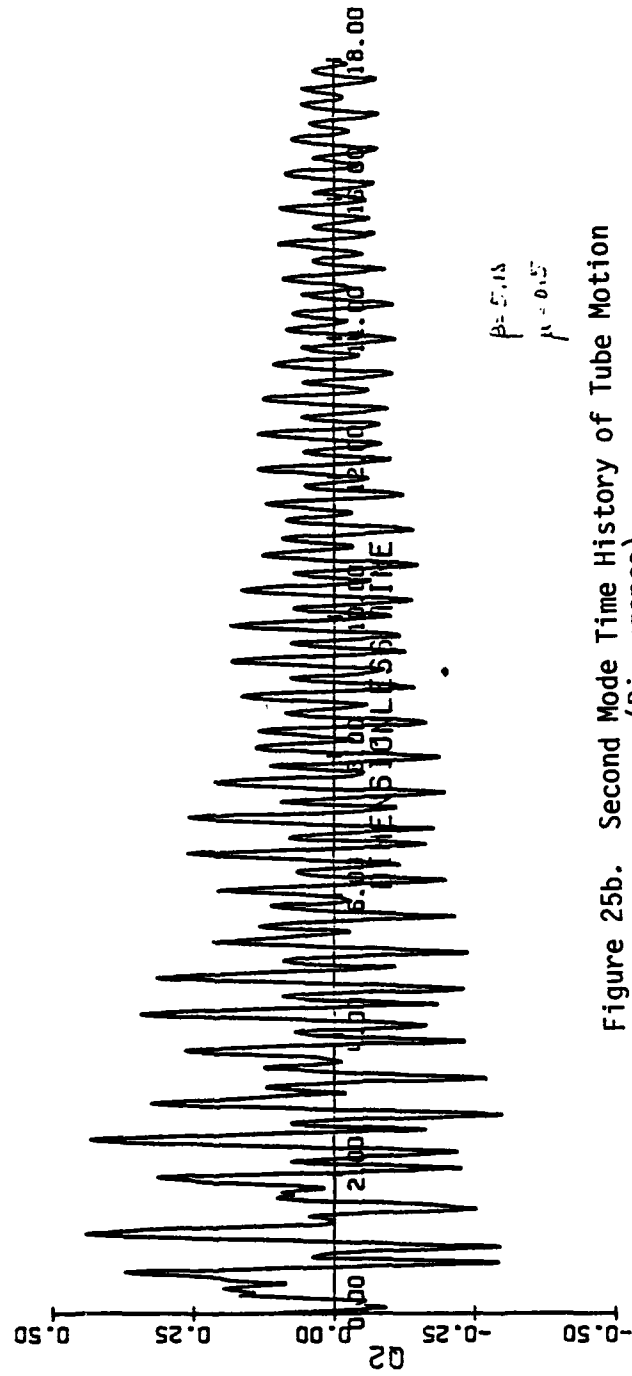


Figure 25a. First Mode Time History of Tube Motion
(Divergence)



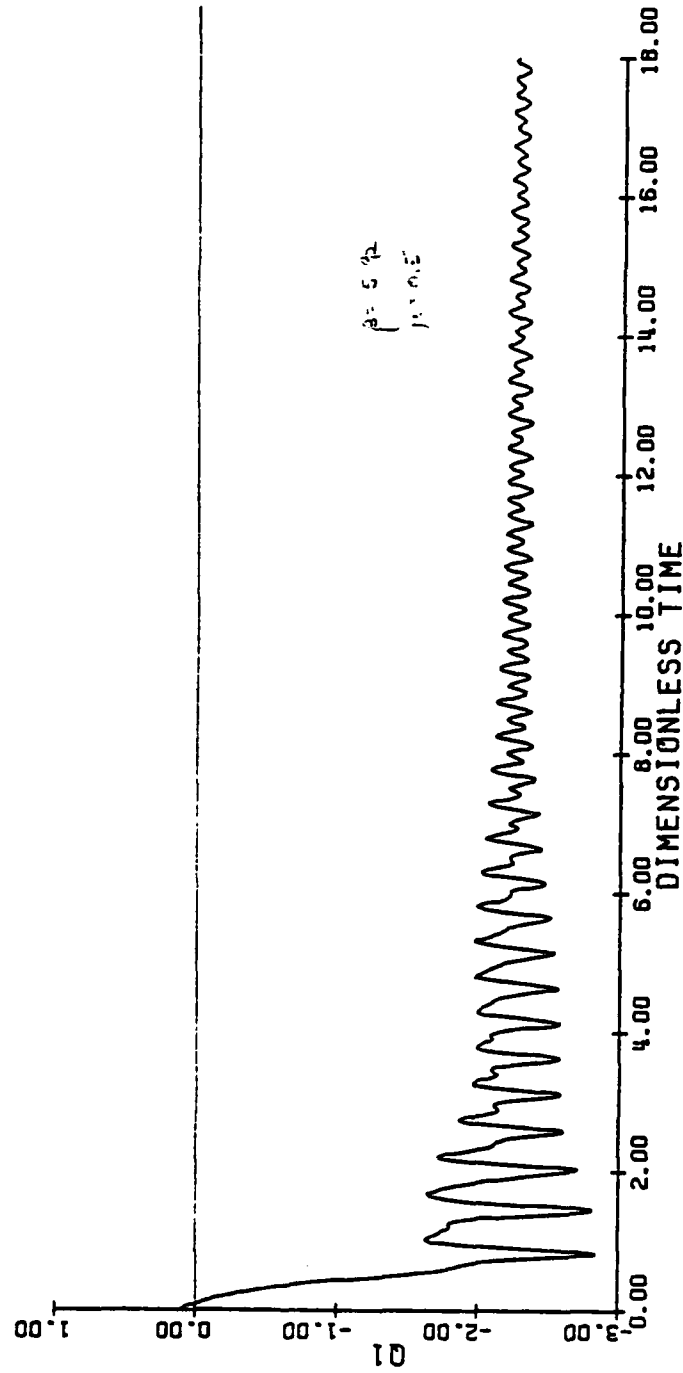


Figure 26a. First Mode Time History of Tube Motion
(Divergence)

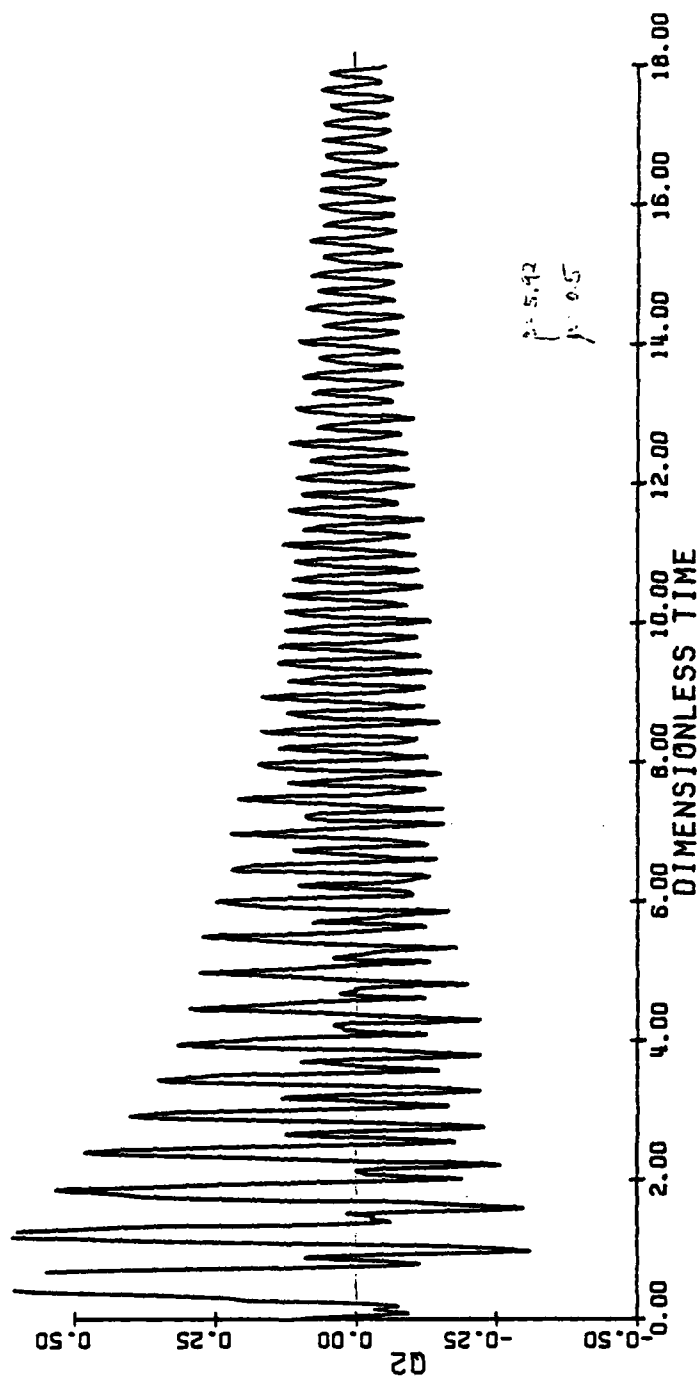


Figure 26b. Second Mode Time History of Tube Motion
(Divergence)

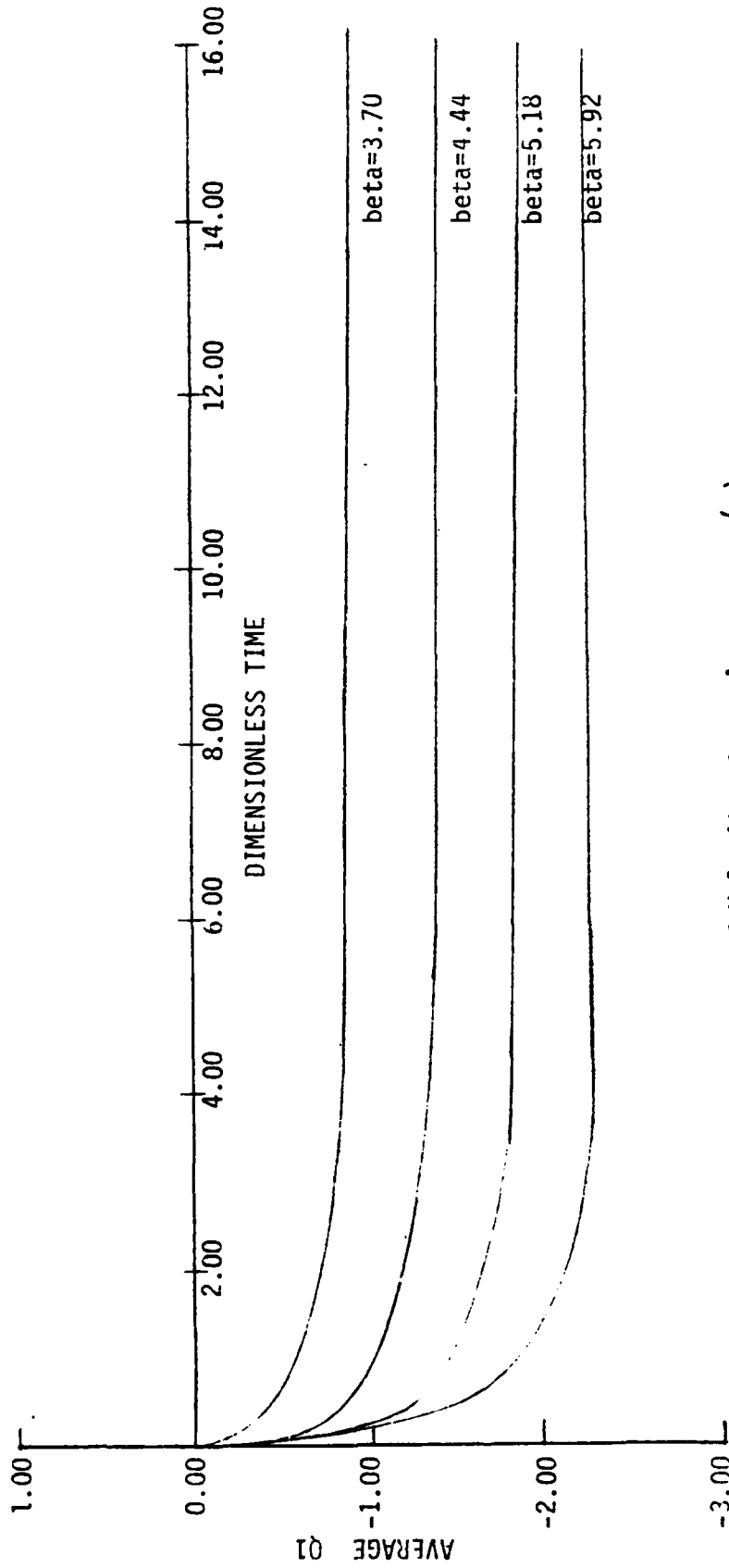


Figure 27. Influence of Velocity, β , on Average $q_1(\tau)$

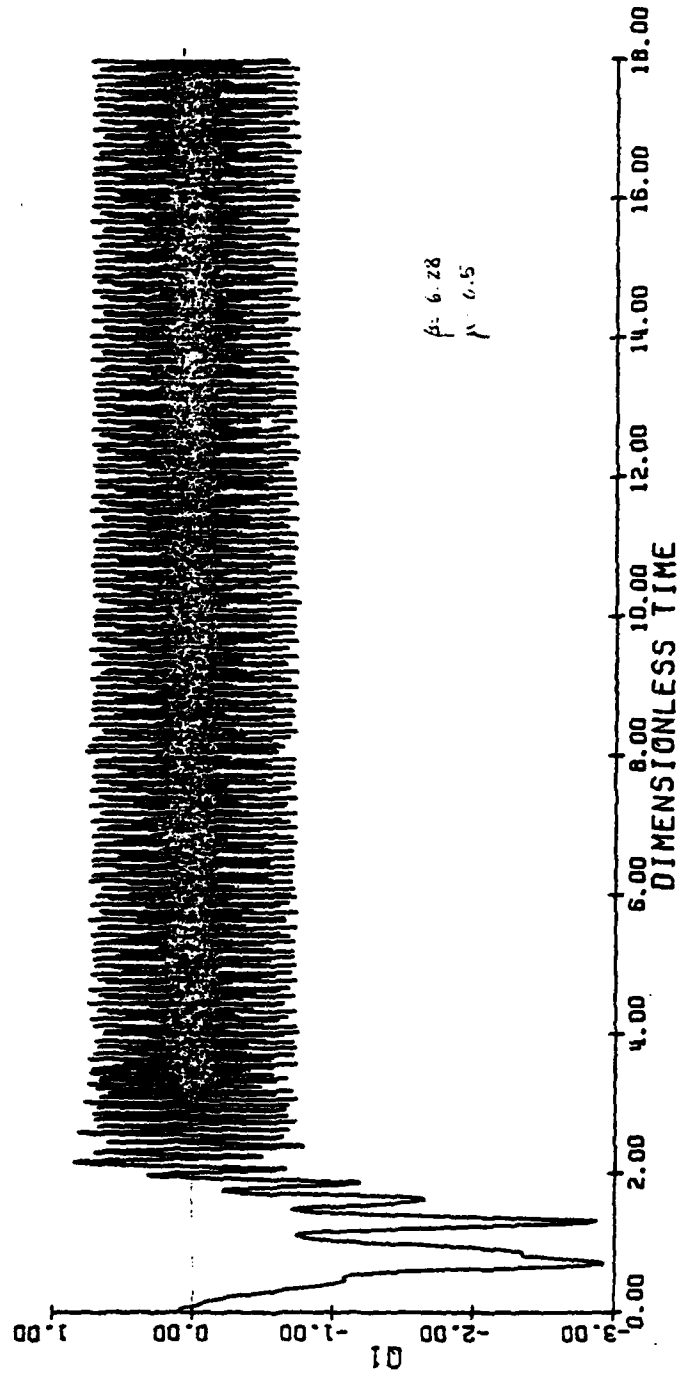
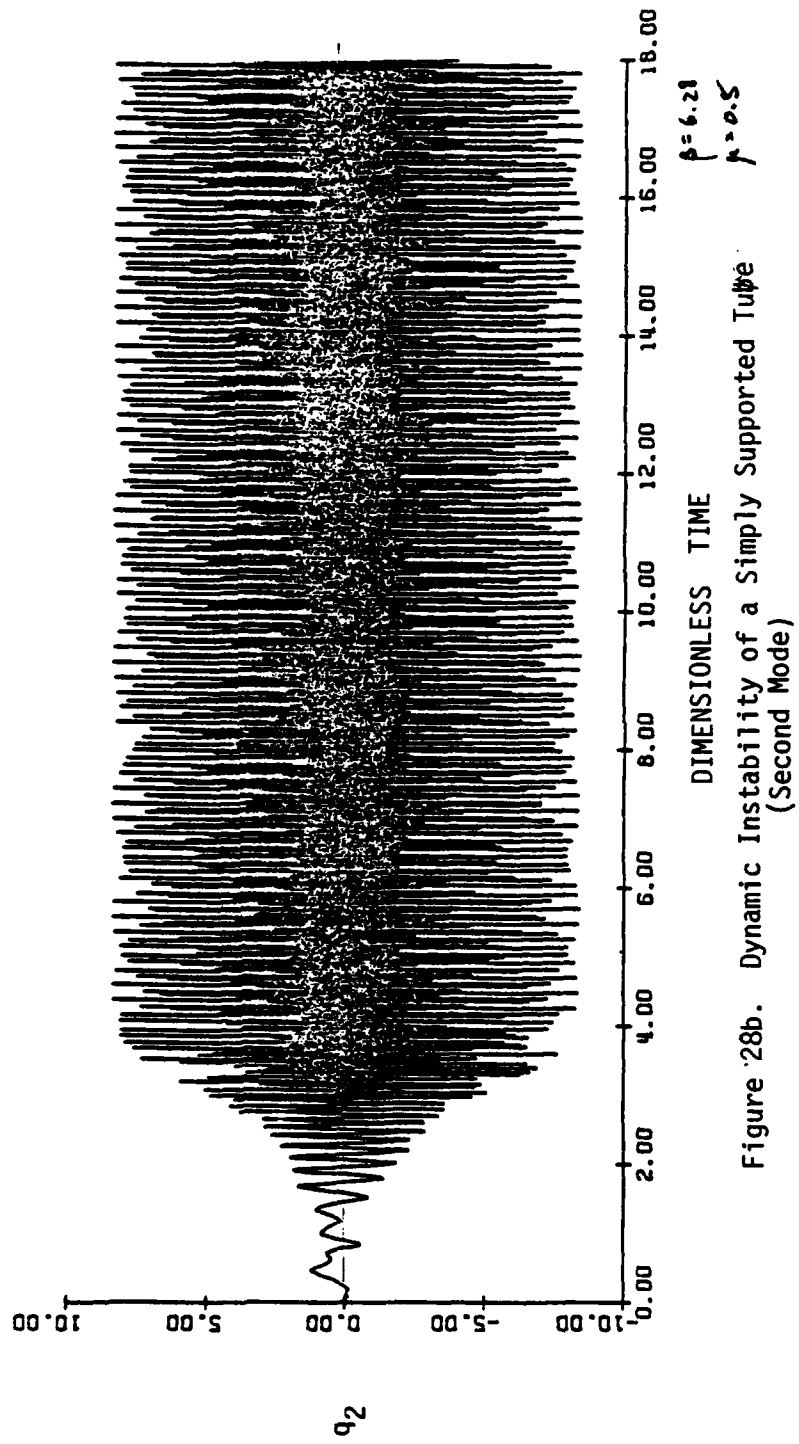


Figure 28a. Dynamic Instability of a Simply Supported Tube
(First Mode)



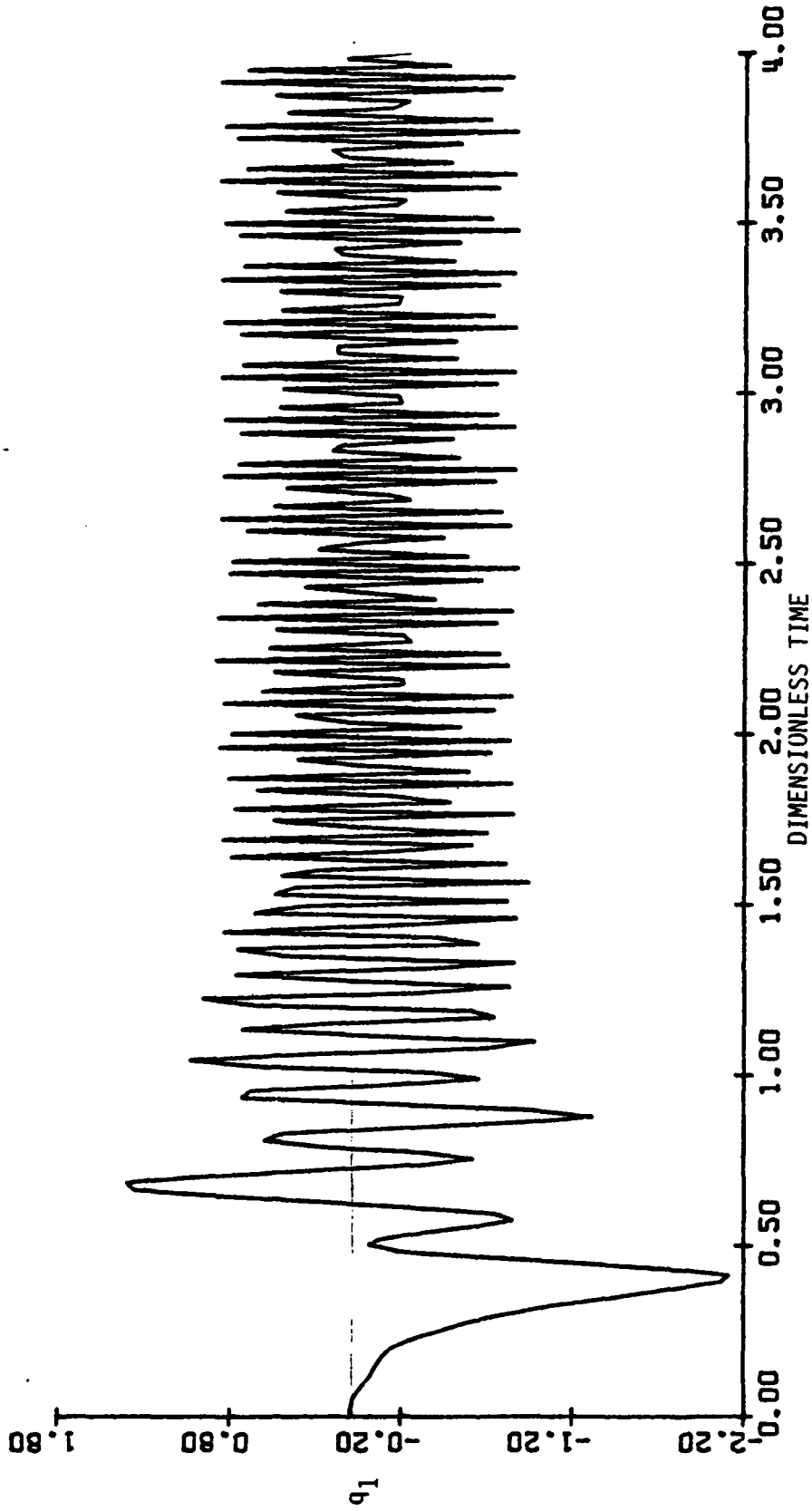


Figure 29a. First Mode Instability
($\mu = 0.5$, $\beta = 7.4$)

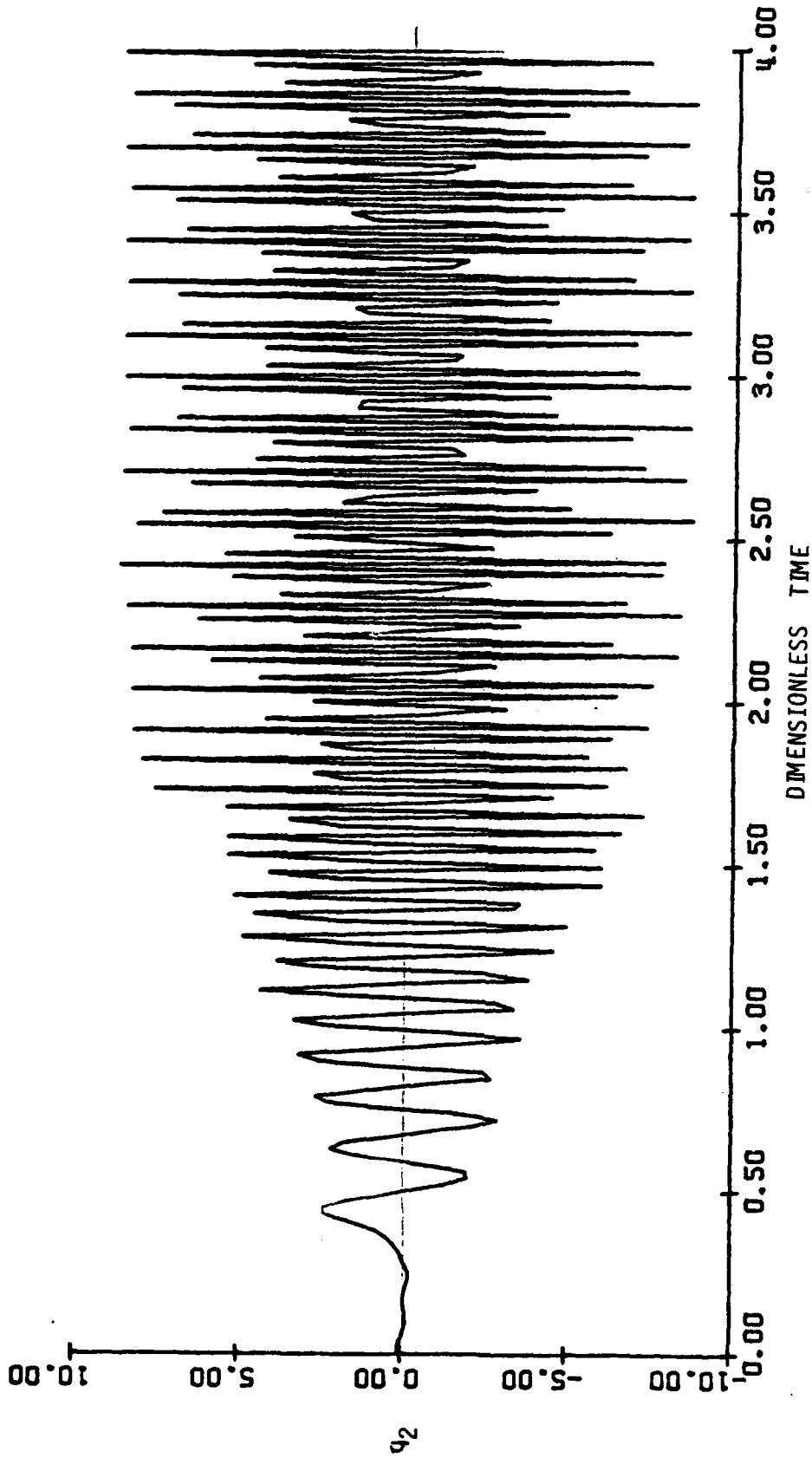


Figure 29b. Second Mode Instability
($\mu = 0.5$, $\beta = 7.4$)

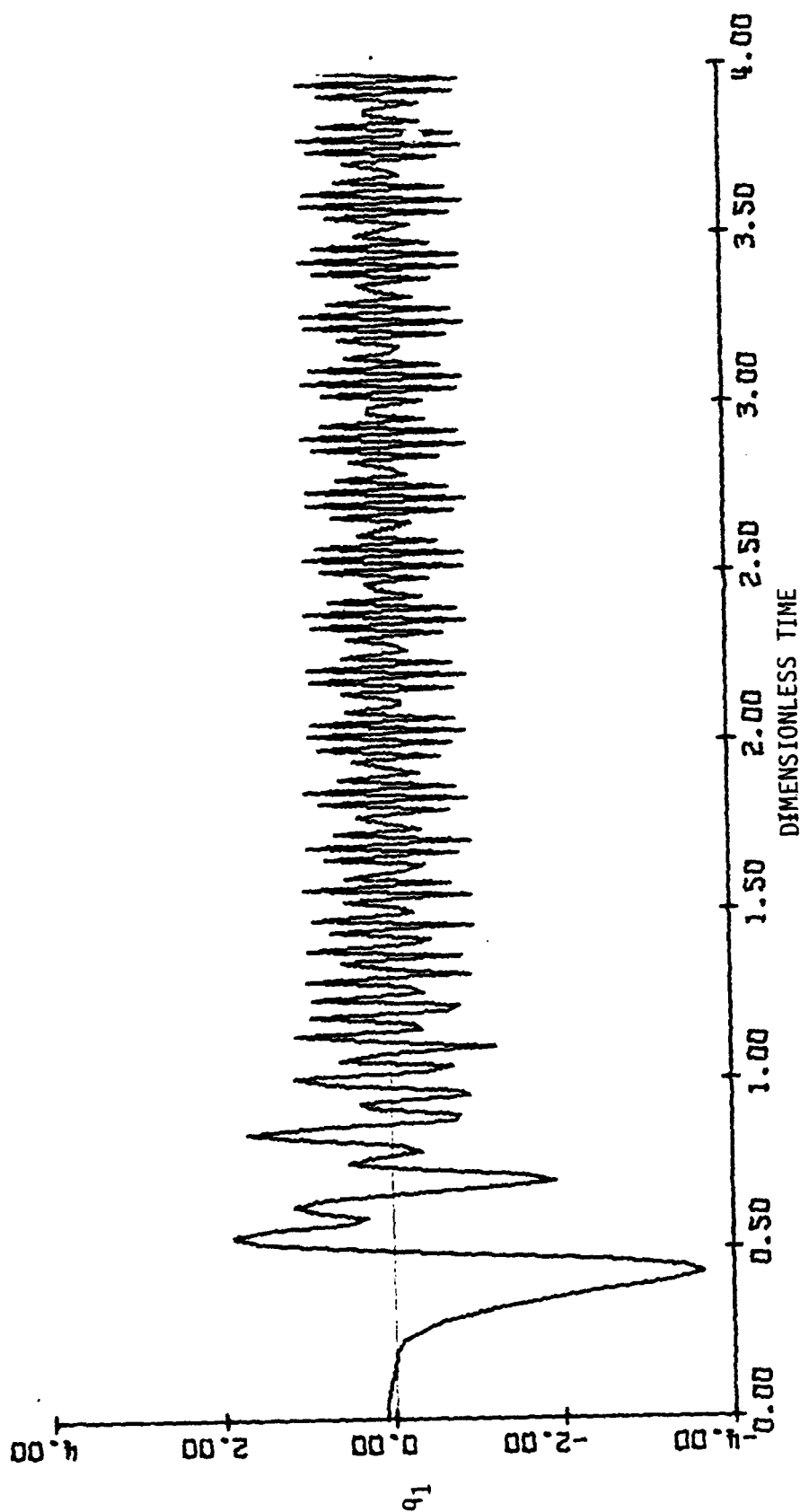


Figure 30a. First Mode Instability
($\mu = 0.5$, $\beta = 8.14$)

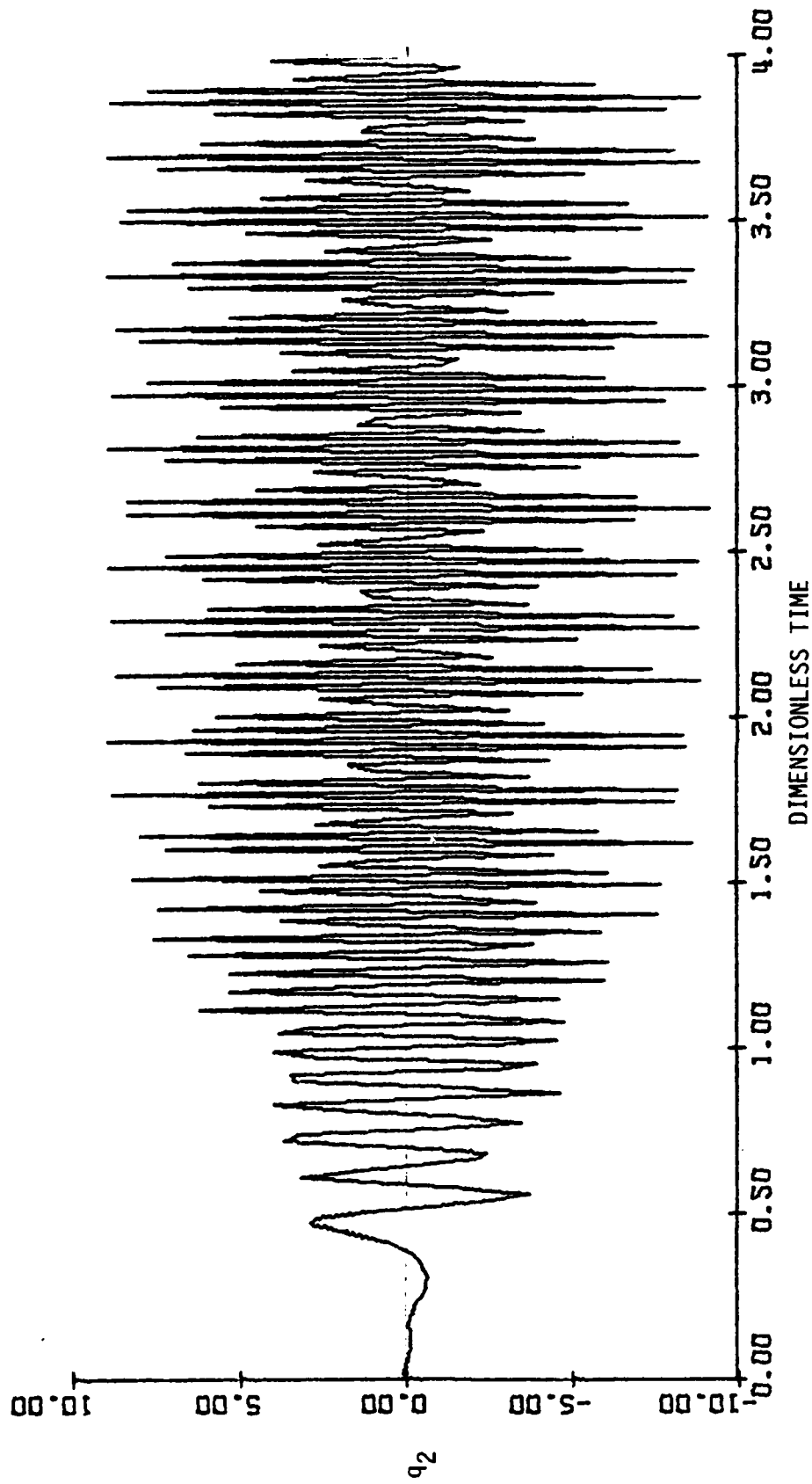


Figure 30b. Second Mode Instability
($\mu = 0.5$, $\beta = 8.14$)

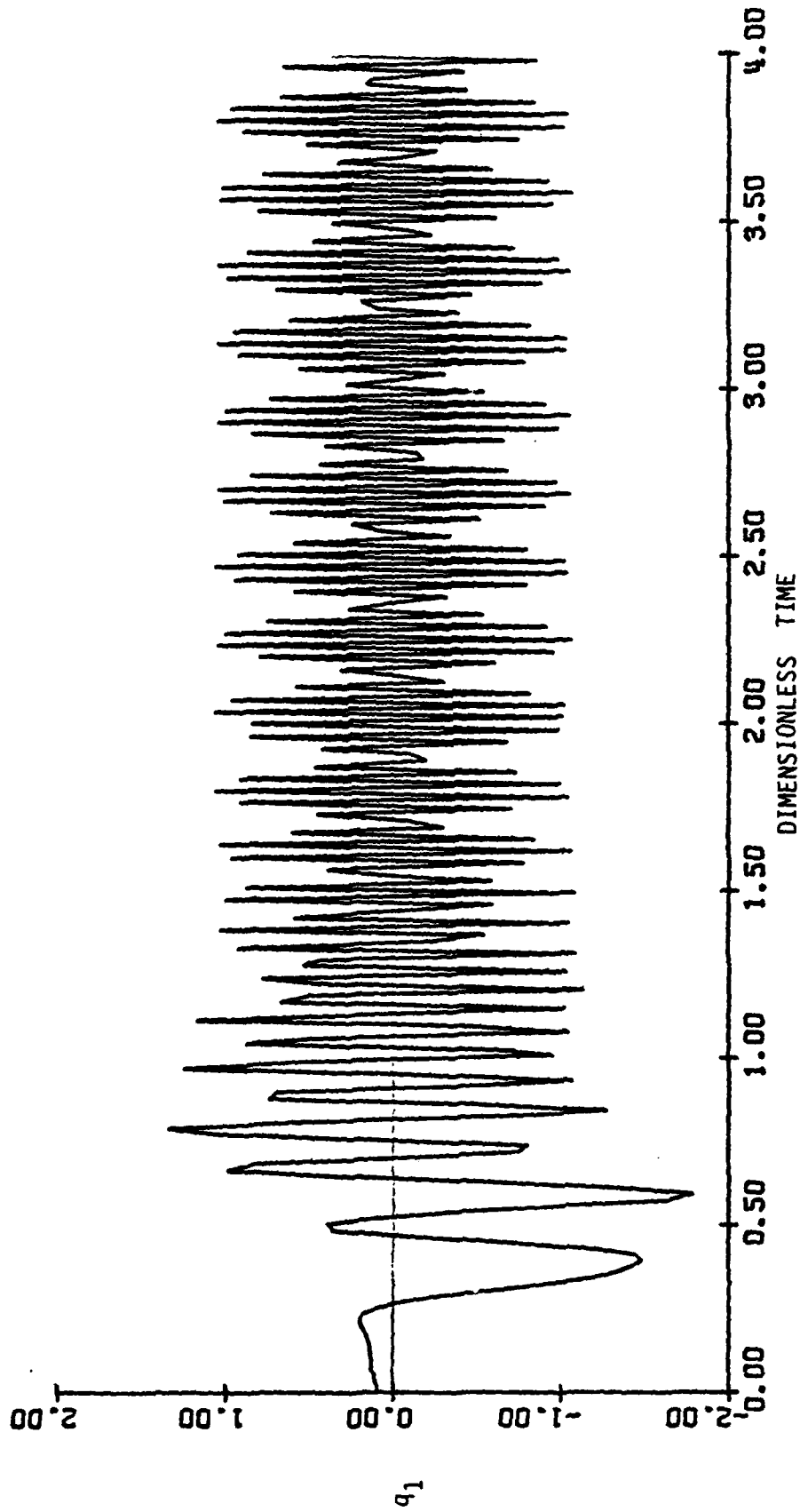


Figure 31a. First Mode Instability
($\mu = 0.5$, $\beta = 8.88$)

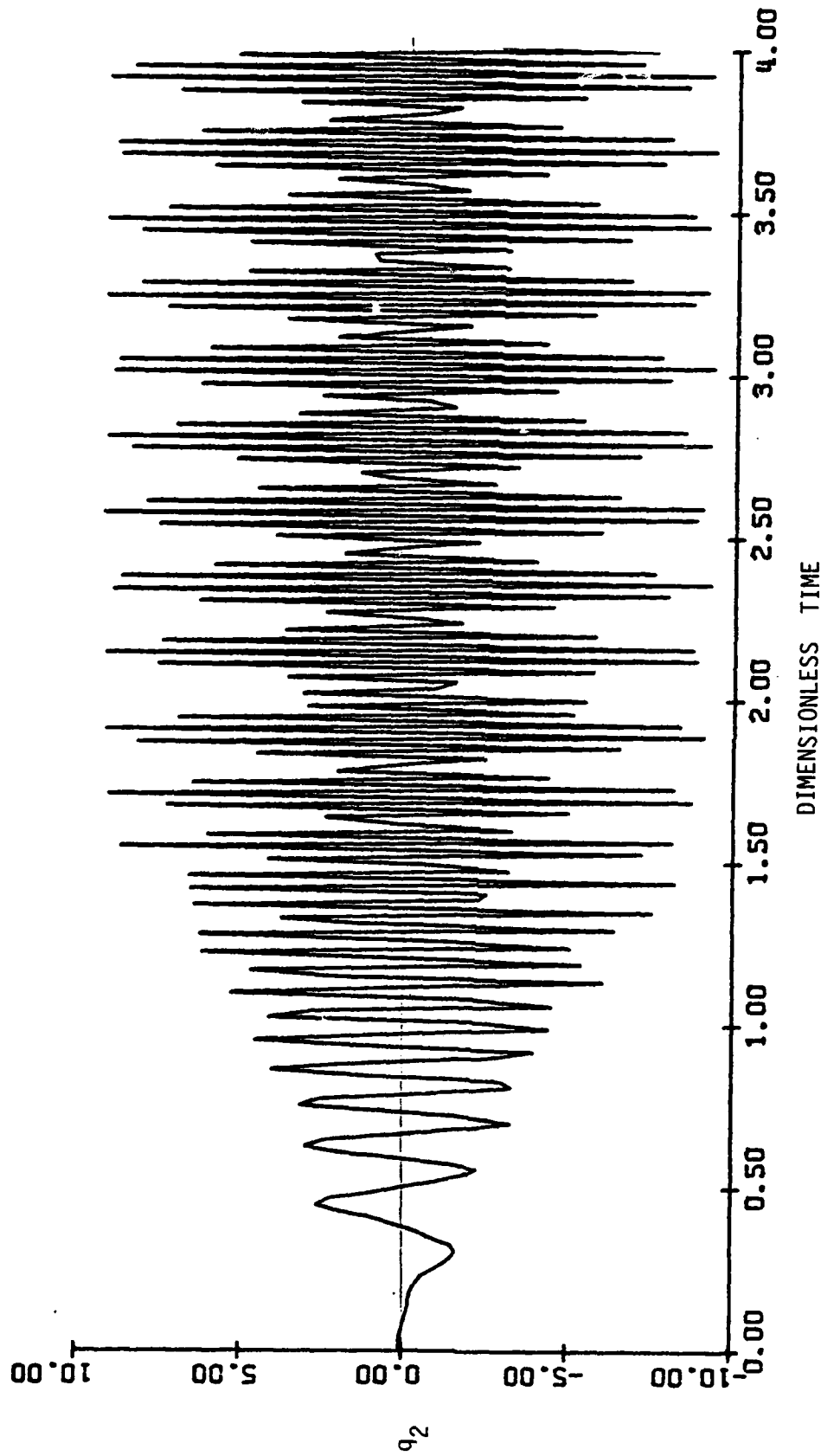


Figure 31b. Second Mode Instability
($\mu = 0.5$, $\beta = 8.88$)

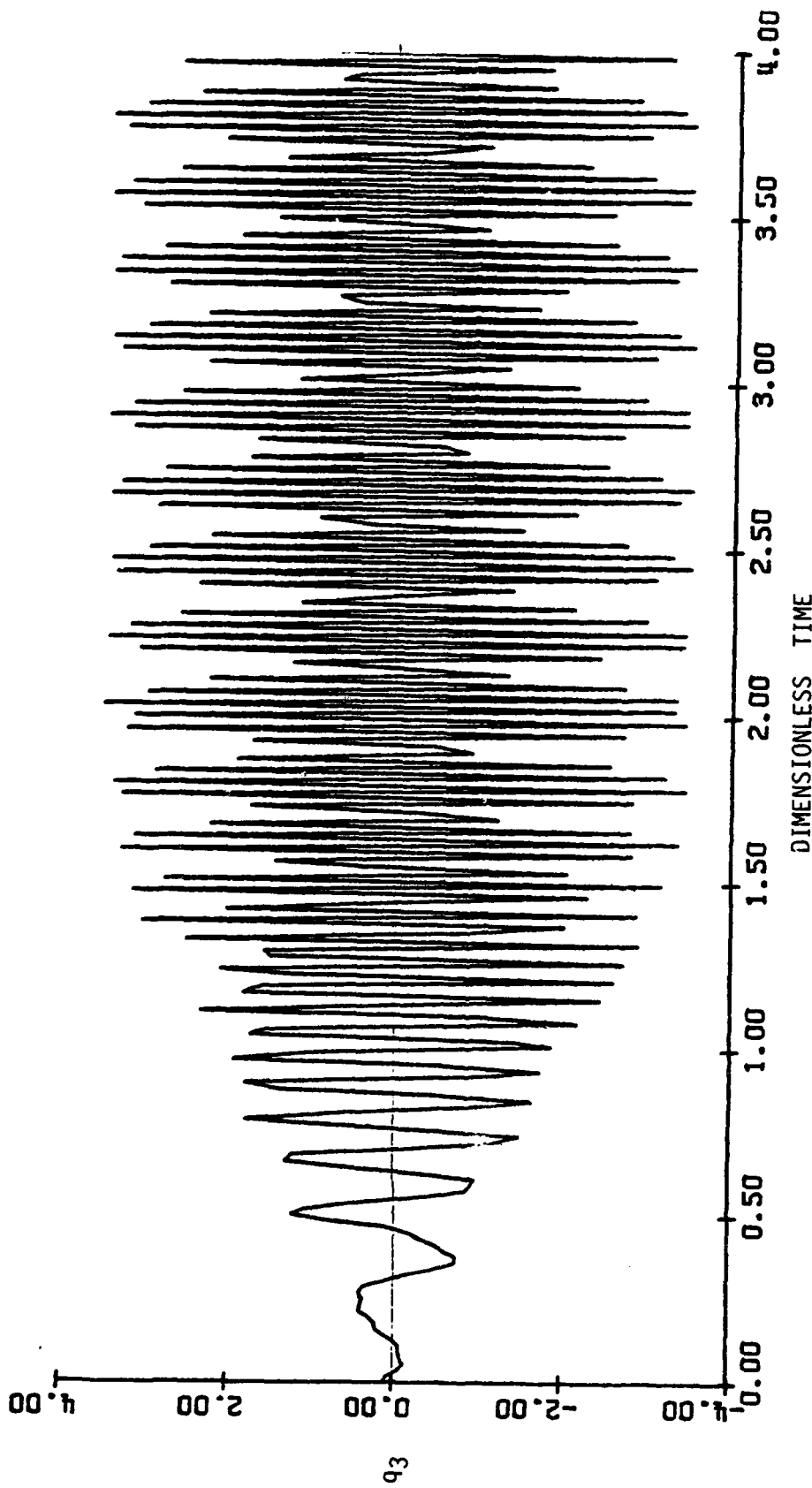


Figure 31c. Third Mode Instability
($\mu = 0.5$, $\beta = 8.88$)

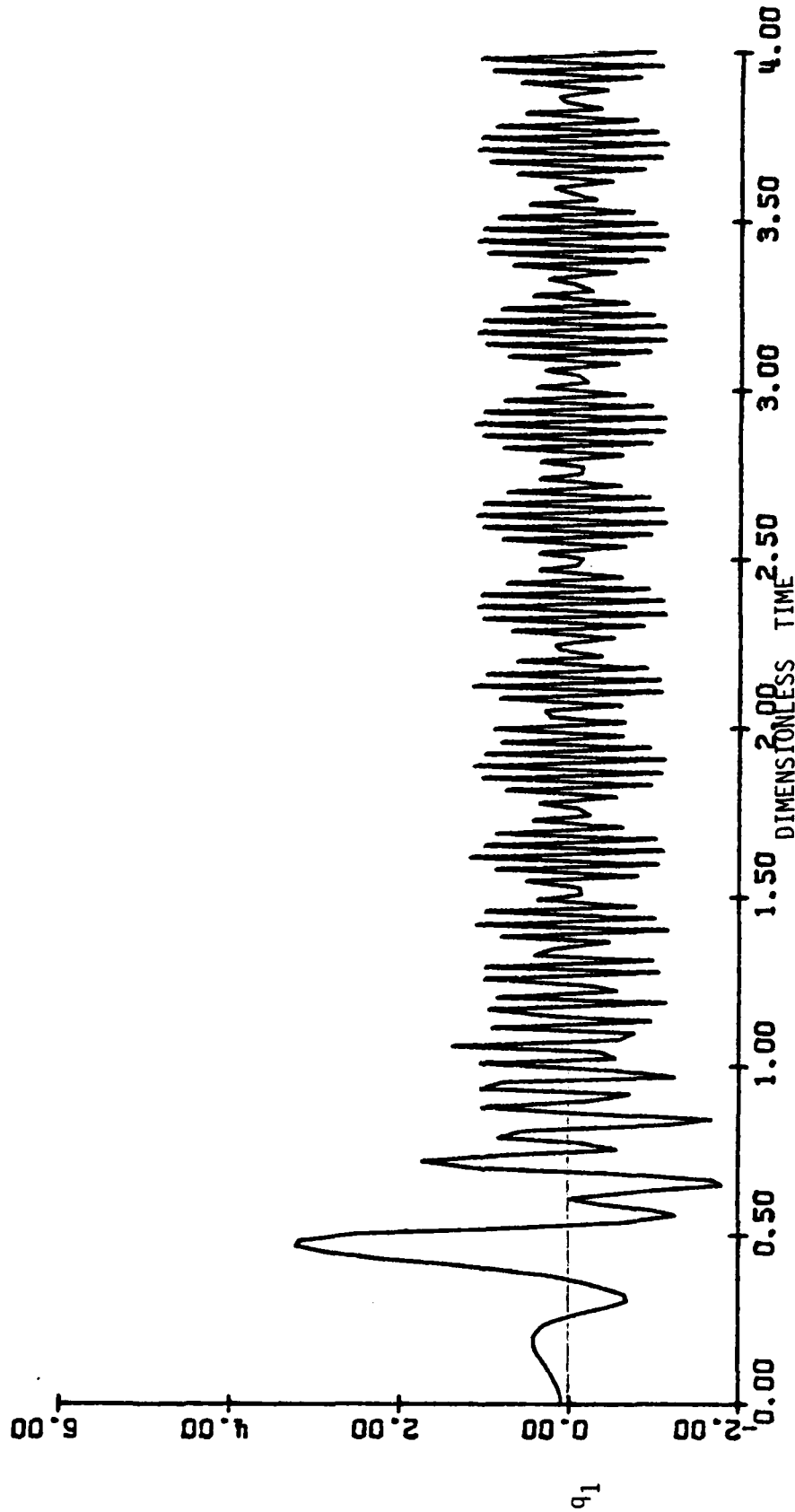


Figure 32a. First Mode Instability
($\mu = 0.5$, $\beta = 9.42$)

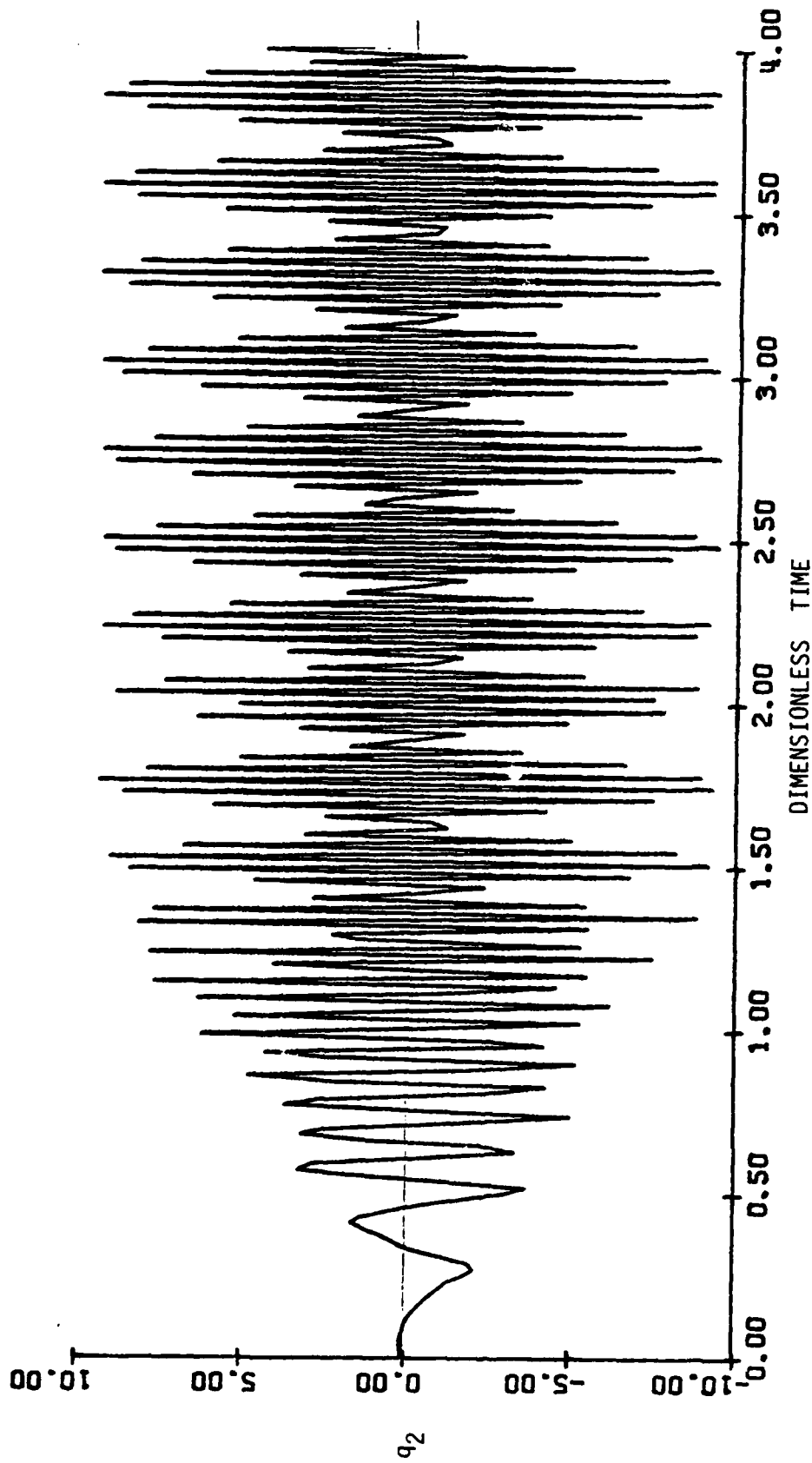


Figure 32b. Second Mode Instability
($\mu = 0.5$, $\beta = 9.42$)

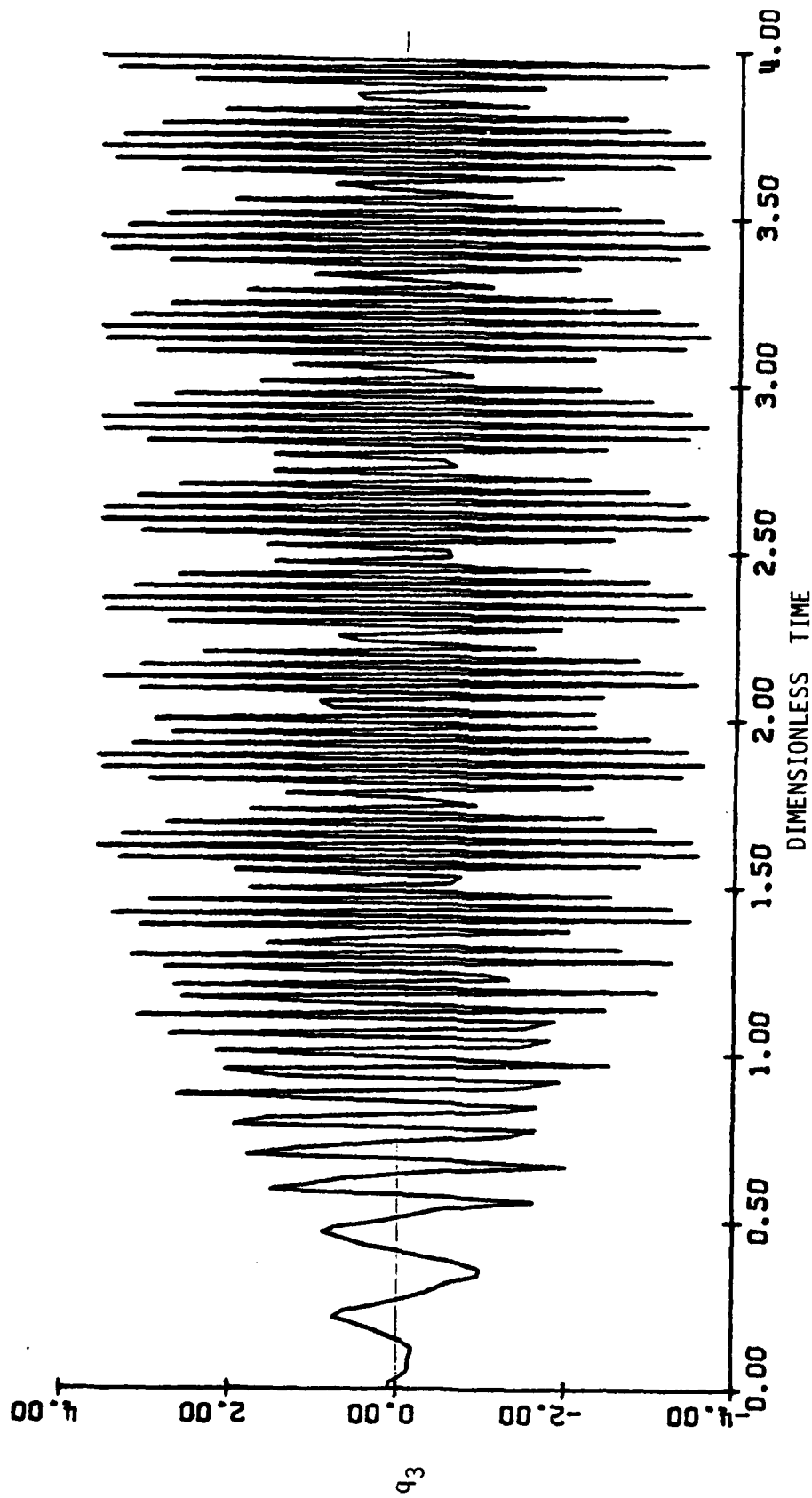


Figure 32c. Third Mode Instability
($\mu = 0.5$, $\beta = 9.42$)

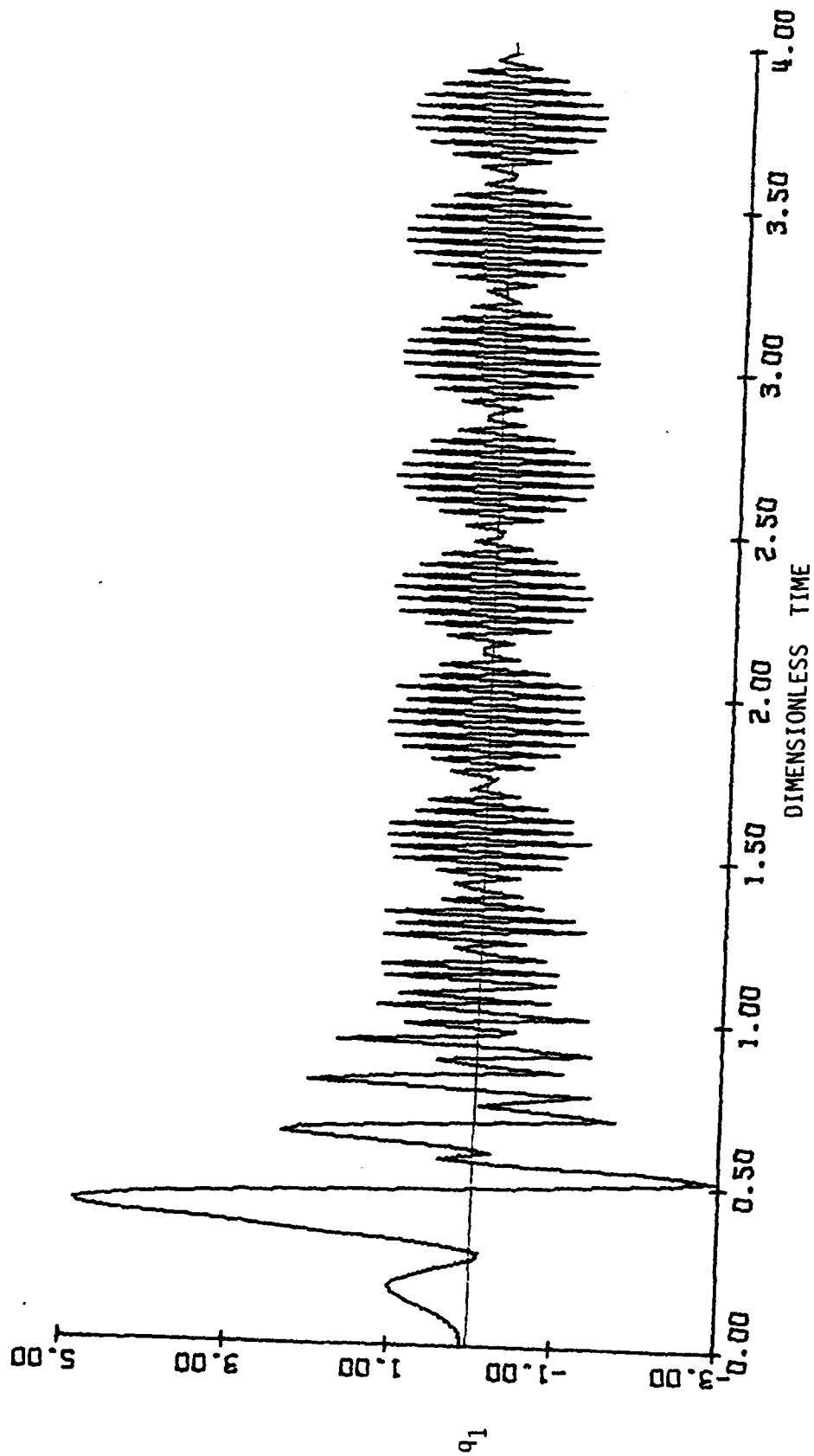


Figure 33a. First Mode Instability
($\mu = 0.5$, $\beta = 10.0$)

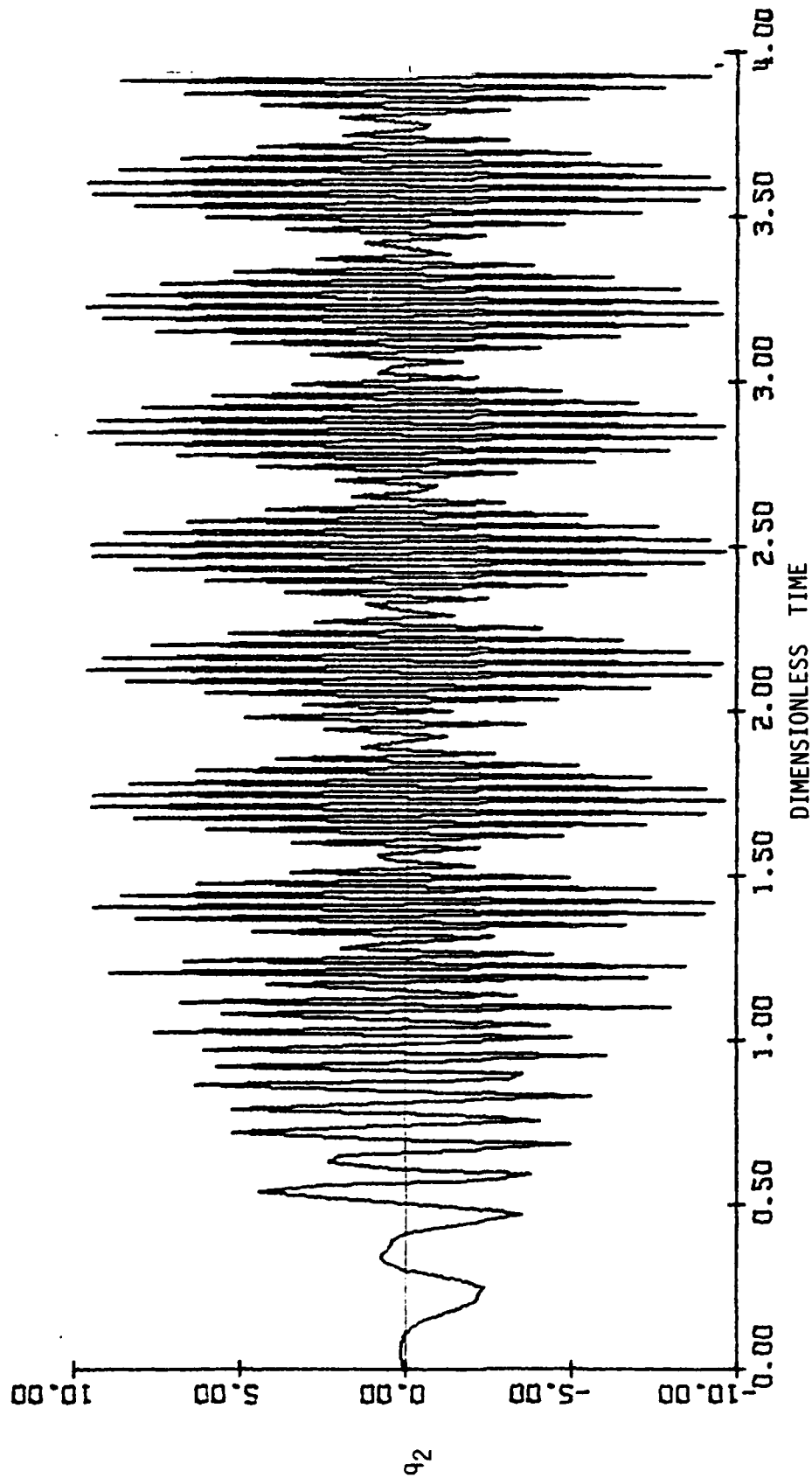


Figure 33b. Second Mode Instability
($\mu = 0.5$, $\beta = 10.0$)

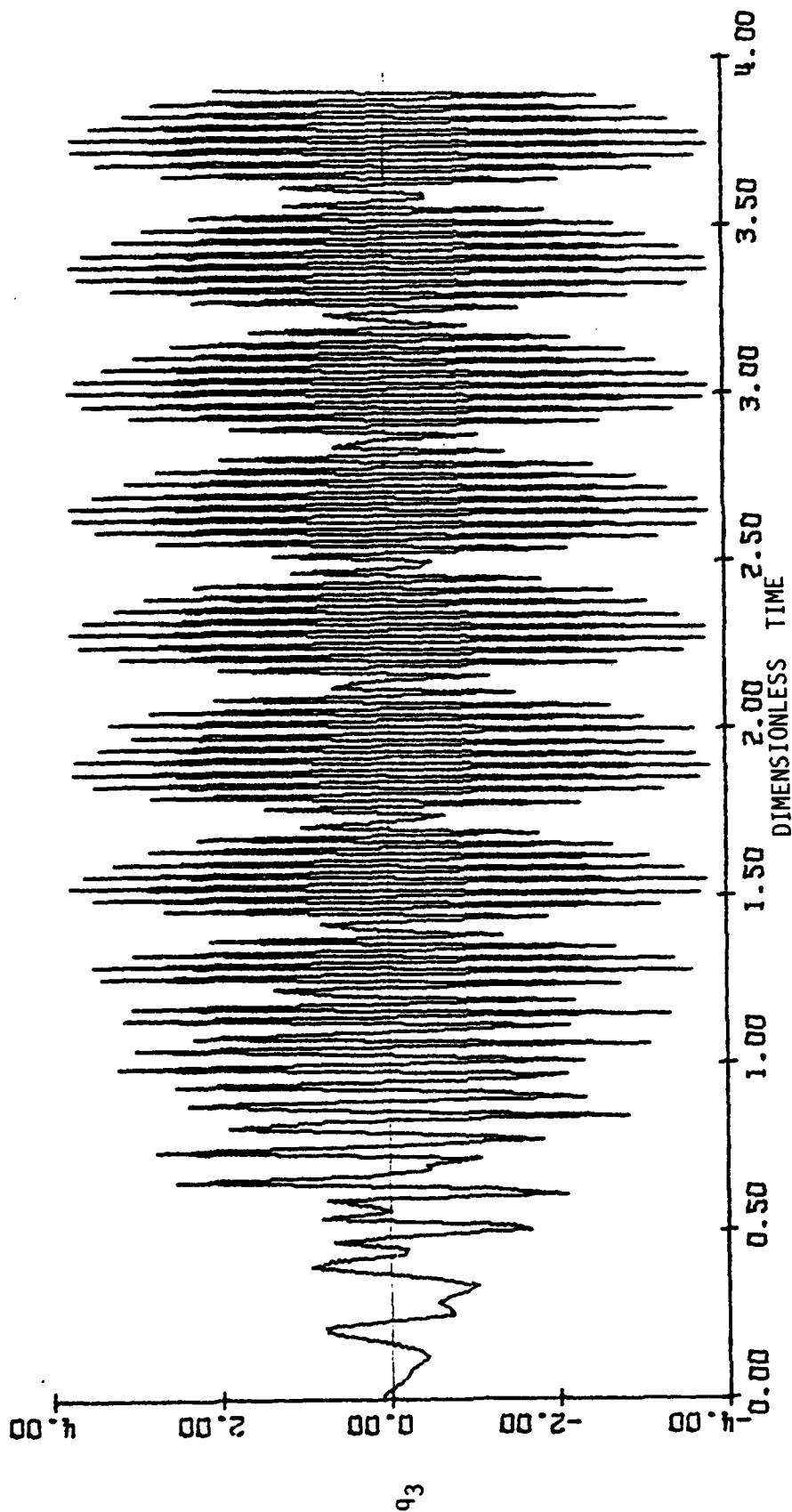


Figure 33c. Third Mode Instability
($\mu = 0.5$, $\beta = 10.0$)

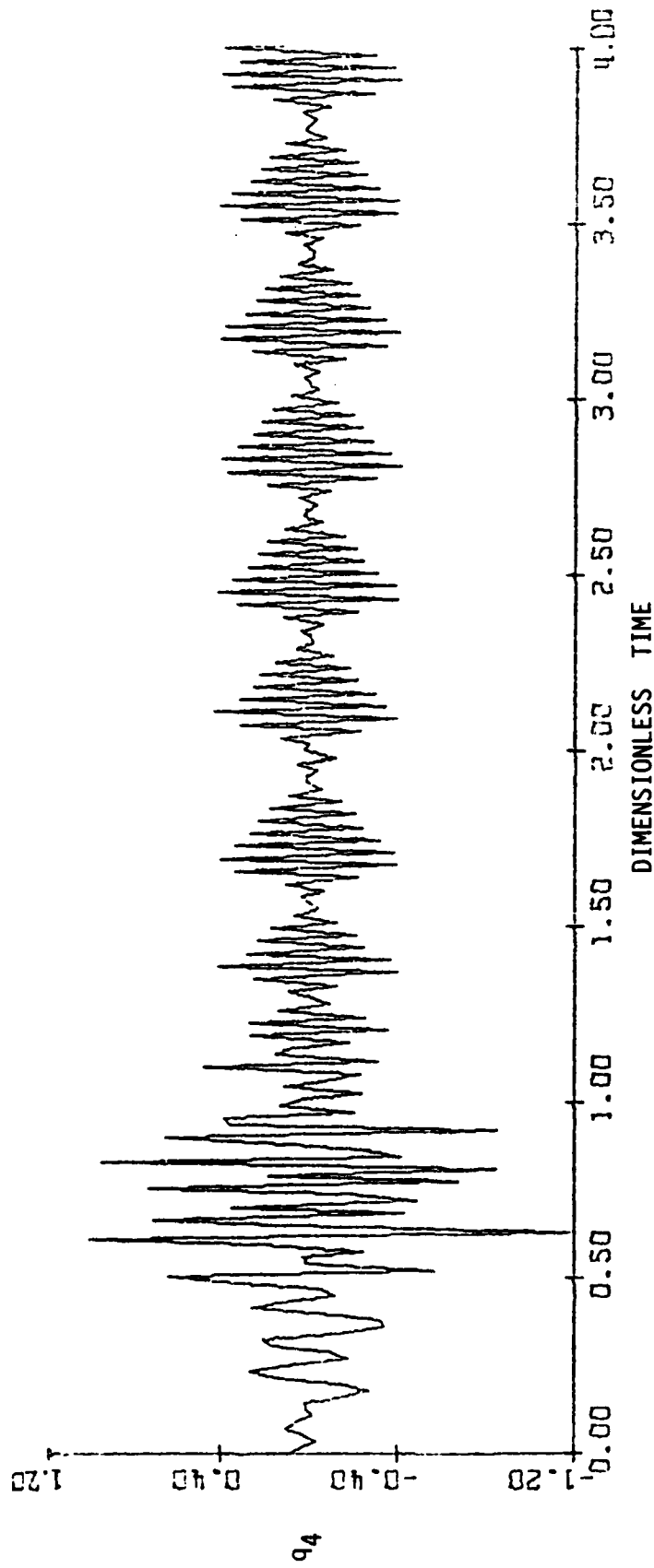


Figure 33d. Fourth Mode Instability
($\mu = 0.5$, $\beta = 10.0$)

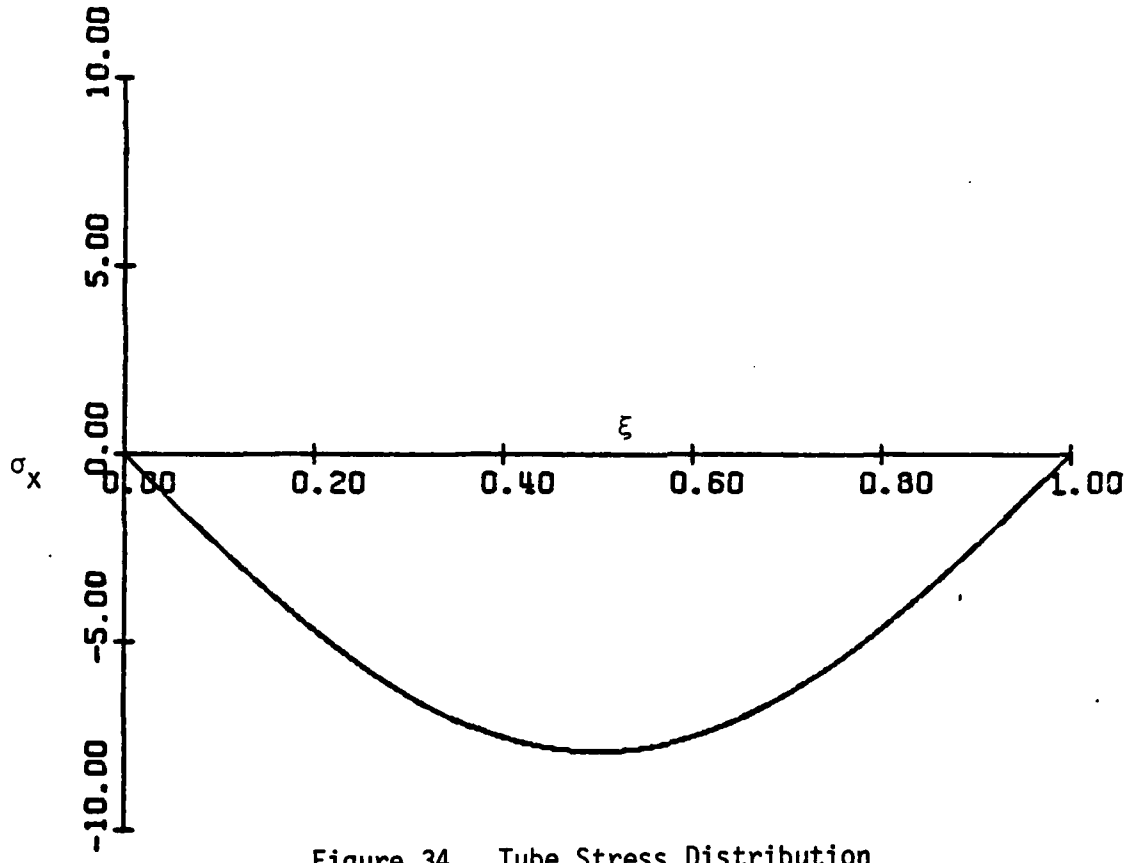


Figure 34. Tube Stress Distribution
at Divergence ($\beta = 5.92$)

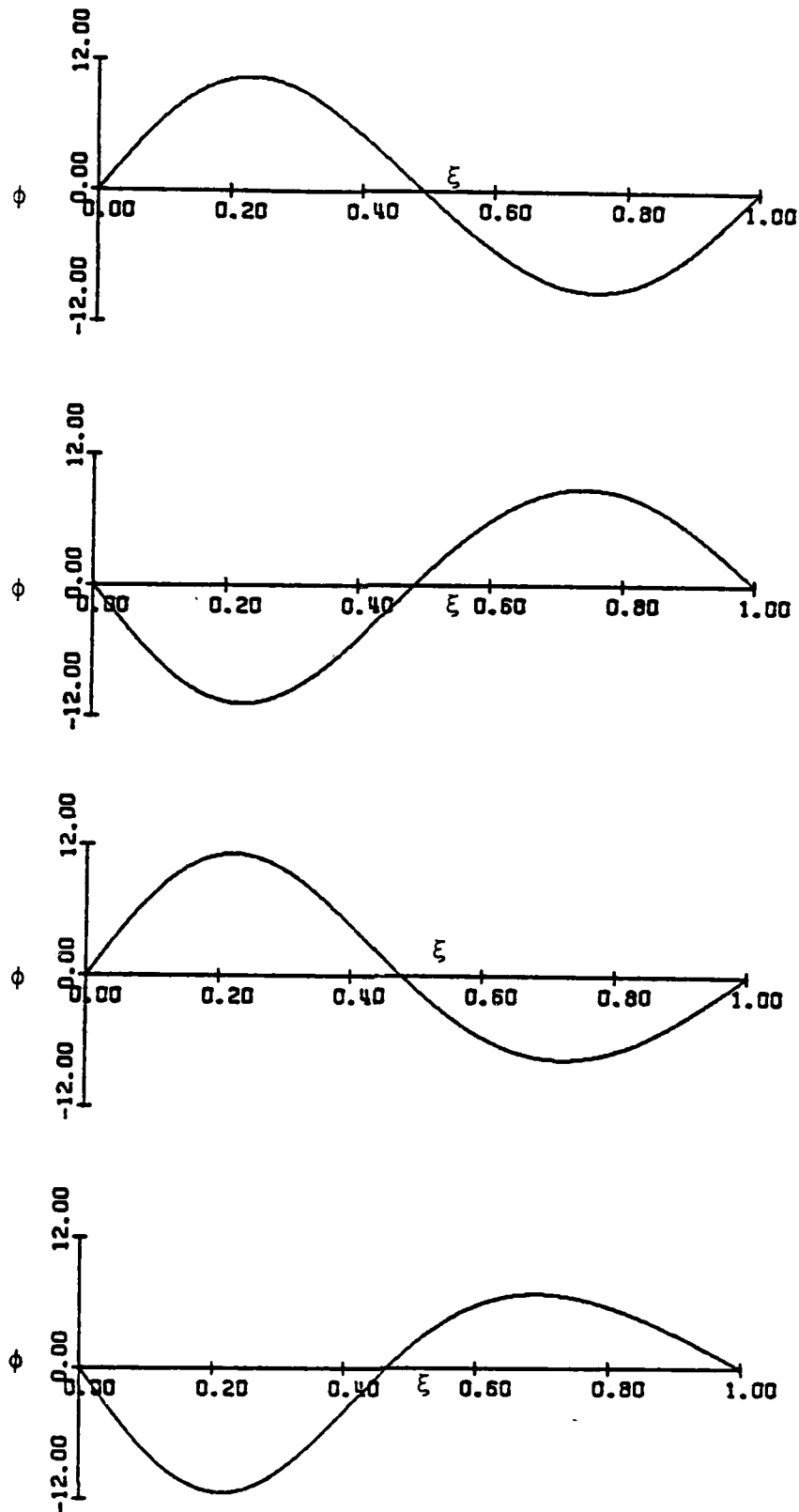


Figure 35a. Tube Deformation Shapes at Various Time Intervals ($\beta = 10.0$)

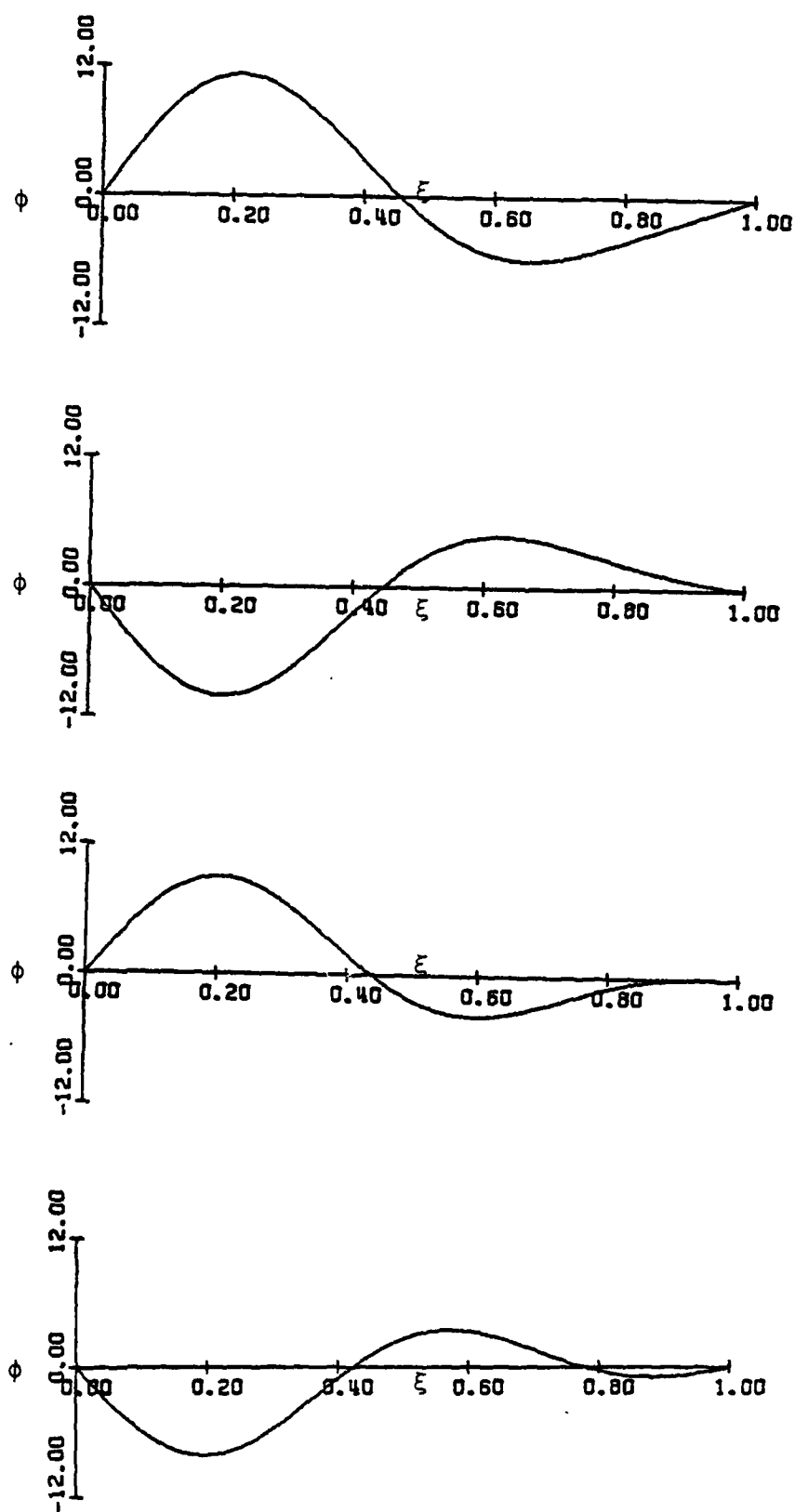


Figure 35b. Tube Deformation Shapes at Various Time Intervals ($\beta = 10.0$)

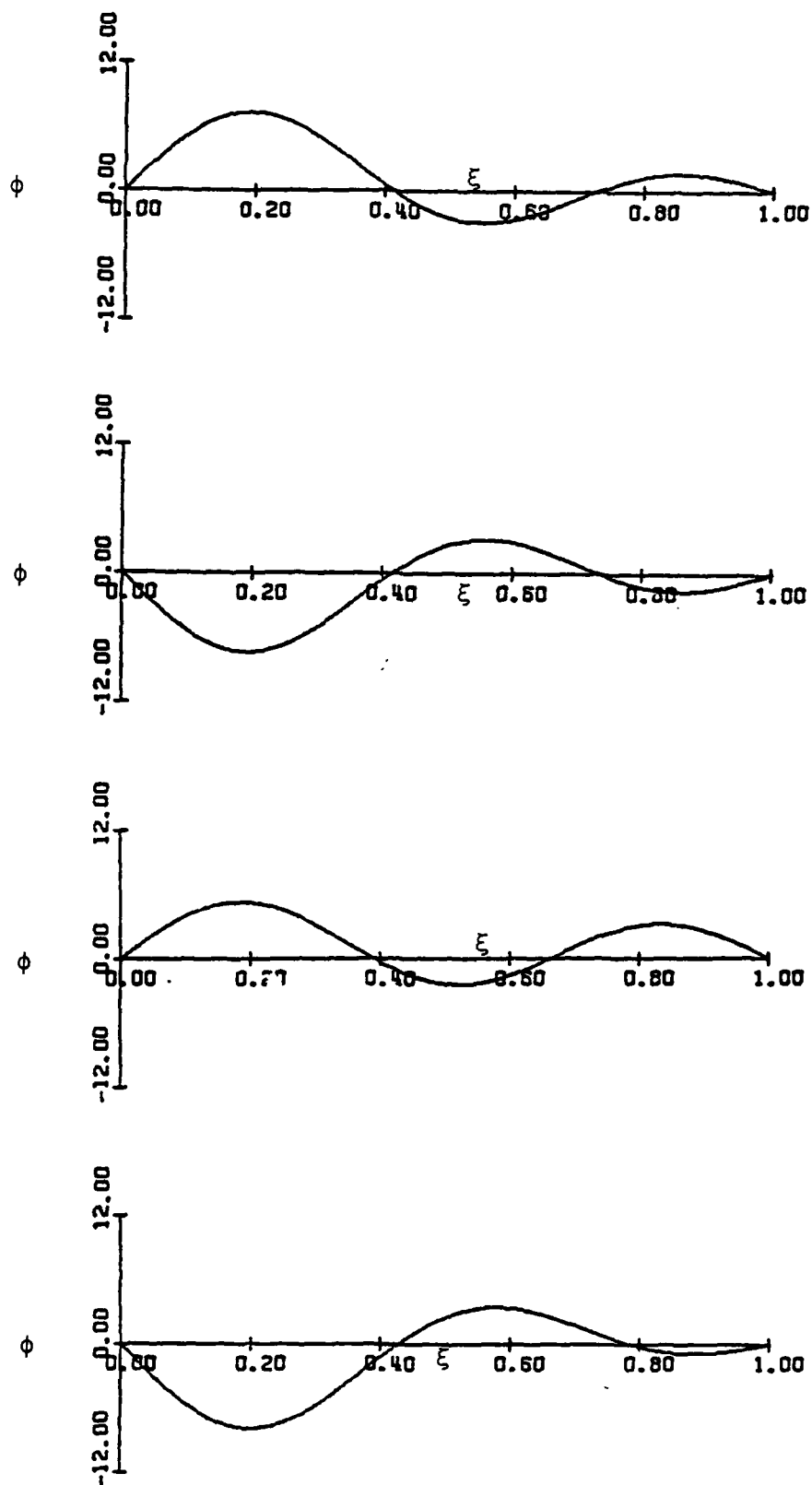


Figure 35c. Tube Deformation Shapes at Various Time Intervals ($\beta = 10.0$)

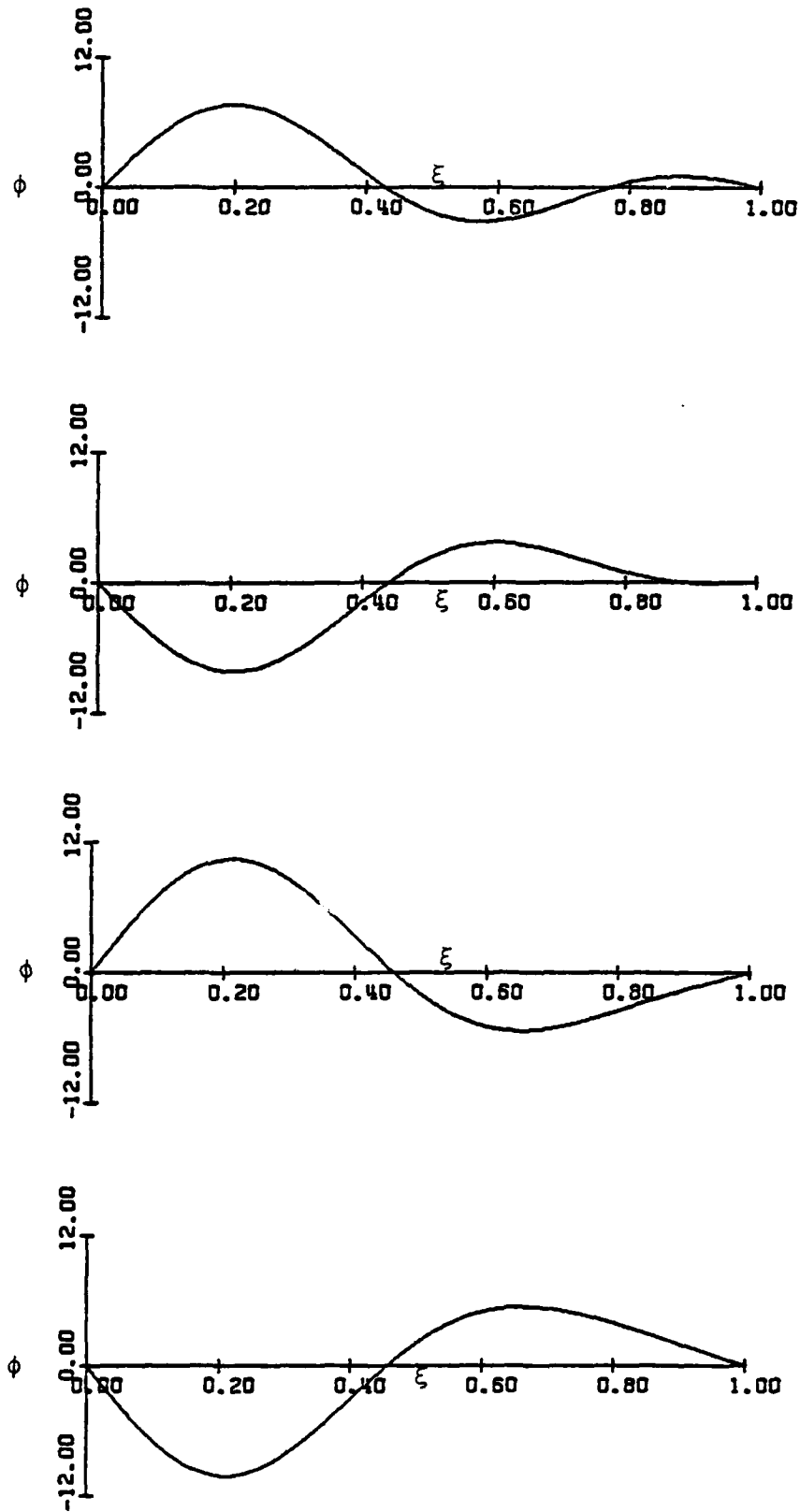


Figure 35d. Tube Deformation Shapes at Various Time Intervals ($\beta = 10.0$)

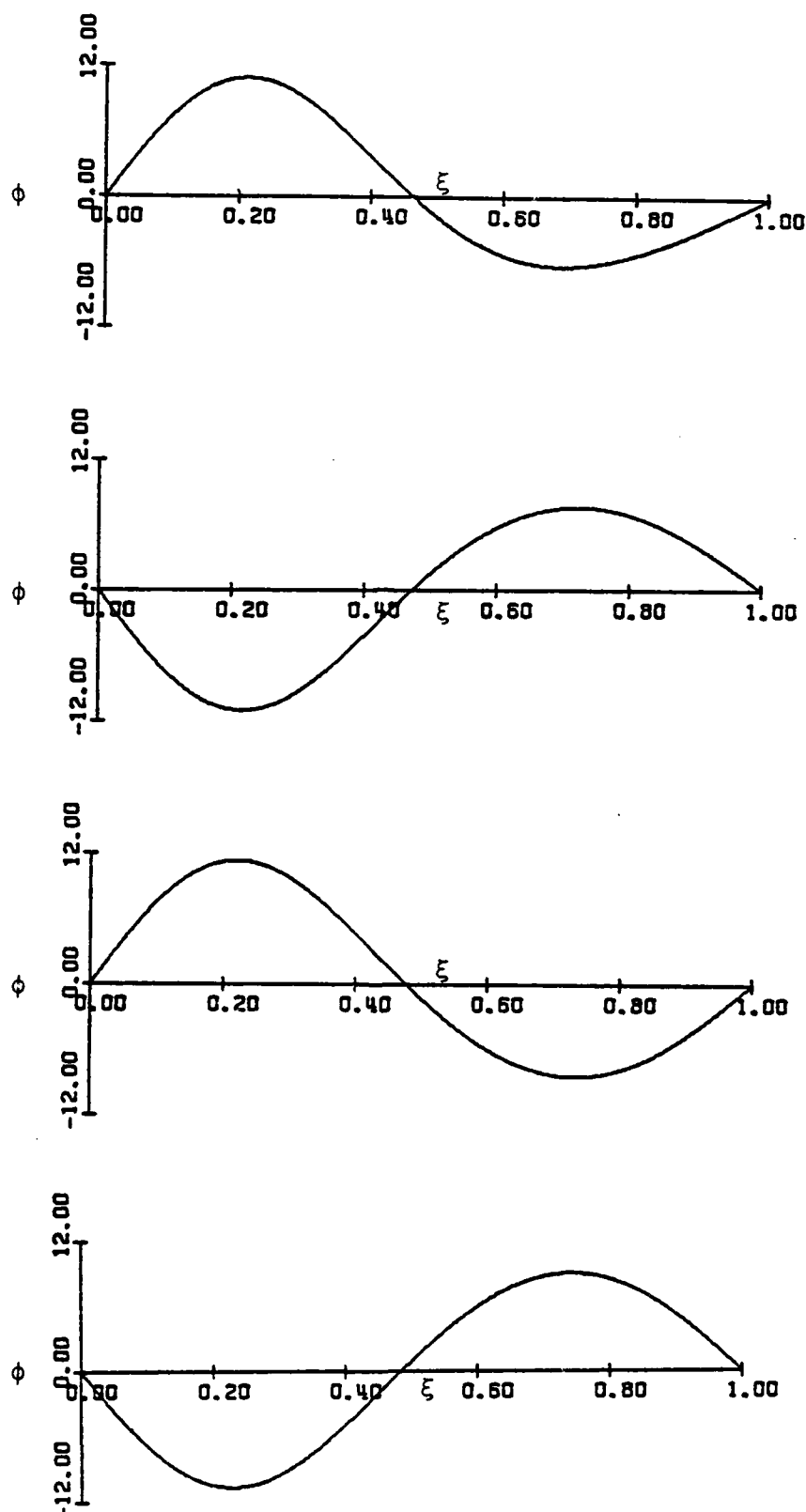


Figure 35e. Tube Deformation Shapes at Various Time Intervals ($\beta = 10.0$)

AD-A132 178

A THEORETICAL ANALYSIS OF NONLINEAR EFFECTS ON THE
FLUTTER AND DIVERGENCE. (U) PRINCETON UNIV N J DEPT OF
AEROSPACE AND MECHANICAL SCIENCES. E CH'NG 02 AUG 77

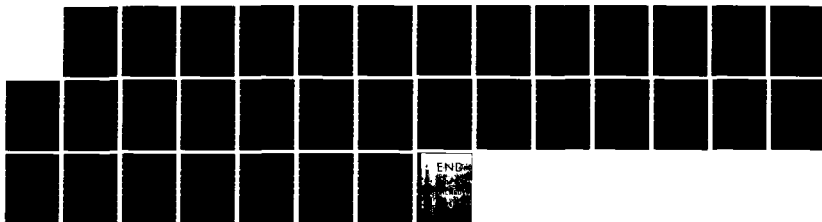
2/2

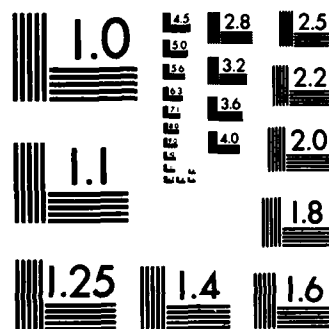
UNCLASSIFIED

PUAMS-1343

F/G 20/4

NL





MICROCOPY RESOLUTION TEST CHART
NATIONAL BUREAU OF STANDARDS-1963-A

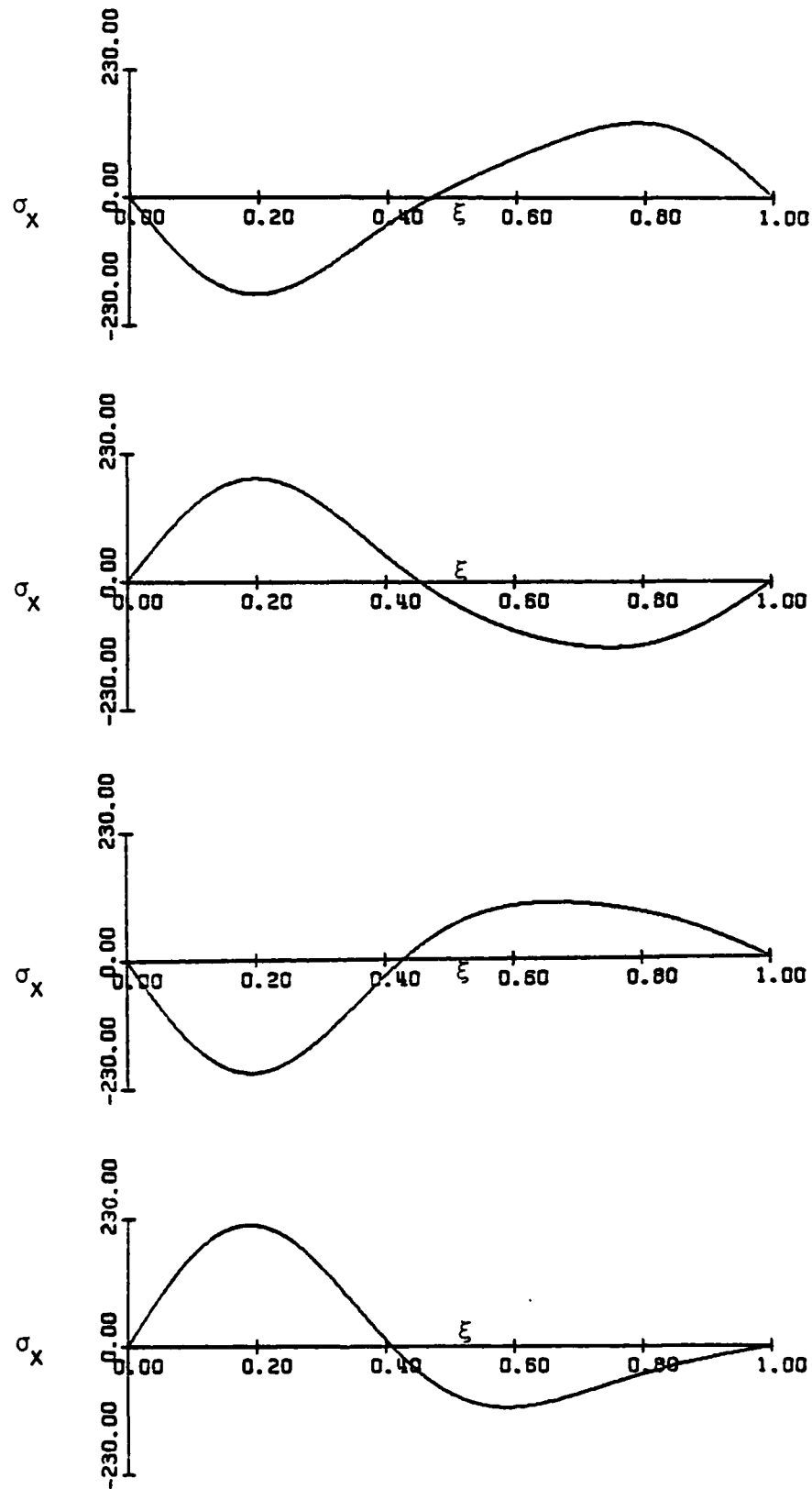


Figure 36a. Tube Stress Distribution at Various Times ($\beta = 10.0$)

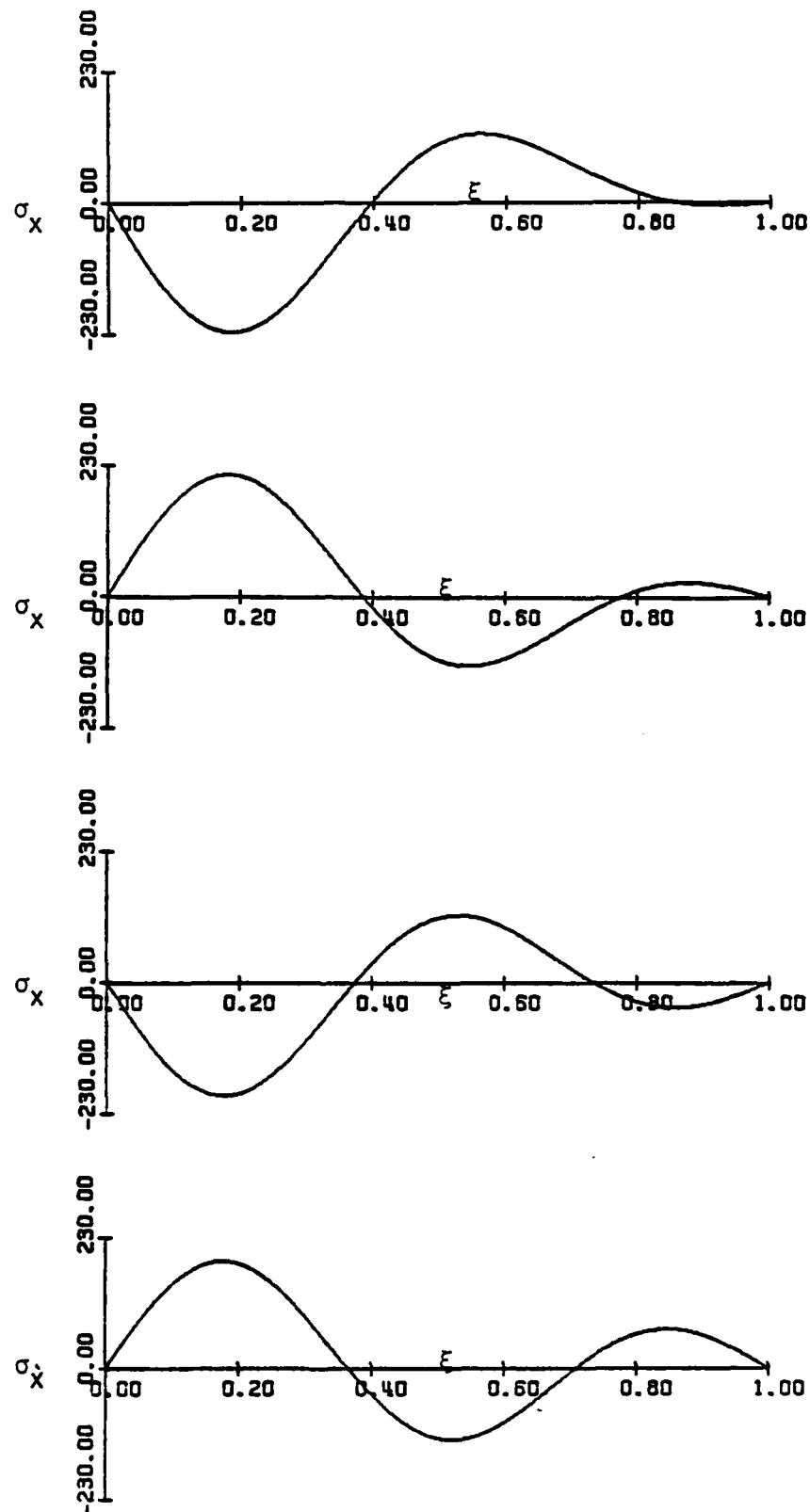


Figure 36b. Tube Stress Distribution at Various Times ($\beta = 10.0$)

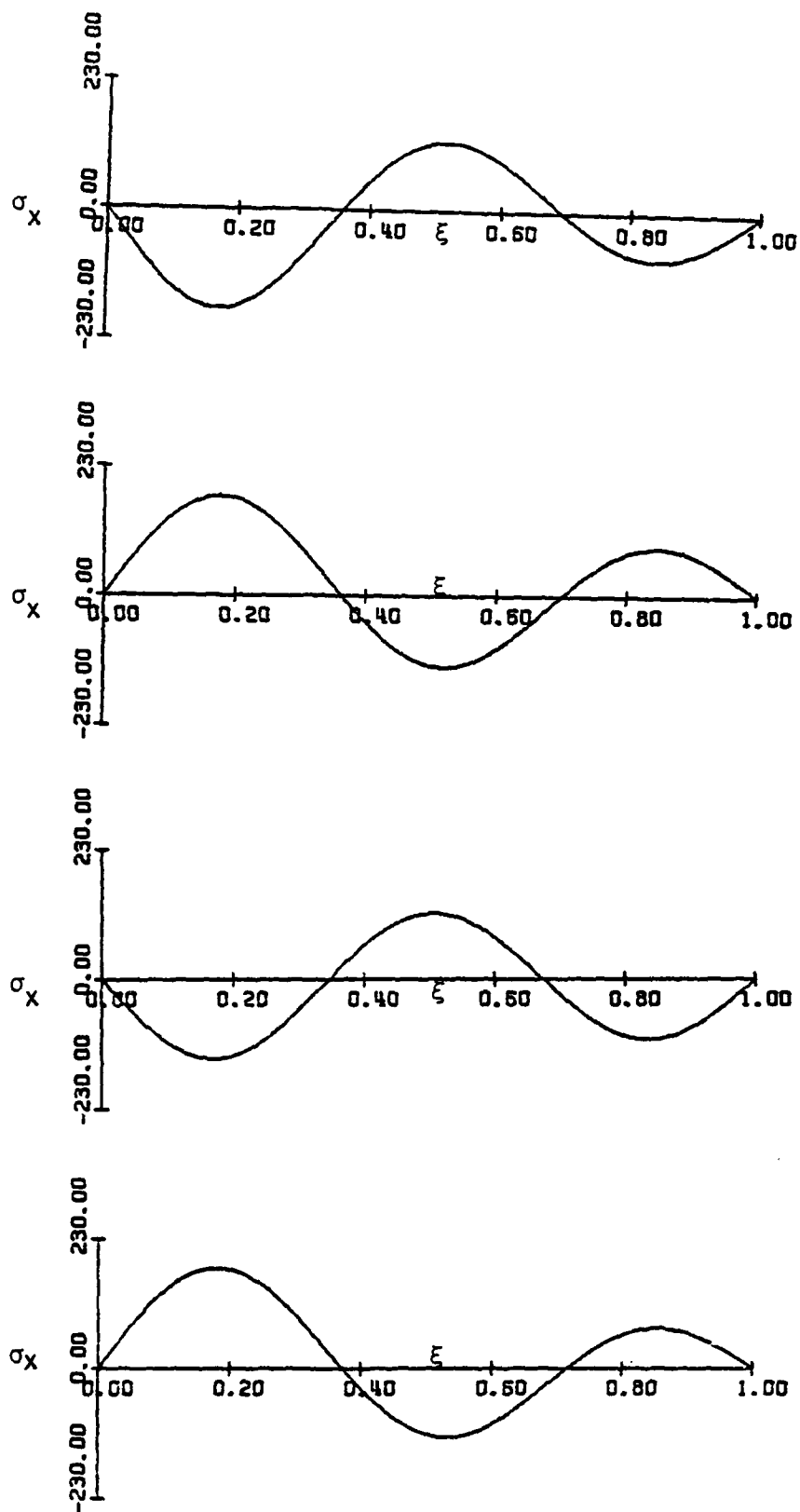


Figure 36c. Tube Stress Distribution at Various Times ($\beta = 10.0$)

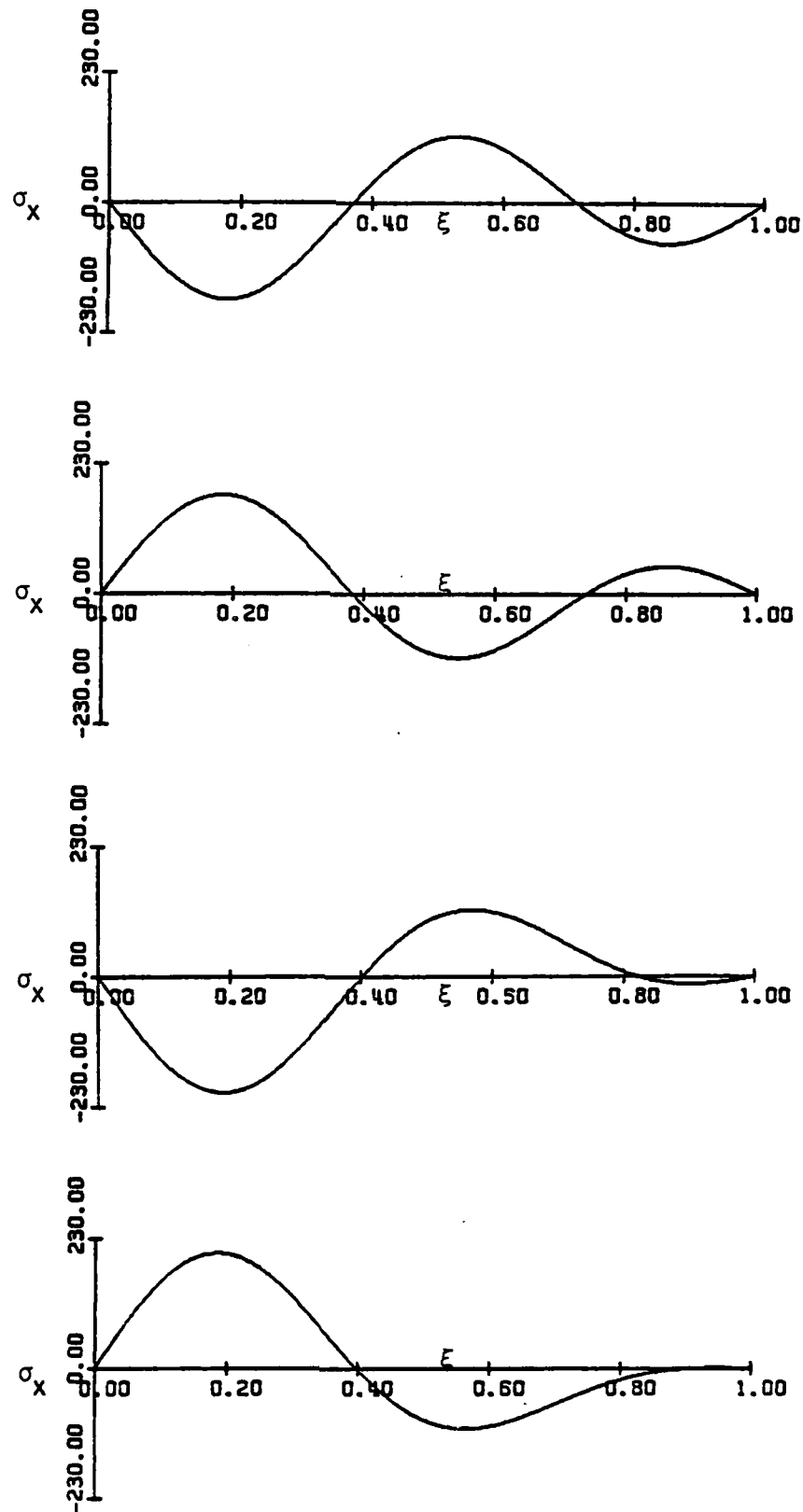


Figure 36d. Tube Stress Distribution at Various Times ($\beta = 10.0$)

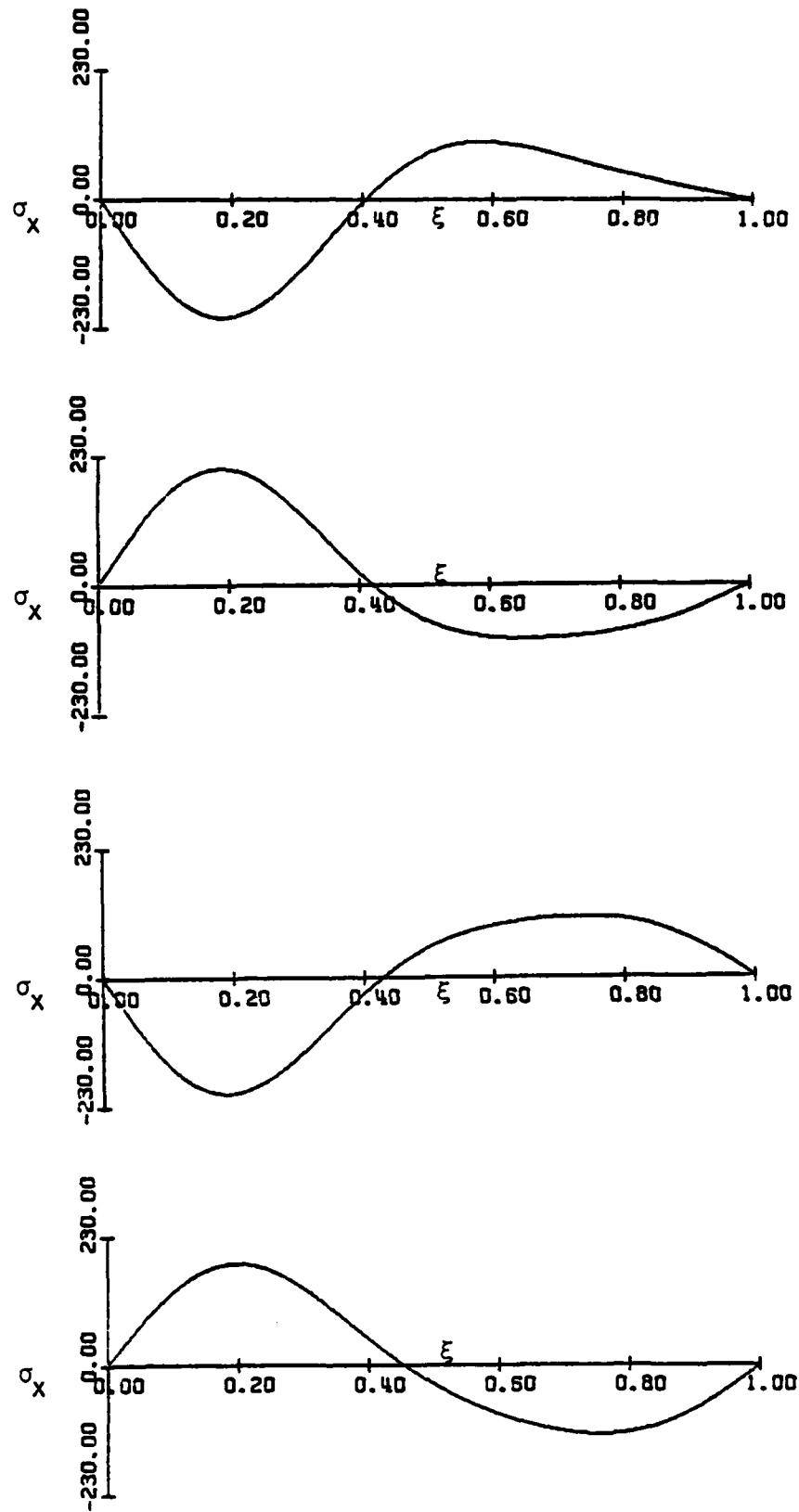


Figure 36e. Tube Stress Distribution at Various Times ($\beta = 10.0$)

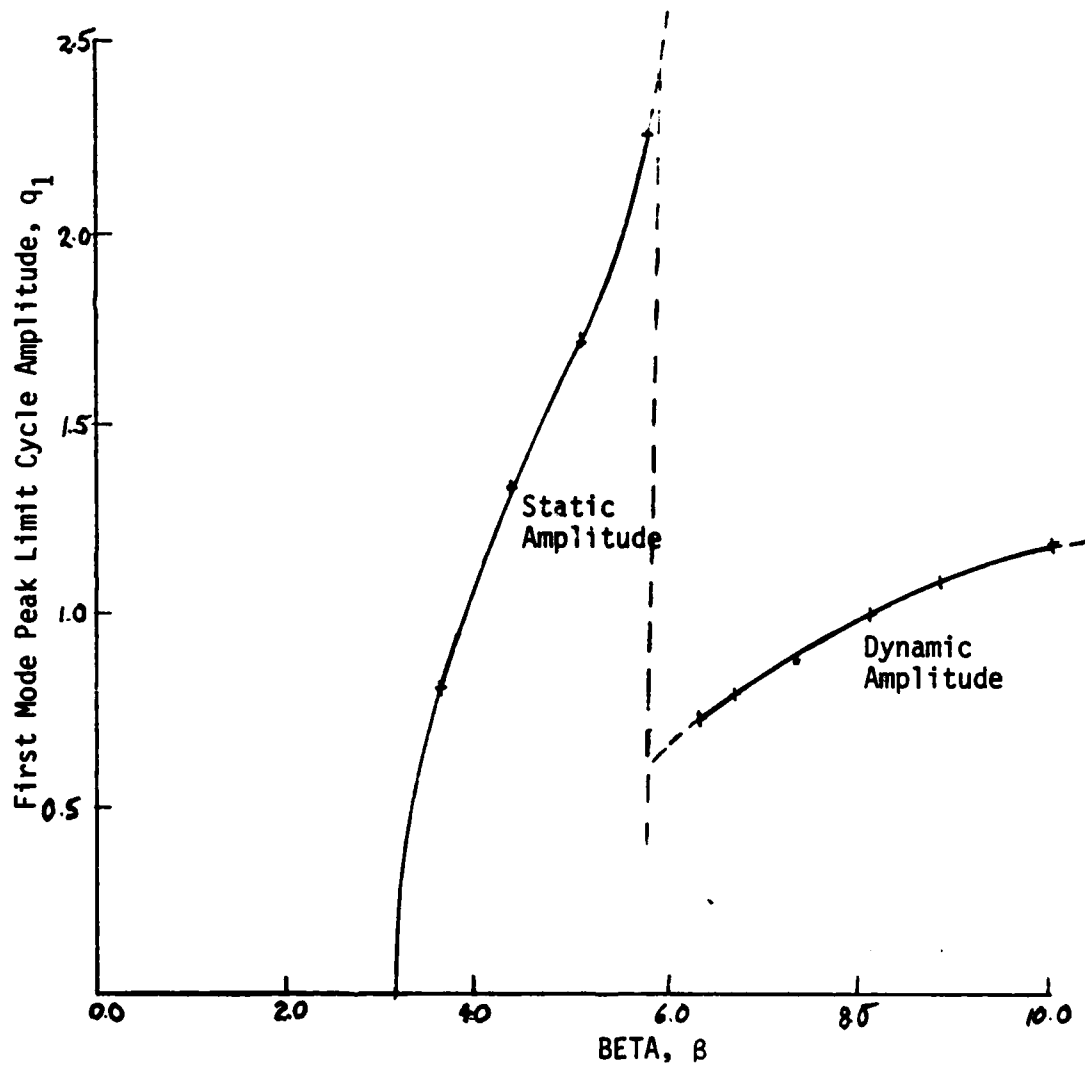


Figure 37a. Effects of β on Peak Amplitude
($\mu = 0.5$)

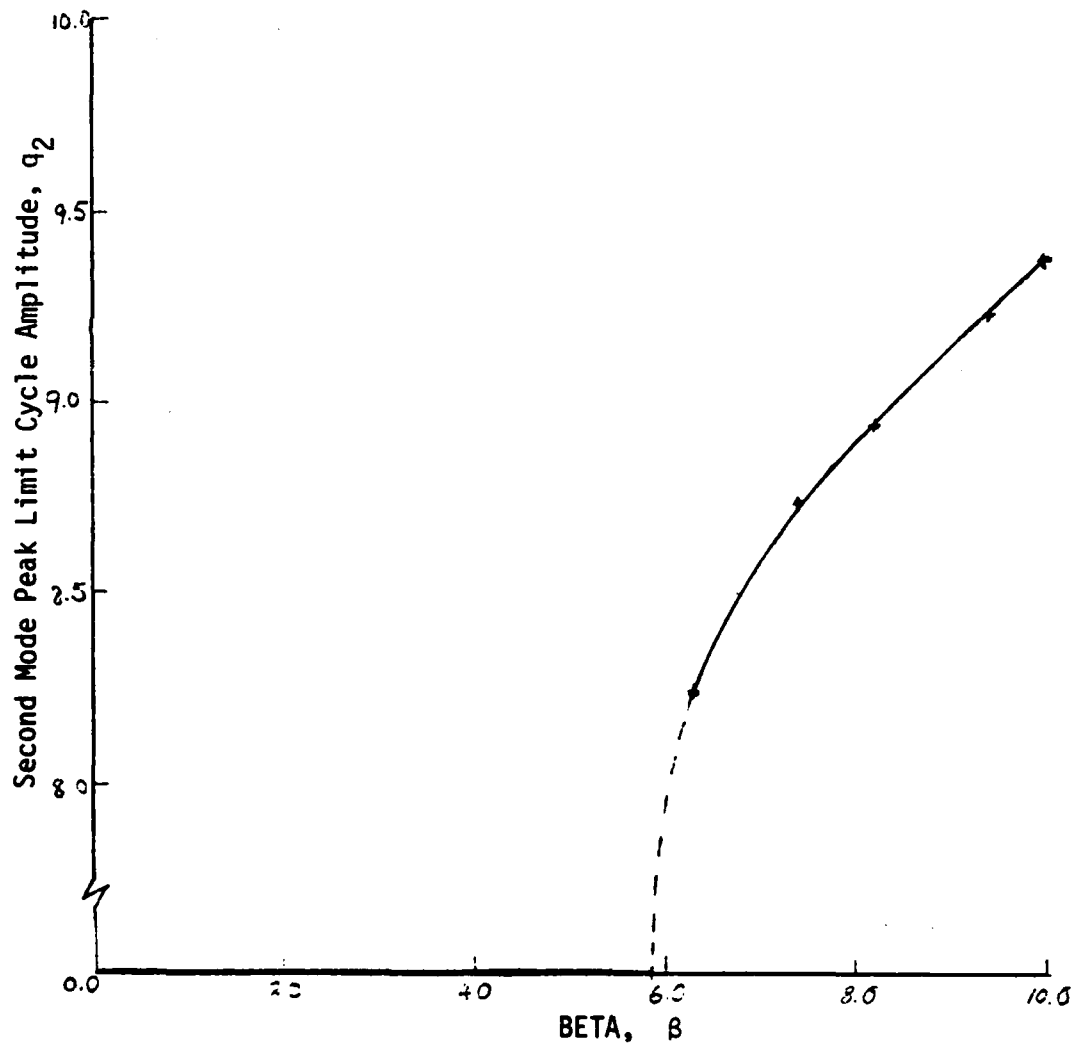


Figure 37b. Effects of β on Peak Amplitude
($\mu = 0.5$)

APPENDIX I

Solving the Energy Equation

Substituting equations (7), (8), and (11) into equation (1) gives

$$\begin{aligned}
 & \frac{1}{2} \delta \int_{t_1}^{t_2} \int_0^l \left\{ m \left(\frac{\partial y}{\partial t} \right)^2 + m_f \left[\left(\frac{\partial y}{\partial t} \right)^2 + 2V \frac{\partial y}{\partial t} \frac{\partial y}{\partial x} + V^2 \left(\frac{\partial y}{\partial x} \right)^2 + V^2 \right] \right. \\
 & - EI \left(\frac{\partial^2 y}{\partial x^2} \right)^2 + mg(l-x) \left(\frac{\partial y}{\partial x} \right)^2 \left. \right\} dx dt - \int_{t_1}^{t_2} \int_0^l 2\zeta_1 \bar{\omega}_1 m \frac{\partial y}{\partial t} \frac{\partial y}{\partial x} dx dt \\
 & + \int_{t_1}^{t_2} m_f \left[\frac{\partial y}{\partial t} (l) + V \frac{\partial y}{\partial x} (l) \right] \cdot dt \delta y (l) = 0 \quad (A-1)
 \end{aligned}$$

In the calculus of variations, δ may be considered as a linear differential operator. Examples:

$$\delta \int_{t_1}^{t_2} \int_0^l m \left(\frac{\partial y}{\partial t} \right)^2 dx dt = \int_{t_1}^{t_2} \int_0^l 2m \frac{\partial y}{\partial t} \delta \frac{\partial y}{\partial t} dx dt \quad (A-2)$$

$$\delta \int_{t_1}^{t_2} \int_0^l m_f V^2 dx dt = \int_{t_1}^{t_2} \int_0^l \delta (m_f V^2) dx dt = 0 \quad (A-3)$$

$$\delta \int_{t_1}^{t_2} \int_0^l 2m_f V \frac{\partial y}{\partial t} \frac{\partial y}{\partial x} dx dt = \int_{t_1}^{t_2} \int_0^l 2m_f V \left(\frac{\partial y}{\partial t} \delta \frac{\partial y}{\partial x} + \frac{\partial y}{\partial x} \delta \frac{\partial y}{\partial t} \right) dx dt \quad (A-4)$$

Similarly, performing variation on equation (A-1) and then rearranging the terms yields

$$\begin{aligned}
& \int_{t_1}^{t_2} \int_0^l \{ (m+m_f) \frac{\partial y}{\partial t} \delta \frac{\partial y}{\partial t} dx dt + m_f V \frac{\partial y}{\partial t} \delta \frac{\partial y}{\partial x} + m_f V \frac{\partial y}{\partial x} \delta \frac{\partial y}{\partial t} \\
& + m_f V^2 \frac{\partial y}{\partial x} \delta \frac{\partial y}{\partial x} - EI \frac{\partial^2 y}{\partial x^2} \delta \frac{\partial^2 y}{\partial x^2} - mg(l-x) \frac{\partial y}{\partial x} \delta \frac{\partial y}{\partial x} \\
& - 2\tau_1 \bar{\omega}_1 m \frac{\partial y}{\partial t} \delta y \} dx dt - \int_{t_1}^{t_2} m_f V \left[\frac{\partial y}{\partial t} (l) + V \frac{\partial y}{\partial x} (l) \right] \delta y(l) dt = 0
\end{aligned} \tag{A-5}$$

Due to the tedious mathematics involved, only representative terms of equation (A-5) will be worked out completely and shown below.

Integration by parts:

$$\begin{aligned}
\int_{t_1}^{t_2} \int_0^l (m+m_f) \frac{\partial y}{\partial t} \delta \frac{\partial y}{\partial t} dx dt &= (m+m_f) \left\{ \int_0^l \left[\frac{\partial y}{\partial t} \delta y \right] \int_{t_1}^{t_2} dx \right. \\
&\quad \left. - \int_0^l \int_{t_1}^{t_2} \frac{\partial^2 y}{\partial t^2} \delta y dx dt \right\}
\end{aligned} \tag{A-6}$$

$$\begin{aligned}
\int_{t_1}^{t_2} \int_0^l (m_f V \frac{\partial y}{\partial t} \delta \frac{\partial y}{\partial x}) dx dt &= m_f V \left\{ \int_{t_1}^{t_2} \left[\frac{\partial y}{\partial t} \delta y \right]_0^l dt - \right. \\
&\quad \left. \int_{t_1}^{t_2} \int_0^l \frac{\partial^2 y}{\partial x \partial t} \delta y dx dt \right\}
\end{aligned} \tag{A-7}$$

$$\int_{t_1}^{t_2} \int_0^l EI \frac{\partial^2 y}{\partial x^2} \delta \frac{\partial^2 y}{\partial x^2} dx dt = EI \left\{ \int_{t_1}^{t_2} \left[\frac{\partial^2 y}{\partial x^2} \delta \frac{\partial y}{\partial x} \right]_0^l dt - \int_{t_1}^{t_2} \int_0^l \frac{\partial^3 y}{\partial x^3} \delta \frac{\partial y}{\partial x} dx dt \right\}$$

$$= EI \left\{ \int_{t_1}^{t_2} \left[\frac{\partial^2 y}{\partial x^2} \delta \frac{\partial y}{\partial x} \right]_0^l dt - \int_{t_1}^{t_2} \left[\frac{\partial^3 y}{\partial x^3} \delta y \right]_0^l dt + \int_{t_1}^{t_2} \int_0^l \frac{\partial^4 y}{\partial x^4} \delta y dx dt \right\} \quad (A-8)$$

$$\int_{t_1}^{t_2} \int_0^l m_f V \frac{\partial y}{\partial x} \delta \frac{\partial y}{\partial x} dx dt = \int_0^l \left\{ \left[-m_f V \frac{\partial y}{\partial x} \delta y \right]_{t_1}^{t_2} - \int_{t_1}^{t_2} m_f V \frac{\partial^2 y}{\partial x \partial t} \delta y dt \right\} dx \quad (A-9)$$

$$\int_0^l m_f V^2 \frac{\partial y}{\partial x} \delta \frac{\partial y}{\partial x} dx = m_f V^2 \frac{\partial y}{\partial x} \delta y \Big|_{x=0}^l - \int_0^l m_f V^2 \frac{\partial^2 y}{\partial x^2} \delta y dx \quad (A-10)$$

$$\int_0^l -mg(l-x) \frac{\partial y}{\partial x} \delta \frac{\partial y}{\partial x} dx = -mg(l-x) \frac{\partial y}{\partial x} \delta y \Big|_{x=0}^l + \int_0^l mg \frac{\partial}{\partial x} [(l-x) \frac{\partial y}{\partial x}] \delta y dx \quad (A-11)$$

and
$$\left[\delta y \right]_{t_1}^{t_2} = 0 \quad (\text{See Ref. 6})$$

To satisfy Eq. (A-5), the integrands have to be zero. The sum of all the integrands of the double integrals give the partial differential equation for the problem,

$$EI \frac{\partial^4 y}{\partial x^4} + (m+m_f) \frac{\partial^2 y}{\partial t^2} + 2m_f V \frac{\partial^2 y}{\partial t \partial x} + m_f V^2 \frac{\partial^2 y}{\partial x^2} + 2m_f \bar{\omega}_1 \frac{\partial y}{\partial t} - mg \frac{\partial}{\partial x} [(l-x) \frac{\partial y}{\partial x}] = 0 \quad (A-12)$$

Also the several end point terms must be zero. Thus

$$EI \frac{\partial^2 y}{\partial x^2} \delta \left(\frac{\partial y}{\partial x} \right) \Big|_{x=0, l} = 0 \quad (A-13)$$

For a cantilevered tube (A-13) is satisfied by

$$\left. \frac{\partial y}{\partial x} \right|_{x=0} = 0$$

(A-13c)

and

$$EI \left. \frac{\partial^2 y}{\partial x^2} \right|_{x=l} = 0$$

For a simply-supported tube,

$$EI \left. \frac{\partial^2 y}{\partial x^2} \right|_{x=0, l} = 0$$

(A-13s)

The other end point conditions are

$$\left[EI \frac{\partial^3 y}{\partial x^3} - mg(l-x) \frac{\partial y}{\partial x} \right] \delta y \Big|_{x=0, l} = 0$$

(A-14)

For a cantilevered tube, (A-14) is satisfied by

$$y|_{x=0} = 0$$

(A-14c)

and

$$\left[EI \frac{\partial^3 y}{\partial x^3} - mg(l-x) \frac{\partial y}{\partial x} \right]_{x=0} = 0$$

For a simply-supported tube,

$$y|_{x=0, l} = 0$$

(A-14ss)

It should be noted that in obtaining (A-14) from (A-5) to (A-11), there has been a cancellation of terms involving the last term in (A-5) and the first terms on the right hand side of (A-7) and (A-10) for $x=l$ to give the same form in (A-14) for the boundary conditions at both $x=0$ and $x=l$.

APPENDIX II

Mode Shape Integrals of a Cantilevered Beam

Integrals containing the characteristic functions and their derivatives are referred to as mode shape integrals in this paper. They can be evaluated by the method of partial integration along with their orthogonality properties. Special formulas for those mode shape integrals which occur frequently in engineering application may be found in references 10 and 11. They are given in terms of α_n and β_n for five common boundary conditions: clamped-clamped, clamped-free, clamped-supported, free-free, and free-supported.

As an illustration, consider

$$c_{hi} = \int_0^1 \gamma_h'(\xi) \gamma_i'(\xi) d\xi \quad (A-15)$$

for a cantilevered uniform beam. Combining formulas (6) and (16) of reference (7) yields.

$$c_{hi} = \begin{cases} \alpha_h \beta_h (2 + \alpha_h \beta_h), & h = i \\ \frac{4\beta_h \beta_i}{\beta_h^4 - \beta_i^4} [(-1)^{h+i} (\alpha_i \beta_h^3 - \alpha_h \beta_i^3) - \beta_h \beta_i (\alpha_h \beta_h - \alpha_i \beta_i)], & h \neq i \end{cases}$$

The corresponding α 's and β 's can be found in reference 11. They are

n	α_n	β_n
1	0.7341	1.8751
2	1.0185	4.6940
3	0.9992	7.8546
4	1.0000	10.9955

Numerical values of c_{hi} are given in Table 2. The computations were done on the IBM 360/91

APPENDIX III

Radius of gyration, r

(i) For a thin cylindrical tube, the area moment is

$$I = \int z^2 da \equiv r^2 a$$

Now

$$a = 2\pi \bar{R} t$$

and

$$da = \bar{R} \cdot t \cdot d\theta$$

Also

$$z = \bar{R} \cos \theta$$

Thus

$$\begin{aligned} I &= \int_0^{2\pi} \bar{R}^2 \cos^2 \theta \bar{R} d\theta t \\ &= \bar{R}^3 t \int_0^{\pi} \cos^2 \theta d\theta \\ &= \bar{R}^3 t \pi \end{aligned}$$

Hence

$$r^2 a = \bar{R}^3 t \pi$$

Solving,

$$r^2 = \frac{\bar{R}^3 t \pi}{2\pi \bar{R} t}$$

or

$$\begin{aligned} r^2 &= \frac{\bar{R}^2}{2} \\ r &= \sqrt{\frac{\bar{R}^2}{2}} \end{aligned}$$

(II) For a tube with a thick wall,

$$I = \int_0^{2\pi} \int_{\bar{R}_1}^{\bar{R}_2} \bar{R}^2 \cos^2 \theta \bar{R} d\bar{R} d\theta$$

$$= \int_0^{2\pi} [(\bar{R}_2^4 - \bar{R}_1^4)/4] \cos^2 \theta \, d\theta$$

$$= \frac{\pi}{4} [\bar{R}_2^4 - \bar{R}_1^4]$$

$$a = \int_0^{2\pi} \int_{\bar{R}_1}^{\bar{R}_2} \bar{R} \, d\bar{R} \, d\theta$$

$$= \int_0^{2\pi} \frac{1}{2} (\bar{R}_2^2 - \bar{R}_1^2) \, d\theta$$

$$= \pi [\bar{R}_2^2 - \bar{R}_1^2]$$

Hence

$$r^2 = I/a$$

$$= \frac{\pi [\bar{R}_2^4 - \bar{R}_1^4]}{4\pi [\bar{R}_2^2 - \bar{R}_1^2]}$$

$$= \frac{1}{4} [\bar{R}_2^2 + \bar{R}_1^2]$$

APPENDIX IV

A LISTING OF WATFIV PROGRAMS FOR CANTILEVERED TUBE

(Linear and Nonlinear)

0761536.SELF¹⁰⁴BIN=1.82

```

*****
+
+   NUMERICAL SOLUTION FOR STATIC AND   +
+   DYNAMIC INSTABILITIES OF A PROPELLANT +
+   LINE.  (FOUR MODES ANALYSIS)      +
+   NR:  WITH FORMULA OF OPEN TYPES    +
+
*****

```

n n n n n n n n n

Q1, Q2, Q3, ... ARE INITIAL CONDITIONS
DQ(N)'S ARE PSEUDO INITIAL CONDITIONS
I1, I2 ARE MODE SHAPE PARAMETERS
L = LENGTH OF PIPE
Z1 = CRITICAL DAMPING RATIO
M = MASS OF PIPE
MF = MASS OF FLUID
VF = FLUID VELOCITY
I = INERTIA
E = MODULUS OF ELASTICITY
A11, A12, ..., B11, B12, ... ARE MODE SHAPE INTEGRALS

ccc

BEFL = DIMENSIONLESS FLUID VELOCITY
MU = MASS RATIO

C NU = VISCOUS DAMPING COEFFICIENT

C

32 BETA = VF*SQRT(MF*L**2./(E*I))
 33 MU = MF/(MF+M)
 34 NU = 7.04*Z1*SQRT(1.-MU)

C

35 WRITE (6,1012)
 36 WRITE (6,1003) A11,A12,A13,A14,A21,A22,A23,A24
 37 1003 FORMAT (' ','A(1,J)=' ,4F20.4,/, ' ','A(2,J)=' ,4F20.4)
 38 WRITE (6,3011) A31,A32,A33,A34,A41,A42,A43,A44
 39 3011 FORMAT (' ','A(3,J)=' ,4F20.4,/, ' ','A(4,J)=' ,4F20.4)
 40 WRITE (6,3001) B11,B12,B13,B14,B21,B22,B23,B24
 41 3001 FORMAT (' ','B(1,J)=' ,4F20.4,/, ' ','B(2,J)=' ,4F20.4)
 42 WRITE (6,3111) B31,B32,B33,B34,B41,B42,B43,B44
 43 3111 FORMAT (' ','B(3,J)=' ,4F20.4,/, ' ','B(4,J)=' ,4F20.4)
 44 WRITE (6,1004) Q1,Q2,Q3,Q4,Q5,Q6,Q7,Q8
 45 1004 FORMAT (' ','Q(N)=' ,4F20.4,/,6X,4F20.4)
 46 WRITE (6,1005) BETA,MU,NU
 47 1005 FORMAT (' ','BETA=' ,1F15.4,5X, 'MU=' ,1F15.4,5X, 'NU=' ,1F15.4)
 48 WRITE (6,1006) VF,L1,L2,L3,L4,L,Z1
 49 1006 FORMAT (' ','VF=' ,1F15.4,5X, 'L1 ... ARE' ,4F10.5,/, ' ','L=' ,1F10.4,
 15X, 'Z1=' ,1F10.4)
 50 WRITE (6,1007) M,MF,I,E
 51 1007 FORMAT (' ','M,MF,I,E ARE' ,4E20.3)
 52 WRITE (6,1008)
 53 1008 FORMAT (//,30X, 'MATRIX IS',//)

C

54 RMU = SQRT(MU)

C

C

C

C

C

C

C

C

C

C

C

C

C

C

C

C

C

C

C

C

C

C

C

C

C

C

C

C

C

C

C

C

C

C

C

C

C

C

C

C

C

C

DQ(1,1) = 0.0
 DQ(1,2) = 0.0
 DQ(2,1) = 0.0
 DQ(2,2) = 0.0
 DQ(3,1) = 0.0
 DQ(3,2) = 0.0
 DQ(4,1) = 0.0
 DQ(4,2) = 0.0
 DQ(5,1) = 0.0
 DQ(5,2) = 0.0
 DQ(6,1) = 0.0
 DQ(6,2) = 0.0
 DQ(7,1) = 0.0
 DQ(7,2) = 0.0
 DQ(8,1) = 0.0
 DQ(8,2) = 0.0
 K(1,1) = 0.0
 K(1,2) = 0.0
 K(1,3) = 0.0
 K(1,4) = 0.0
 K(1,5) = 1.0
 K(1,6) = 0.0
 K(1,7) = 0.0
 K(1,8) = 0.0
 K(2,1) = 0.0

```

80      K(2,2) = 0.0
81      K(2,3) = 0.0
82      K(2,4) = 0.0
83      K(2,5) = 0.0
84      K(2,6) = 1.0
85      K(2,7) = 0.0
86      K(2,8) = 0.0
87      K(3,1) = 0.0
88      K(3,2) = 0.0
89      K(3,3) = 0.0
90      K(3,4) = 0.0
91      K(3,5) = 0.0
92      K(3,6) = 0.0
93      K(3,7) = 1.0
94      K(3,8) = 0.0
95      K(4,1) = 0.0
96      K(4,2) = 0.0
97      K(4,3) = 0.0
98      K(4,4) = 0.0
99      K(4,5) = 0.0
100     K(4,6) = 0.0
101     K(4,7) = 0.0
102     K(4,8) = 1.0
103     K(5,1) = -(L1**4.+BETA**2.*B11)
104     K(5,2) = -BETA**2.*B12
105     K(5,3) = -BETA**2.*B13
106     K(5,4) = -BETA**2.*B14
107     K(5,5) = -(2.*BETA*RMU*A11+NU)
108     K(5,6) = -2.*BETA*RMU*A12
109     K(5,7) = -2.*BETA*RMU*A13
110     K(5,8) = -2.*BETA*RMU*A14
111     K(6,1) = -BETA**2.*B21
112     K(6,2) = -(L2**4.+BETA**2.*B22)
113     K(6,3) = -BETA**2.*B23
114     K(6,4) = -BETA**2.*B24
115     K(6,5) = -2.*BETA*RMU*A21
116     K(6,6) = -(2.*BETA*RMU*A22+NU)
117     K(6,7) = -2.*BETA*RMU*A23
118     K(6,8) = -2.*BETA*RMU*A24
119     K(7,1) = -BETA**2.*B31
120     K(7,2) = -BETA**2.*B32
121     K(7,3) = -(L3**4.+BETA**2.*B33)
122     K(7,4) = -BETA**2.*B34
123     K(7,5) = -2.*BETA*RMU*A31
124     K(7,6) = -2.*BETA*RMU*A32
125     K(7,7) = -(2.*BETA*RMU*A33+NU)
126     K(7,8) = -2.*BETA*RMU*A34
127     K(8,1) = -BETA**2.*B41
128     K(8,2) = -BETA**2.*B42
129     K(8,3) = -BETA**2.*B43
130     K(8,4) = -(L4**4.+BETA**2.*B44)
131     K(8,5) = -2.*BETA*RMU*A41
132     K(8,6) = -2.*BETA*RMU*A42
133     K(8,7) = -2.*BETA*RMU*A43
134     K(8,8) = -(2.*BETA*RMU*A44+NU)

C
135     WRITE (6,1009) ((K(II,JJ), JJ=1,8), II=1,8)
136     1009 FORMAT (' ',8F12.4)
C
137     N1 = 1

```

```

138      AQ(1,N1) = Q1
139      AQ(2,N1) = Q2
140      AQ(3,N1) = Q3
141      AQ(4,N1) = Q4
142      AQ(5,N1) = Q5
143      AQ(6,N1) = Q6
144      AQ(7,N1) = Q7
145      AQ(8,N1) = Q8
146      100  CONTINUE
      C
147      DC 101 I1=1,8
148      V(I1) = AQ(I1,N1)
149      101  CONTINUE
      C
150      AT(N1) = T
151      NNN = N1 + 2
152      N1 = N1+1
      C
      C      ++++++
      C      +
      C      +          MATRIX MULTIPLICATION          +
      C      +
      C      ++++++
      C
153      DC 102 I3=1,8
154      DUMMY = 0.
155      DC 102 I2=1,8
156      MATM = K(I3,I2)*V(I2)
157      DUMMY = DUMMY + MATM
158      102  CONTINUE
159      DC(I3,NNN) = DUMMY
160      AQ(I3,N1) = DELT*(1.9167*IQ(I3,NNN)-1.3333*DQ(I3,NNN-1)
2+0.4167*DQ(I3,NNN-2)) + V(I3)
161      103  CONTINUE
      C
162      I = T+DELT
163      IF (TMAX.GT.T) GO TO 100
164      WRITE (6,1010)
165      1010  FORMAT (//,5X,'T,Q1,Q2,Q3,Q4 ARE AS FOLLOWED:',/)
      C
      C      NOTE: ONLY EVERY FIFTH VALUE IS PRINTED
      C
166      WRITE (6,1011) (AT(J), (AQ(I3,J), I3=1,4), J=1,N1,5)
167      1011  FORMAT (' ',5E15.4)
      C
      C      ++++++
      C      +
      C      +          PLOTTING FUNCTION          +
      C      +
      C      ++++++
      C
      C      NOTE: ONLY EVERY FIFTH VALUE IS PLOTTED
168      N3 = 0
169      DC 104 N2=1,N1,5
170      N3 = N3 + 1
171      IT(N3) = AT(N2)
172      IQ1(N3)=AQ(1,N2)
173      IQ2(N3) = AQ(2,N2)
174      IQ3(N3) = AQ(3,N2)

```



```

175      IC4(N3) = AQ(4,N2)
176      104      CONTINUE
      C
177      WRITE (6,1012)
178      1012      FORMAT ('1')
179      CALL WFL0T1 (TT,TQ1,N3,12,'DISPLACEMENT')
180      WRITE (6,1013) TT(1),TMAX,DELT
181      1013      FORMAT (40X,'DISPLACEMENT(1) AS A FUNCTION OF TAU',///,20X,
182      1'T=' ,1F7.4,10X,'TMAX=' ,1F7.4,10X,'DELT=' ,1F7.4)
183      WRITE (6,1012)
184      CALL WFL0T1 (TT,TQ2,N3,12,'DISPLACEMENT')
185      WRITE (6,1014) TT(1),TMAX,DELT
186      1014      FORMAT (40X,'DISPLACEMENT(2) AS A FUNCTION OF TAU',///,20X,
187      1'T=' ,1F7.4,10X,'TMAX=' ,1F7.4,10X,'DELT=' ,1F7.4)
188      WRITE (6,1012)
189      CALL WFL0T1 (TT,TQ3,N3,12,'DISPLACEMENT')
190      WRITE (6,1015) TT(1),TMAX,DELT
191      1015      FORMAT (40X,'DISPLACEMENT(3) AS A FUNCTION OF TAU',///,20X,
192      1'T=' ,1F7.4,10X,'TMAX=' ,1F7.4,10X,'DELT=' ,1F7.4)
193      WRITE (6,1012)
194      CALL WFL0T1 (TT,TQ4,N3,12,'DISPLACEMENT')
195      WRITE (6,1016) TT(1),TMAX,DELT
196      1016      FORMAT (40X,'DISPLACEMENT(4) AS A FUNCTION OF TAU',///,20X,
197      1'T=' ,1F7.4,10X,'TMAX=' ,1F7.4,10X,'DELT=' ,1F7.4)
198      WRITE (6,1012)
      GC TC 998
      999      CONTINUE
      STOP
      END

```

SENTRY

\$JCF

0761536.SELFED PIN=A82

C
C
C
C
C
C
C
C
C
C
C
C
C

```

*****
+
+   NUMERICAL SOLUTION FOR STATIC AND
+   DYNAMIC INSTABILITIES OF A PROPELLANT
+   LINE. (FOUR MODES ANALYSIS)
+   NB: WITH FORMULA OF OPEN TYPES
+   NONLINEAR AND IMPROVED
+
*****

```

```

1  INTEGER IT
2  INTEGER IA, IB, IC, ID1, ID2
3  INTEGER I1, I2, I3, I4, I5, I6
4  INTEGER JT
5  INTEGER J1, J2, J3, J4, J5, J6
6  REAL DUMMY, MATM
7  REAL EMU
8  REAL BETA, MU, NU, M, MF, I, E
9  REAL Q1, Q2, Q3, Q4, Q5, Q6, Q7, Q8
10 REAL LAM(4), VF
11 REAL L, Z1, T, TMAX, DELT
12 REAL DEL(4,4)
13 REAL DO(8,3200)
14 REAL A(4,4), B(4,4), C(4,4)
15 REAL K(8,38), AQ(8,3200), AP(3200), V(28)
16 REAL TQ1(500), TQ2(500), TQ3(500), TQ4(500)
17 REAL IT(500)

C
C   Q1, Q2, Q3, ... ARE INITIAL CONDITIONS
C   TQ(N)'S ARE PSEUDO INITIAL CONDITIONS
C   LAM(N) ARE MODE SHAPE PARAMETERS
C   VF = FLUID VELOCITY
C   L = LENGTH OF PIPE
C   Z1 = CRITICAL DAMPING RATIO
C   M = MASS OF PIPE
C   MF = MASS OF FLUID
C   I = INERTIA
C   E = MODULUS OF ELASTICITY
C   A(N), B(N), C(N) ARE MODE SHAPE INTEGRALS
C

18 REAL (5,1000) Q1,Q2,Q3,Q4,Q5,Q6,Q7,Q8
19 1000 FORMAT (8F10.4)
20 READ (5,1005) (LAM(I1), I1=1,4)
21 READ (5,1005) ((A(I1,J1), J1=1,4), I1=1,4)
22 READ (5,1005) ((B(I1,J1), J1=1,4), I1=1,4)
23 READ (5,1005) ((C(I1,J1), J1=1,4), I1=1,4)
24 1005 FORMAT (4F10.4)
25 READ (5,1010) M,MF,I,E
26 1010 FORMAT (4E10.3)
27 998 READ (5,1011,FND=999) VF,L,Z1,T,DELT,TMAX
28 1011 FORMAT (F12.4,5F10.4)

C
C   BETA = DIMENSIONLESS FLUID VELOCITY
C   MU = MASS RATIO
C   NU = VISCOUS DAMPING COEFFICIENT
C

```

```

29      BEIA = VF*SQRT(MF*L**2./(E*I))
30      MU = MF/(MF+M)
31      NU = 7.04*Z1*SQRT(1.-MU)

C
32      WRITE (6,1015)
33 1015   FORMAT ('1')
34      WRITE (6,1020) ((A(I2,J2), J2=1,4), I2=1,4)
35 1020   FORMAT ('1','A(I,J)=' ,4F20.4,/3(8X,4F20.4,/))
36      WRITE (6,1025) ((B(I2,J2), J2=1,4), I2=1,4)
37 1025   FORMAT ('1','B(I,J)=' ,4F20.4,/3(8X,4F20.4,/))
38      WRITE (6,1030) ((C(I2,J2), J2=1,4), I2=1,4)
39 1030   FORMAT ('1','C(I,J)=' ,4F20.4,/3(8X,4F20.4,/))
40      WRITE (6,1035) Q1,Q2,Q3,Q4,Q5,Q6,Q7,Q8
41 1035   FORMAT ('1','Q(N)=' ,4F20.4,/6X,4F20.4)
42      WRITE (6,1040) BETA,MU,NU
43 1040   FORMAT ('1','BETA=' ,1F15.4,5X,'MU=' ,1F15.4,5X,'NU=' ,1F15.4)
44      WRITE (6,1045) VF,L,Z1,(IAM(II), II=1,4)
45 1045   FORMAT ('1','VF=' ,1F15.4,5X,'L=' ,1F10.4,5X,'Z1=' ,1F10.4,/,'1',
* 'LAMBDA(N)=' ,4F10.4)
46      WRITE (6,1050) M,MF,I,E
47 1050   FORMAT ('1','M,MF,I,E ARE',4E20.3)
48      WRITE (6,1055)
49 1055   FORMAT (//,30X,'MATRIX IS')
50      WRITE (6,1056)
51 1056   FORMAT ('1','(DUE TO SPACE LIMITATION, MATRIX IS PRINTED AS (2',
* ' INSTEAD OF (8,28)',/))

C
52      RMU = SQRT(MU)

C
C      ++++++
C      +
C      +          ENTRIES OF MATRIX          +
C      +
C      ++++++

C      NOTE: DELTA FUNCTION

C
53      DC 110 ID1=1,4
54      DC 100 ID2=1,4
55      DEL(ID1,ID2) = 0.0
56 100    CONTINUE
57      DEL(ID1,ID1) = 1.0
58 110    CONTINUE

C
59      DC 120 I4=1,8
60      DC(14,1) = 0.0
61      DC(14,2) = 0.0
62 120    CONTINUE

C
C      NOTE: DO-LOOP TO FILL IN 0'S & 1'S

C
63      IC = 4
64      DC 140 IA=1,4
65      DC 130 IB=1,28
66      K(IA,IB) = 0.0
67 130    CONTINUE
68      IC = IC + 1
69      K(IA,IC) = 1.0
70 140    CONTINUE

C

```

Copy available to DTIC does not
 permit fully legible reproduction

NOTE: ENTRIES WITH RECOGNIZED PATTERN

```

C
C
71      DC 160  I5=5,8
72      IT = I5-4
73      DC 150  J5=1,4
74      K(I5,J5) = -(DEL(IT,J5)*LAM(IT)**4.0+BETA**2.0*B(IT,J5))
75      150    CCNTINUE
76      DC 155  J3=5,8
77      JT= J3-4
78      K(I5,J3) = -(2.0*BETA*RMU*A(IT,JT)+DEL(IT,JT)*NU)
79      155    CCNTINUE
C
80      K(I5,9) = B(IT,1)*C(1,1)
81      K(I5,10) = B(IT,1)*C(2,2)+B(IT,2)*(C(1,2)+C(2,2))
82      K(I5,11) = B(IT,1)*C(3,3)+B(IT,3)*(C(1,3)+C(3,1))
83      K(I5,12) = B(IT,1)*C(4,4)+B(IT,4)*(C(1,4)+C(4,1))
84      K(I5,13) = B(IT,1)*(C(1,2)+C(2,1))+B(IT,2)*C(1,1)
85      K(I5,14) = B(IT,1)*(C(1,3)+C(3,1))+B(IT,3)*C(1,1)
86      K(I5,15) = B(IT,1)*(C(2,3)+C(3,2))+B(IT,2)*(C(1,3)+C(3,1))+
      *B(IT,3)*(C(1,2)+C(2,1))
87      K(I5,16) = B(IT,1)*(C(1,4)+C(4,1))+B(IT,4)*C(1,1)
88      K(I5,17) = B(IT,1)*(C(2,4)+C(4,2))+B(IT,2)*(C(1,4)+C(4,1))+
      *B(IT,4)*(C(1,2)+C(2,1))
89      K(I5,18) = B(IT,1)*(C(3,4)+C(4,3))+B(IT,3)*(C(1,4)+C(4,1))+
      *B(IT,4)*(C(1,3)+C(3,1))
90      K(I5,19) = B(IT,2)*C(2,2)
91      K(I5,20) = B(IT,2)*C(3,3)+B(IT,3)*(C(2,3)+C(3,2))
92      K(I5,21) = B(IT,2)*(C(2,3)+C(3,2))+B(IT,3)*C(2,2)
93      K(I5,22) = B(IT,2)*C(4,4)+B(IT,4)*(C(2,4)+C(4,2))
94      K(I5,23) = B(IT,4)*C(2,2)+B(IT,2)*(C(2,4)+C(4,2))
95      K(I5,24) = B(IT,2)*(C(3,4)+C(4,3))+B(IT,3)*(C(2,4)+C(4,2))+
      *B(IT,4)*(C(2,3)+C(3,2))
96      K(I5,25) = B(IT,3)*C(3,3)
97      K(I5,26) = B(IT,3)*C(4,4)+B(IT,4)*(C(3,4)+C(4,3))
98      K(I5,27) = B(IT,4)*C(3,3)+B(IT,3)*(C(3,4)+C(4,3))
99      K(I5,28) = B(IT,4)*C(4,4)
C
100     160    CCNTINUE
C
C
101     WRITE (6,1060) ((K(IA,JA), IA=1,8),JA=1,28)
102     1060    FORMAT (' ',8E14.4)
C
103     N1 = 1
104     AQ(1,N1) = Q1
105     AQ(2,N1) = Q2
106     AQ(3,N1) = Q3
107     AQ(4,N1) = Q4
108     AQ(5,N1) = Q5
109     AQ(6,N1) = Q6
110     AQ(7,N1) = Q7
111     AQ(8,N1) = Q8
112     170    CCNTINUE
C
113     DC 180  IZ1=1,8
114     V(IZ1) = AQ(IZ1,N1)
115     180    CCNTINUE
C
C
C

```

NOTE: HAVE TO ADD NON LINEAR EQUATIONS

Copy available to DTIC does not
 permit fully legible reproduction

C

2

C

c

c

22

22

٢٢

C

C

C

C

C

C

C

C

C

cc

22

2

•

•

Copy available to DTIC does not permit fully legible reproduction

C
C
C

NOTE: ONLY EVERY TENTH VALUE IS PLOTTED

```

154      N3 = 0
155      DC 210  N2=1,N1,10
156      N3 = N3 + 1
157      TT(N3) = AT(N2)
158      TQ1(N3)=AQ(1,N2)
159      TQ2(N3) = AQ(2,N2)
160      TQ3(N3) = AQ(3,N2)
161      TQ4(N3) = AQ(4,N2)
162      210  CCNTINUE
C
163      WRITE (6,1015)
164      CALL WFLC11 (TT,TQ1,N3,12,'DISPLACEMENT')
165      WRITE (6,1071)  TT(1),TMAX,DELT
166      1071  FORMAT (40X,'DISPLACEMENT (1) AS A FUNCTION OF TAU',///,20X,
1'I=',1F7.4,10X,'TMAX=',1F7.4,10X,'DELT=',1F7.4)
167      WRITE (6,1015)
168      CALL WFLC11 (TT,TQ2,N3,12,'DISPLACEMENT')
169      WRITE (6,1075)  TT(1),TMAX,DELT
170      1075  FORMAT (40X,'DISPLACEMENT (2) AS A FUNCTION OF TAU',///,20X,
1'I=',1F7.4,10X,'TMAX=',1F7.4,10X,'DELT=',1F7.4)
171      WRITE (6,1015)
172      CALL WFLC11 (TT,TQ3,N3,12,'DISPLACEMENT')
173      WRITE (6,1080)  TT(1),TMAX,DELT
174      1080  FORMAT (40X,'DISPLACEMENT (3) AS A FUNCTION OF TAU',///,20X,
1'I=',1F7.4,10X,'TMAX=',1F7.4,10X,'DELT=',1F7.4)
175      WRITE (6,1015)
176      CALL WFLC11 (TT,TQ4,N3,12,'DISPLACEMENT')
177      WRITE (6,1085)  TT(1),TMAX,DELT
178      1085  FORMAT (40X,'DISPLACEMENT (4) AS A FUNCTION OF TAU',///,20X,
1'I=',1F7.4,10X,'TMAX=',1F7.4,10X,'DELT=',1F7.4)
179      WRITE (6,1015)
180      GC TC 998
181      999  CCNTINUE
182      STOP
183      END

```

SENTRY

Copy available to DTIC does not
 permit fully legible reproduction

APPENDIX V

Mode Shape Integrals of a Simply Supported Beam

$$\int_0^1 \gamma_j \gamma_k^{iv} d\xi = k^4 \pi^4 \int_0^1 \sin j\pi\xi \sin k\pi\xi d\xi \quad (\text{A-21})$$

$$= \begin{cases} \frac{k^4 \pi^4}{2} & j=k \\ 0 & j \neq k \end{cases}$$

$$= \frac{k^4 \pi^4}{2} \delta_{jk}$$

$$\int_0^1 \gamma_j \gamma_k d\xi = \int_0^1 \sin j\pi\xi \sin k\pi\xi d\xi \quad (\text{A-22})$$

$$= \begin{cases} \frac{1}{2} & j=k \\ 0 & j \neq k \end{cases}$$

$$= \frac{1}{2} \delta_{jk}$$

$$\int_0^1 \gamma_j \gamma_k' d\xi = k\pi \int_0^1 \sin j\pi\xi \cos k\pi\xi d\xi \quad (\text{A-23})$$

$$= a_{jk} \quad (\text{values of } a_{jk} \text{ are tabulated in Table 4})$$

$$\int_0^1 \gamma_j \gamma_k'' d\xi = -k^2 \pi^2 \int_0^1 \sin j\pi\xi \sin k\pi\xi d\xi \quad (\text{A-24})$$

$$= \begin{cases} \frac{-k^2 \pi^2}{2} & j=k \\ 0 & j \neq k \end{cases}$$

$$= \frac{-k^2 \pi^2}{2} \delta_{jk}$$

$$= b_{jk}$$

$$\int_0^1 \gamma_h' \gamma_i' d\xi = h i \pi^2 \int_0^1 \cos h\pi\xi \cos i\pi\xi d\xi \quad (\text{A-25})$$

$$= \begin{cases} \frac{h^2 \pi^2}{2} & h=i \\ 0 & h \neq i \end{cases}$$

$$= \frac{-k^2 \pi^2}{2} \delta_{hi}$$

$$= c_{hi}$$

APPENDIX VI

A LISTING OF FORTRAN IV PROGRAM FOR
SIMPLY SUPPORTED TUBE

```

      +-----+
      +               +
      +               +
      +               +
      +               +
      +               +
      +               +
      +               +
      +-----+

```

DIVERGENCE
SIMPLY-SUPPORTED
SPECIAL EDITION

```

0001      REAL  A(4,4), B(4,4), C(4,4)
0002      REAL  DEL(4,4)
0003      REAL  MATM,MU,NU,M,MF,I
0004      REAL  LAM(4),L
0005      REAL  DO(8,2500)
0006      REAL  K(8,28),AO(8,2020),AT(2020),V(28)
0007      REAL  TQ1(2020),TT(2020),TQ2(2020)

C
C
0008      READ (5,1000)  (AO(IU,1), IU=1,8)
0009      1000  FORMAT (8F10.4)
0010      READ (5,1005)  ((A(I1,J1), J1=1,4), I1=1,4)
0011      1005  FORMAT (4F10.4)
0012      READ (5,1010)  M,MF,T,E
0013      1010  FORMAT (4E10.3)
0014      READ (5,1011)  VF,L,Z1
0015      1011  FORMAT (F12.4,2F10.4)
0016      N3 = 0

C
C
0017      BETA = VF*SQRT(MF*L**2./(E*I))
0018      MU = MF/(MF+M)
0019      NU = 7.04*Z1*SQRT(1.-MU)

C
0020      WRITE (6,1015)
0021      1015  FORMAT ('1')

C
C      NOTE:  DELTA FUNCTION
C             B(J,K),C(E,I) ... ARE DIFFERENT
C

0022      DO 110  ID1=1,4
0023      DO 100  ID2=1,4
0024      DEL(ID1,ID2) = 0.0
0025      B(ID1,ID2) = 0.0
0026      C(ID1,ID2) = 0.0
0027      100  CONTINUE
0028      DEL(ID1,ID1) = 0.5
0029      LAM(ID1) = 3.14159*ID1
0030      E(ID1,ID1) = -0.5*LAM(ID1)**2
0031      C(ID1,ID1) = 0.5*LAM(ID1)**2
0032      110  CONTINUE

C
C
0033      RMU = SQRT(MU)

```

```

C
C      ++++++
C      +
C      +          ENTRIES OF MATRIX          +
C      +
C      ++++++
C
0034      DO 120 I4=1,8
0035      DQ(I4,1) = 0.0
0036      DQ(I4,2) = 0.0
0037      120 CONTINUE
C
C      NOTE: DO-LOOP TO FILL IN 0'S & 1'S
C
0038      IC = 4
0039      DO 140 IA=1,4
0040      DO 130 IB=1,28
0041      K(IA,IB) = 0.0
0042      130 CONTINUE
0043      IC = IC + 1
0044      K(IA,IC) = 1.0
0045      140 CONTINUE
C
C      NOTE: ENTRIES WITH RECOGNIZED PATTERN
C
0046      DO 160 I5=5,8
0047      IT = I5-4
0048      DO 150 J5=1,4
0049      K(I5,J5) = -(DEL(IT,J5)*LAM(IT)**4.0+BETA**2.0*B(IT,J5))
0050      150 CONTINUE
0051      DO 155 J3=5,8
0052      JT= J3-4
0053      K(I5,J3) = -(2.0*BETA*PMU*L(IT,JT)+DEL(IT,JT)*MU)
0054      155 CONTINUE
C
0055      K(I5,9) = B(IT,1)*C(1,1)
0056      K(I5,10) = B(IT,1)*C(2,2)+B(IT,2)*(C(1,2)+C(2,2))
0057      K(I5,11) = B(IT,1)*C(3,3)+B(IT,3)*(C(1,3)+C(3,1))
0058      K(I5,12) = B(IT,1)*C(4,4)+B(IT,4)*(C(1,4)+C(4,1))
0059      K(I5,13) = B(IT,1)*(C(1,2)+C(2,1)) + B(IT,2)*C(1,1)
0060      K(I5,14) = B(IT,1)*(C(1,3)+C(3,1)) + B(IT,3)*C(1,1)
0061      K(I5,15) = B(IT,1)*(C(2,3)+C(3,2)) + B(IT,2)*(C(1,3)+C(3,1))
0062      K(I5,16) = B(IT,1)*(C(1,4)+C(4,1)) + B(IT,4)*C(1,1)
0063      K(I5,17) = B(IT,1)*(C(2,4)+C(4,2)) + B(IT,2)*(C(1,4)+C(4,1))
0064      K(I5,18) = B(IT,1)*(C(3,4)+C(4,3)) + B(IT,3)*(C(1,4)+C(4,1))
0065      K(I5,19) = B(IT,2)*C(2,2)
0066      K(I5,20) = B(IT,2)*C(3,3) + B(IT,3)*(C(2,3)+C(3,2))
0067      K(I5,21) = B(IT,2)*(C(2,3)+C(3,2)) + B(IT,3)*C(2,2)
0068      K(I5,22) = B(IT,2)*C(4,4)+B(IT,4)*(C(2,4)+C(4,2))
0069      K(I5,23) = B(IT,2)*C(2,2)+B(IT,2)*(C(2,4)+C(4,2))
0070      K(I5,24) = B(IT,2)*(C(3,4)+C(4,3)) + B(IT,3)*(C(2,4)+C(4,1))
0071      K(I5,25) = B(IT,3)*C(3,3)

```

```

0072      K(I5,26) = B(IT,3)*C(4,4)+E(IT,4)*(C(3,4)+C(4,3))
0073      K(I5,27) = B(IT,4)*C(3,3)+E(IT,3)*(C(3,4)+C(4,3))
0074      K(I5,28) = E(IT,4)*C(4,4)

```

```

C
0075      160  CONTINUE

```

```

C
C      2 CONTINUATION CARDS JUST IN CASE
0076      165  CONTINUE

```

```

C
0077      READ (5,1012,EVD=999)  T,DELT,TMA
0078      1012  FORMAT (3F10.4)
0079      WRITE (6,5554)  T,DELT,TMAX
0080      5554  FORMAT( ' ',3F20.4)
0081      N1 = 1

```

```

C
0082      170  CONTINUE

```

```

C
0083      DO 180  IZ1=1,8
0084      V(IZ1) = AQ(IZ1,N1)
0085      180  CONTINUE

```

```

C
C
C      NOTE:  HAVE TO ADD NON LINEAR EQUATIONS
C

```

```

0086      V(9) = AQ(1,N1)**3
0087      V(10) = AQ(1,N1)*AQ(2,N1)**2
0088      V(11) = AQ(1,N1)*AQ(3,N1)**2
0089      V(12) = AQ(1,N1)*AQ(4,N1)**2
0090      V(13) = AQ(1,N1)**2*AQ(2,N1)
0091      V(14) = AQ(1,N1)**2*AQ(3,N1)
0092      V(15) = AQ(1,N1)*AQ(2,N1)*AQ(3,N1)
0093      V(16) = AQ(1,N1)**2*AQ(4,N1)
0094      V(17) = AQ(1,N1)*AQ(2,N1)*AQ(4,N1)
0095      V(18) = AQ(1,N1)*AQ(3,N1)*AQ(4,N1)
0096      V(19) = AQ(2,N1)**3
0097      V(20) = AQ(2,N1)*AQ(3,N1)**2
0098      V(21) = AQ(2,N1)**2*AQ(3,N1)
0099      V(22) = AQ(2,N1)*AQ(4,N1)**2
0100      V(23) = AQ(2,N1)**2*AQ(4,N1)
0101      V(24) = AQ(2,N1)*AQ(3,N1)*AQ(4,N1)
0102      V(25) = AQ(3,N1)**3
0103      V(26) = AQ(3,N1)*AQ(4,N1)**2
0104      V(27) = AQ(3,N1)**2*AQ(4,N1)
0105      V(28) = AQ(4,N1)**3

```

```

C
C
0106      AT(N1) = T
0107      NNN = N1 + 2
0108      N1 = N1+1

```

```

C
C      ++++++
C      +
C      +          MATRIX MULTIPLICATION          +
C      +
C      ++++++

```

[illegible]

END

FILMED

9-83

DTIC